LUND UNIVERSITY
Faculty of Science

Rigshospitalet

# Impact of PET in the Radiation Therapy Planning for Pediatric Cancer

Master of Science Thesis

Josefine Ståhl Kornerup
Lund University, Faculty of Science
Rigshospitalet, Copenhagen University Hospital
January – August 2012

Supervisors: Patrik Brodin, MSc, Charlotte Birk Christensen, MD, Thomas Björk Eriksson, MD, Assoc prof, and Per Munck af Rosenschöld, MSc, PhD, MPE, Assoc. prof.

Radiation Medicine Research Center,
Department of Radiation Oncology, Rigshospitalet,
Copenhagen University Hospital.
Medical Radiation Physics, Clinical Sciences,
Lund University.

# Acknowledgements

Apart from thanking my lucky star for getting this project in the first place, I would like to extend sincere thanks to the following persons:

- MD:s Anne Kiil-Berthelsen and Elena Markova: for meticulously delineating the OAR:s and GTV:s.
- Marianne C Aznar, PhD, Ivan R Vogelius, PhD, Christine Ritter, MSc, and Christian Hollensen, MSc: for generously helping me with treatment planning, statistics, programming etc.

In particular, I owe many special thanks to my four supervisors for their dedication, guidance and support:

- Charlotte Birk Christensen: for structuring the patient data and guiding me through the PET-parts of the project.
- Thomas Björk-Eriksson: for delineating the CTV:s and for always being encouraging and enthusiastic whenever I needed help.
- Per Munck af Rosenschöld: for sharing experience and knowledge as well as keeping a critical eye to my work.
- Patrik Brodin: for invaluable help and mentoring and for always taking time to explain to me with a seemingly endless patience, through every step of this work.

*Josefine*

# Table of Contents

# Abstract


## Purpose:

The purpose of this study was to evaluate the impact of including PET (Positron Emission Tomography) in the process of pediatric radiation therapy planning.

The aim was to study the effect on target volumes and how this in turn affects the resulting treatment plans. This study also aims to compare the estimated risks of various long-term complications and how the use of PET influences these risks.

## Methods:

Eleven pediatric sarcoma, NSCLC (non-small-cell lung cancer) and nasopharyngeal cancer patients, treated at Rigshospitalet in 2005-2011, were included in this study. The target volumes (GTV:s and CTV:s) were delineated by senior clinicians specialized in nuclear medicine, diagnostic radiology and radiation oncology. The delineation was performed without and subsequently with access to the PET scan information, on separate CT-sets. A margin of 6 mm was added to each CTV to render the PTV.
Treatment plans were generated for three different photon therapy modalities and intensity-modulated proton therapy. Dose-effects models based on published studies were derived to evaluate and compare the risks of complications.
Moreover, a rough estimation of the effective dose from the PET/CT scan and the associated risk was made.

## Results:

The target volumes were evaluated with respect to volume size as well as shape. For the patients in this study, there was no significant change of the size of the target volumes: the average CTV size was 257 $cm^3$ (range: 71.10-462.40 $cm^3$, median 259.60 $cm^3$) and 254 $cm^3$ (range: 63.43-497.30 $cm^3$, median 211.90 $cm^3$) without and with PET respectively. Using PET did in some cases alter the shape of the treatment volumes, resulting in a mean Dice index of 0.91 (range: 0.86-0.95).
The radiation therapy plans based on PET data were not significantly different from the noPET-plans, in neither the risk of normal tissue complications, nor the risk of secondary cancers. The impact of PET did not differ between the four treatment modalities.

## Conclusions:

The main conclusion from this study is that while including PET in the radiation therapy treatment planning process of pediatric cancer patients may change the shape and size of the target volume, it does not significantly impact the risks attributable to the radiation therapy, neither of normal tissue complications nor secondary cancers. The risk of radiation-induced complications from the PET/CT scan is very small.
The target volume may be decreased by including PET, when areas dubious on the CT are FDG-negative. This gives the potential to reduce the irradiated normal tissue volume. The PET-based target volume may be expanded for FDG-positive areas that are undistinguishable on the CT-images. This will likely decrease the risk of leaving malignant tissue untreated.

The results suggest that there will be no significant differences between radiation therapy plans made with or without PET-data. The plans appear to be of comparable quality (provided that the therapeutic efficacy is maintained) and the risk of long-term complications is not changed. A vast amount of published results from more than a decade of research and clinical experience, indicate the usefulness and diagnostic value of including PET-data into the care of cancer patients – adults as well as children. Taking these factors into consideration, along with the very low risks of radiation-induced side effects from the PET/CT scan itself, the conclusion is that PET should be used as a complementary tool in target volume delineation for radiation therapy planning of pediatric patients.

# Populärvetenskaplig sammanfattning

I Sverige drabbas omkring 300 barn av cancer varje år och majoriteten av dem är bara fyra-fem år gamla när de får sin diagnos. Omkring två tredjedelar av barncancerdiagnoserna utgörs av leukemier, lymfom och hjärntumörer, medan den sista tredjedelen är olika solida tumörformer som njurtumörer och nervvävnadstumörer i buken.

Cancersjukvårdens utveckling under de senaste årtiondena har medfört en avsevärt förbättrad prognos för flertalet cancerdiagnoser. Ungefär tre fjärdedelar av barncancerpatienterna blir idag helt botade. De främsta behandlingsmetoderna är kirurgi, kemoterapi (cellgifter) och strålbehandling och de kan kombineras på olika sätt. I Sverige strålbehandlas ungefär hälften av alla cancerpatienter, och cirka en tredjedel av barncancerpatienterna, någon gång under sin sjukdomstid.

Strålbehandlingen går ut på att en viss stråldos levereras till en specifik målvolym, som oftast utgörs av själva tumören inklusive marginaler. Strålningen som används har tillräckligt hög energi för att orsaka skador på kroppens celler, till exempel genom att jonisera atomer och bryta molekylbindningar. Detta kan bland annat påverka DNA-molekylen i cellkärnan.
Tyvärr är det ofrånkomligt att även friska celler bestrålas, och givetvis kan strålningen orsaka bestående påverkan även inuti dessa. Skadorna motarbetas dock av de reparationsprocesser som ständigt pågår i kroppen och lyckligtvis nog sker reparationen oftast betydligt mer effektivt i de friska cellerna än i tumörceller. För att undvika skador i frisk vävnad är det dock viktigt att inte bestråla en onödigt stor volym. Att skona den friska vävnaden men samtidigt leverera en tillräckligt hög dos till tumören är en av de största utmaningarna inom modern strålbehandling. Detta är ännu viktigare för unga patienter, eftersom barn är extra känsliga för strålning och riskerna för negativa bieffekter är större än hos vuxna. Dessutom har barn fler levnadsår framför sig än vuxna patienter, vilket innebär fler år för komplikationer att hinna utvecklas och ge besvär.

Inom extern strålbehandling har det under de senaste årtiondena utvecklats nya behandlingstekniker. I kombination med CT-baserad (Computed Tomography, datortomografi) dosplanering har dessa förbättrat möjligheterna att mer exakt leverera stråldos till den önskade målvolymen. Denna mer konforma dosfördelning gör det möjligt att öka den absorberade dosen till tumören utan att öka stråldosen till omgivande frisk vävnad. Den gör det också möjligt att minska behandlingsmarginalerna, men detta innebär i sin tur att det blir ännu viktigare säkerställa vilken volym som behöver behandlas. Behovet av att komplettera traditionella undersökningsmetoder som CT med andra informationskällor har ökat.

PET (positronemissionstomografi) är en nuklearmedicinsk bildtagningsmodalitet som blivit ett allt viktigare komplement till CT vid diagnostisering och behandlingsplanering av cancersjukdomar. Precis som vid de flesta nuklearmedicinska undersökningar injiceras ett radioaktivt preparat i patienten. Aktiviteten fördelar sig i patientens kropp och kan avbildas med hjälp av olika detektorer. Genom att fästa den radioaktiva isotopen till en molekyl med känt biologiskt rörelsemönster kan man till viss del styra var i kroppen aktiviteten ska hamna. Vid PET-scanning används ofta den radioaktiva isotopen fluor-18 som fästs vid en glukosliknande molekyl. Glukos (druvsocker) är en viktig energikälla och tas upp av celler i proportion till deras ämnesomsättning. Detta innebär att radioaktiviteten ackumuleras i celler med hög metabolism – något som ofta är fallet med maligna tumörceller. PET-bilden kan därmed vara till stor hjälp vid inritningen av målvolymer.

Syftet med denna studie är att studera om – och i så fall hur – målvolymerna ändras av att den kliniska informationen kompletteras med PET-bilder. Strålbehandlingsplaner har gjorts till båda varianter och för ett flertal strålbehandlingstekniker. Målet är att med hjälp av teoretiska modeller baserade på publicerade data försöka upptäcka och kvantifiera skillnader mellan planerna med och utan PET, med avseende på risken för komplikationer.

Resultaten visar att användningen av PET kan förändra målvolymerna till såväl storlek som form. Trots detta var det inte möjligt att påvisa någon signifikant förändring av riskerna för komplikationer av själva strålbehandlingen.

# 1. Introduction

Radiation therapy has undergone a considerable evolution during the last decade. The widespread implementation of intensity-modulated therapy techniques, proton irradiation and stereotactic body radiation therapy (SBRT) has drastically improved the ability to deliver a more conformal dose to the target volume.

An improved conformity of the dose distribution has made it possible to increase the dose to the tumor, while maintaining – or even reducing – the dose to surrounding normal tissue and organs at risk (OAR). However, with the ability to deliver dose to a very specific area comes an increasing importance of knowing the optimal volume to treat. This is where imaging techniques such as positron emission tomography (PET) and magnetic resonance imaging (MRI) can contribute with valuable diagnostic information to complement the traditional computed tomography (CT) images.

The therapeutic advances in pediatric oncology have dramatically increased the number of childhood and adolescent cancer survivors that reach adulthood. However, childhood cancer survivors have significant long-term morbidity attributable to their cancer therapy and the side effects of the treatment are numerous (1, 2). As a result of the increased cure rates, the need to address questions regarding their long-term quality of life and the risk of therapy-related late side effects has become more important.

## 1.1 Aim

The purpose of this study was to evaluate the impact of including PET in the process of pediatric radiation therapy planning.
Besides studying the target volumes, the aim was to try to quantify the impact on the treatment plans in terms of risk of complications. The study also includes an attempt to compare different treatment modalities.

In short, this study aims to answer the following questions:

1. Does PET change the size of the target volumes?
2. Does PET change the shape of the target volumes?
3. Does PET improve the outcome of radiation therapy in terms of reduced normal tissue toxicity and/or secondary cancer risk?
4. If there are any benefits from using PET in radiation therapy planning, do they depend on the choice of treatment technique?

Whether the use of PET in radiation therapy treatment planning affects the tumor control probability is an issue that will not be addressed. It is assumed that tumor control probability (TCP) will be comparable with and without PET.

# 2. Background

## 2.1 Radiation therapy

Radiation therapy is one of the principal cancer treatment methods, along with surgery and chemotherapy. In Sweden, about 50 % of all cancer patients – and one third of the pediatric cancer patients – receive radiation therapy. It is to thank for about 30 % of the cured patients (3).

The radiation treatment may aim to cure the patient (curative treatment), to shrink the tumor before surgery (neoadjuvant treatment), to prevent relapses after surgery (adjuvant treatment) or to relieve a patient from pain and discomfort from an incurable disease (palliative treatment). The radiation can be given by a source located near-by the patient (external radiation therapy) or through so-called Brachy-therapy, with the radiation source placed within the tumor (interstitial therapy) or in a cavity adjacent to the tumor (intracavitary therapy).

The main purpose of radiation therapy is to deliver an absorbed dose to a target volume, in general the tumor with margins. The radiation used has sufficient energy to cause ionizations of atoms and thereby change the structures of molecules, such as the DNA-molecule located within the nucleus of the cell. The damages to the DNA-molecule are mostly caused indirectly by hydroxyl radicals produced by chemical reactions following the radiolysis of water.

The cell damages can be severe enough to kill the cell or just keep the cell from growing and dividing. These reactions are desired in the malignant cells, but unfortunately it is inevitable to irradiate and damage healthy cells too. The radiation-induced damages are thwarted by repairing-processes constantly taking place in human cells. Non-malignant cells are usually more capable of repairing the damages caused by the radiation, but – depending on the level of radiosensitivity of the healthy organ – are still at risk of acute and permanent damages. Thus, one of the major challenges of modern radiation therapy is to minimize the absorbed dose to healthy organs and tissues while delivering a high dose to the target volume.

Sparing the healthy tissue is one of the main reasons to fractionate the radiation regimen: instead of giving the entire dose at one occasion, the prescribed dose is usually given in smaller portions (fractions). The time in-between the treatment sessions allows for the non-malignant cells to repair some of the damage and enhances the recovery of healthy tissues.

The traditional radiation used for therapy is photon beams, but the use of particle radiation, such as protons and ions, is increasing.

- Photons are quantized amounts of electromagnetic energy, just like visible light and X-rays. The photons used for radiation therapy have higher energy and shorter wave length than the X-rays used for diagnostic purposes. The photon radiation is delivered by a linear accelerator (linac), capable to rotate around the patient.
- Protons are elementary particles. Along with neutrons, protons make up the major part of the visible mass in our universe as these two particles, in different proportions, are the building blocks of the nucleus in all atoms. The accelerator used to produce clinical proton beams is circular, usually referred to as a cyclotron.

When used for radiation therapy, there are some important differences between the two. For example, as can be seen in Figure 1, photons deposit most of their energy quite shallow in the attenuating matter, whereas the energy of a proton beam is mainly deposited at a relatively focused depth. This characteristic maximum of the energy deposited by particle radiation is called the Bragg peak.

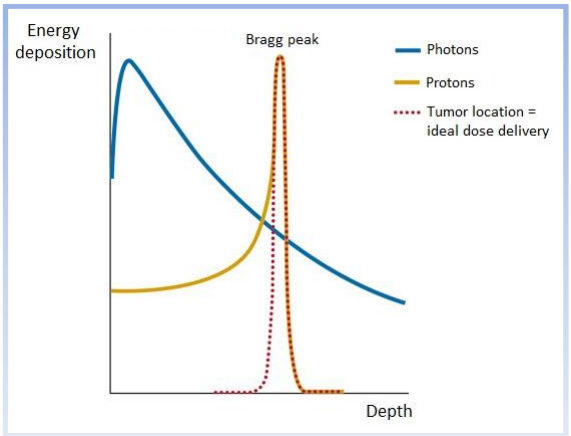


Figure 1: Schematic image of the characteristics in the energy-deposition of photons and protons.

## 2.1.1 3DCRT

Two-dimensional (2D) radiation therapy is a rather old-fashioned – and out of date – technique which uses blocks to form square-edged radiation fields. The treatment planning is made from planar X-ray images and generalized approximations.

In modern radiation therapy planning (RTP) the planar X-ray images have been replaced by three-dimensional CT images, improving the ability to localize the diseased area and making the plans more individualized. Incorporating the CT images into the treatment process has led to today's three-dimensional conformal radiation therapy, 3DCRT. This modality is quite similar to 2D radiation therapy, however much more advanced. The radiation can be delivered at various angles and the shape of each radiation beam is controlled by collimators, often multi-leaf collimators (MLC:s), to conform the dose to the tumor.

Figure 2: Conventional radiation therapy.

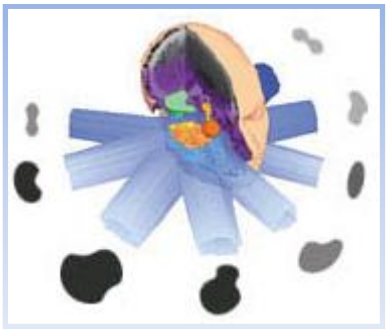

Figure 3: 3DCRT.

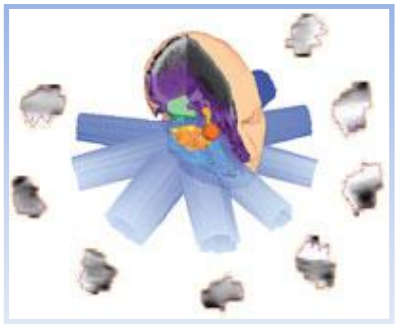

Figure 4: IMRT.

## 2.1.2 IMRT

Intensity-Modulated Radiation Therapy (IMRT) is an important refinement of 3DCRT and revolutionized radiation therapy in the 1990s (4). In IMRT, each field includes numerous of radiation beams and the intensity of the radiation in each field is varied, or modulated. The MLC:s have two important roles: the first is to give the desired shape of the radiation beam and the second is to change the intensity within each beam.

The non-uniform intensities result from a procedure called inverse treatment planning. This planning process is based on defining dose objectives for the target volume as well as the surrounding normal tissues. The inverse planning software uses optimization algorithms to calculate the photon fluence fulfilling the dose objectives. The algorithm also calculates the optimal motion of the MLC:s to realize this fluence.

IMRT permits irradiation of patients with more complexly shaped tumors and at problematic locations. The modulated intensity allows for concave dose distributions, as oppose to the conventional treatment techniques. IMRT thus enables radiation treatment of tumors growing around sensitive organs, such as the medulla. For example, the implementation of IMRT in radiation therapy clinics has drastically improved the ability to treat head and neck cancers while decreasing the prevalence as well as the severity of some common complications (5, 6).

The cost of this highly modulated treatment is however an increased volume of healthy normal tissue receiving low radiation doses. The size of this low-dose area usually increases with the number of fields. Low doses are likely to be of more significance for pediatric patients, but in selected cases the quality of the IMRT plan and the benefit of increased tumor control outweighs the risks associated with the so-called low-dose bath (7). The increase of the low-dose volume, compared to conventional techniques, has led to changes in the clinical manifestations of normal tissue morbidity (8).

### 2.1.3 IMAT

Intensity-Modulated Arc Therapy (IMAT) can be described as rotational version of IMRT and the treatment planning is based on a similar optimizing method.
Instead of delivering the intensity-modulated radiation at fixed angles, the linear accelerator used for IMAT has a donut-shaped gantry enabling the radiation to be delivered continuously while rotating. This technique is sometimes able to produce even more conform target doses than IMRT (9).

### 2.1.4 IMPT

There are two techniques used clinically for radiation therapy with protons: passive scattering and active scanning. In the former, a scattering material is placed in the proton pencil beam as it exits the accelerator. This primary scatterer, making the beam diverge and broaden, is followed by a second scatterer used to shape the beam to the target. The latter technique uses magnets to focus the beam and the dose is delivered in discrete spots. As the depth-wise location of the Bragg peak depends on the energy of the proton beam, altering its energy makes it possible to control the width of the Bragg plateau, defined by the spread out Bragg peak (SOBP). The magnets are used to steer the beam in the plane and modifying energy of the incident beam allows for the entire target volume to be scanned.

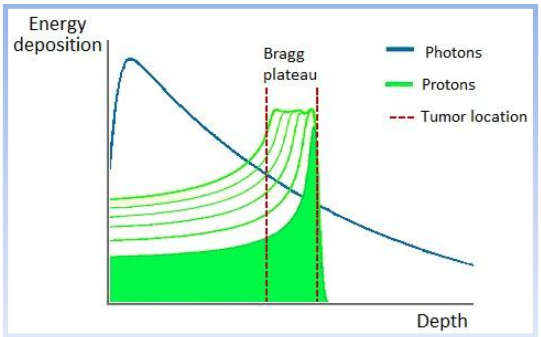


Figure 5: SOBP.

The discrete spot-scanning technique can be used in different ways to obtain optimal target-coverage and dose-distribution. In what is usually referred to as Intensity-Modulated Proton Therapy (IMPT) a number of individually inhomogeneous fields are combined to form a homogenous and conform dose to the target volume. The position and weight of each spot is determined by algorithms, through the same sort of optimizing process used for IMAT- and IMRT-planning.
Actively scanned high-energy proton beams are often able to provide an even more conform dose-distribution than most photon modalities, and reduce the dose of healthy tissues. A number of studies show the potential of reducing treatment-related side effects, including secondary cancers, when using proton therapy instead of photons (6, 9-11).

# 2.2 Positron Emission Tomography

Positron Emission Tomography (PET) is a nuclear medicine imaging technique. Nuclear medicine imaging involves administering a very small amount of a radioactive substance to the patient and measuring the emitted radiation from the outside via advanced systems of detectors and imaging devices. The radioactivity, referred to as a radiopharmaceutical or a radiotracer, can for example be administered to the patient orally, injected intravenously or inhaled as a gas.

The radiotracer consists of a radioactive isotope connected to a molecule (the pharmaceutical) with a known biological behavior. By correctly combining the appropriate isotope with a suitable substance, the activity is forced to accumulate in certain areas of the body. The activity gradually diminishes via physical decay as well as biological excretion. The combined effective half-life as well as the time for the radiotracer to accumulate in the desired location are important factors when deciding the appropriate time interval between the administration of the activity and the imaging procedure.

## 2.2.1 $^{18}$F-fluoro-2-deoxy-D-glucose, FDG

$^{18}$F-FDG, fluorodeoxyglucose, is the most widely available PET tracer and the most commonly used for PET and PET/CT scans.

$^{18}$F has a physical half-life of 109.8 minutes and the decay is dominated (97%) by positron emission to a stable oxygen isotope ($^{18}$O). The emitted positron has a maximum energy of 635 keV and its maximal range in water is approximately 2.4 mm. In other words, its range inside the human body is limited and the positrons themselves cannot be detected to generate an image. However, the emitted positron annihilates when it collides with an electron. The electron-positron annihilation results in the production of two 511 keV-photons, which are relatively penetrating and make it possible to depict the accumulated activity (or to be more precise, the location of the annihilation event).

The fluorine used for PET is usually produced in a cyclotron. These are only available on some hospitals, but the relatively long half-life of $^{18}$F allows for the activity to be produced at a different location a couple of hours before the examination and transported to the clinic.

The radiotracer is synthesized in a process where the $^{18}$F-atom takes the place of one of the hydroxyl groups in the glucose molecule, which then becomes fluorodeoxyglucose. Inside the body, this glucose analog mimics the regular glucose and enters the first step of glycolysis. This initial step is a phosphorylation reaction and turns FDG into FDG-6-$PO_4$, which resists further enzyme processes and is retained in the cell (12, 13).
In other words, FDG accumulates preferentially in cells with high metabolic turnover, a high glucose metabolism, and this intracellular entrapment provides a measure for the rate of glycolysis in the cell. Since neoplastic cells often have a high rate of glycolysis, the activity tends to accumulate in tumors (12, 13). The accumulation depends on the tumor blood flow, the effectiveness and activity of the glucose transport and enzymes as well as the cellular glucose consumption.

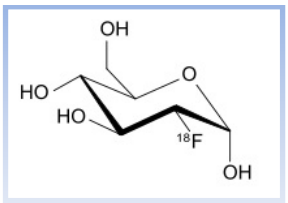


Figure 6: The FDG molecule.

Unfortunately, FDG is not a specific tracer for detecting tumor cells: non-malignant tissues can show an increased FDG uptake, for example due to inflammatory processes, and there may be a physiological high FDG-uptake in several organs, such as brain, heart and kidneys.

Throughout this thesis, the terms PET and PET/CT are always referring to $^{18}$F-FDG PET, unless otherwise stated.

### 2.2.1.2 Principles of FDG-PET

The biologically active molecule, labeled with the positron emitting radioisotope, is injected intravenously. It distributes throughout the patient's body via the bloodstream and enters into organs and cells.

There are blocks of independent scintillation detectors arranged around the ring of the PET scanner, each containing 32 to 64 detector elements adding up to a total of tens of thousands of elements. The two annihilation photons are electronically detected as a coincidence event when they strike opposing detectors simultaneously, i.e. if one detector registers an event, one of the opposite detectors must also register an event within a certain and very small time interval. All single-events are ignored and omitted from the information used for image reconstruction. The coincidence detection is one of the features giving PET-images better resolution than most other nuclear imaging techniques (such as SPECT, Single-Photon Emission Tomography).
Figure 7 below illustrates one line of coincidence. During a real PET scan, about 6-70 million detector-pair combinations record events from many different angles around the patient. Each detector communicates with countless of other detectors, and the number of lines of response (LOR) denotes how many. In modern 3D-PET systems, coincidence planes between all detector rings are possible, resulting in an increased sensitivity compared to older versions.

The collected data is corrected for photon attenuation and tomographic images of the activity concentration in the tissue are reconstructed. The reconstruction software takes the coincidence events measured at all angular and linear positions to reconstruct the image depicting the localization and concentration of the FDG within a plane of the scanned organ.

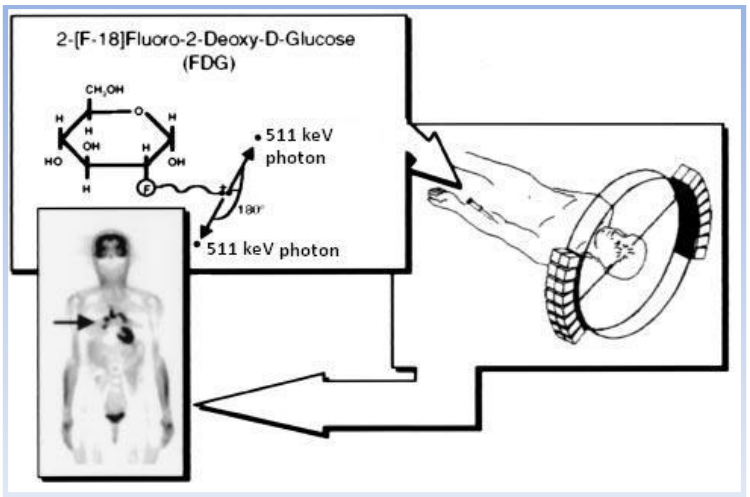


**Figure 7: Principles of FDG-PET. The image shows a patient with metastasis bilaterally to the lung (arrow) (14). The brain and heart shows a normally high uptake and the bladder contains some activity as well.**

The photons are attenuated (i.e. the number of photons emerging from the patient is reduced) as they pass through tissues and interact with the electrons of the tissue. The number of photons emerging from the patient depends on the amount of tissue and its composition (e.g. electron density). Due to the attenuation, measuring the same activity from different angles around the patient will result in a variety of count rates caused only by the density variations between different organs and tissues. As the ideal PET-image should show how and where the activity has accumulated, the effects caused by attenuation must be corrected for.
To correct for the attenuated photons, information about the electron density in the patient is needed. In the early days of PET, an external radiation source – preferably one emitting photons with energies near 511 keV – rotating around the patient was used to measure the attenuation. Today, the attenuation corrections are based on a CT or low-dose CT scan, ideally performed with the patient in the exact same position as in the PET scan. This attenuation correction involves correcting for the much lower photon energies used in a CT-scan (energy scaling). Other corrections of the PET-image, such as scattering corrections, are also often necessary. The scatter correction is one of the main advantages of PET over SPECT, as the technique used in PET gives an improved sensitivity.

## 2.2.2 PET/CT

A major limitation of a PET scan is the lack of anatomical information. To provide an anatomical background, the PET-image is combined with a CT or MRI scan. Without the anatomical data, and due to the inferior spatial resolution of PET images, it can be difficult to determine whether the FDG uptake is due to malignant activity, normal physiological uptake or benign reactions such as inflammatory reactions, post-surgical changes or post-radiation changes (15). A combined PET/CT image provides the means to correlate tumor activity with anatomic features generated by CT. Compared to the individual modalities (CT alone and PET alone), combined PET/CT scans shows a higher sensitivity[1] and accuracy. An advantage of hybrid imaging, compared with PET alone, is the potential of reduced number of suspicious lesions, e.g. lesions difficult to distinctly classify as malignant or benign (15). Reducing these equivocal areas could result in excluding sites of physiological or benign uptake, which would be especially beneficial for pediatric cancer patients.

When clinical PET first became available, the PET and diagnostic CT images were simply displayed side by side and the oncologist could only visually incorporate the PET information when contouring the GTV. This method is however not optimal when the CT contrast between tumor and normal tissues is low. Combining the PET and CT data effectively and displaying the PET information and the CT information simultaneously can nowadays be done in different ways.
One option is to superimpose the nuclear medicine images with CT images, a technique known as image fusion or co-registration. Fusion of two PET/CT scans can be done to view treatment response, but is generally not used for anatomical mapping.
The other option is to use combined PET/CT units, so called hybrids, able to perform both images in one single image session. This minimizes uncertainties due to repositioning of the patient and the time between the two scans.

Whether the combination of anatomical information of a CT scan and the functional information of a PET scan in PET/CT hybrids result in even more precise diagnoses has been debated (16). Nevertheless, the use of these combined scanners is increasing and a large number of studies indicate the advantage of acquiring the two data sets in only one session (17-19).

### 2.2.2.1 PET and PET/CT in oncology

Introducing PET/CT in oncology has led to advancements in the diagnosis, staging and monitoring of therapy response and it has become an important and commonly used diagnostic tool (2).

For a variety of cancer sites, it has been shown that PET has a high sensitivity, specificity[2] and accuracy for detection of tumor involvement (12). Compared to CT alone, including PET gives a more accurate staging of the cancer, with regards to primary tumor as well as lymph nodes and distant metastases. The result of a PET/CT scan may thereby alter the TNM-staging[3] and thus directly influence the treatment management (2, 12, 13, 17-23). For instance, a PET/CT scan may lead to a change in treatment intention from radical to palliative, due to detection of distant metastases or locally advanced tumor not suitable for radical treatment.

There is an increasing use of PET in the management of pediatric cancer patients (2). So far, the value of PET imaging in adult oncology is more thoroughly investigated and evidence-based than PET scanning of pediatric patients (2, 20). However, it appears as though PET imaging is just as accurate for children as for adult patients, for example the number of management alterations for pediatric patients are comparable with data for the adult oncology patients (20). In the case of pediatric sarcoma patients, there also appears to be great potential for using PET/CT in staging and to detect distant metastases as well as local recurrence (24, 25).

[1] High sensitivity means few false negative.
[2] High specificity means few false positive.
[3] The TNM classification is a cancer staging system, where T describes the size of the tumor and if it has invaded nearby tissue, N describes whether any regional lymph nodes are involved and M describes distant metastasis.

### 2.2.2.2 PET and PET/CT in radiation treatment planning

As a PET scan may help to differentiate between tumor and non-malignant tissue, it may influence the delineation of radiation therapy target volumes. Many studies have shown a reduction in the inter- and intra-observer variability when information from a PET scan is available, hopefully resulting in the volumes being more accurately defined (4, 12, 26-28).

Incorporating all available functional and structural imaging into the delineation procedure and combining the information makes it possible to produce a biological target volume (BTV) (19, 29). This concept is based on biological imaging such as PET, but in short, it means integrating all available information about the tumor collected from MRI, CT, US and other techniques still in early development stages.

There are a number of automatic tools for PET-based delineation of target-volumes. For example, isocontouring which can be based on either a standardized uptake (SUV) value, on a fixed threshold of the maximum signal intensity or a threshold adapted to the signal-to-background ratio (30). Thresholding techniques are the most widely used, but more advanced methods based on stochastic models and algorithms recognizing patterns are continuously being improved (31). As the choice of segmentation technique heavily influences both volume and shape of the GTV, and no agreement on a universally acceptable automatic method exists, visual interpretation is still the most commonly used method for PET-based tumor delineation (30-32).

Depending on the tumor type, there seem to be a wide range in the accuracy of PET and it is likely that the role and importance of PET and PET/CT in radiation treatment planning to a great extent may vary with the type of tumor and its location, as well as between pediatric and adult patients (17, 23, 32-35).

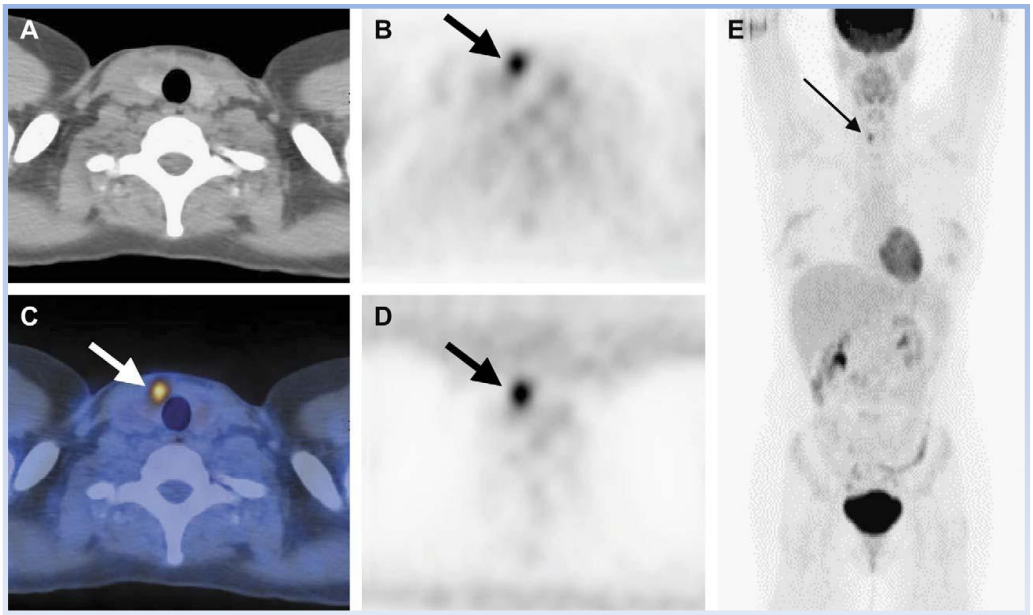


**Figure 8: 18FDG-PET/CT of a patient with a nodule in the right lobe of the thyroid. A) CT scan alone, B) PET scan without attenuation correction, D) PET scan with attenuation correction, C) fused PET/CT and E) whole-body scout. Thyroid nodule is seen in PET and CT scans (arrows). Pathologic examination revealed that this patient had a 1.2-cm papillary cancer (36).**

# 2.3 Normal tissue complications

The long-term effects of the treatment of pediatric malignancies are numerous and include early onset of heart disease, pulmonary fibrosis, endocrine abnormalities, growth impairment, developmental delays, cognitive decline and increased risk of secondary malignancies (1, 2). As childhood cancer survivors presumably have a long life-expectancy, these complications may result in long-lasting compromises of their quality of life. According to estimates done by the Childhood Cancer Group in USA, 73 % of the children surviving cancer will develop one or several chronic physical health conditions. About 40 % will develop a severe, life-threatening or disabling complication or die from a chronic condition (37).

The term radiosensitivity is used to describe the probability of a cell, tissue or organ suffering an effect – damage – per unit dose. This probability is usually higher for highly mitotic (rapidly dividing) and undifferentiated cells. As this is the case with cells in children, they are in general more radiosensitive than adults. For that reason, children are more prone to develop complications, and the risk of many – but not all – normal tissue complications is influenced by the age at irradiation (38).

## 2.3.1 Thorax

### 2.3.1.1 Heart

Radiation therapy, as well as chemotherapy, is known to be cardiotoxic, causing an increased risk of congestive heart failure, myocardial infarction, pericardial disease and valvular abnormalities. Radiation therapy can also contribute to the development of premature coronary artery disease, myocardial fibrosis and dysrhythmias.
In fact, cardiovascular diseases are one of the leading causes of death among childhood cancer survivors (1).

Acute injuries, e.g. pericarditis (inflammation of the heart sac), from radiation therapy are usually transient but can be chronic (39). Acute pericarditis occurring during radiation therapy is relatively rare, whereas delayed pericardial disease is somewhat more common. Delayed pericarditis can occur from months to years after radiation therapy and approximately 20 % develop into chronic conditions.
Late injuries often manifest as congestive heart failure, ischemia, coronary artery disease (CAD) or myocardial infarction. The latency of these late cardiac effects ranges from months to decades.

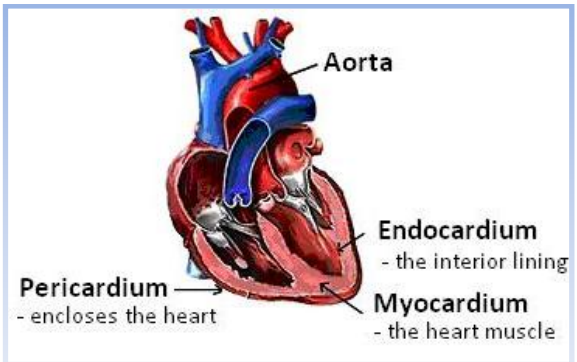


Figure 9: The heart.

Evaluating the dose-response of the heart requires delineating the heart border, which may be difficult to differentiate from liver and diaphragm. The movement of the heart, with the respiratory and cardiac cycles, is however not considered to be an important complicating factor as the degree of movement is quite modest (39).

The risk of cardiac events is probably related to dose as well as the irradiated volume. For example, whole pericardial irradiation leads to a higher rate of pericarditis than irradiation with shielding of the left ventricular and subcarinal areas (39). In adult patients, the risk of pericarditis increases with factors such as a mean pericardium dose above 26 Gy and allowing more than 46 % of the pericardium to receive >30 Gy.

A study on children and adolescents with Hodgkin's disease, all of the excess deaths from heart disease were in patients receiving more than 42 Gy. Another study has found the risk of dying from cardiac disease to be significantly higher in young individuals receiving an average cardiac dose above 5 Gy (40).
For children and adolescents the risk of CAD appears to be much reduced at mean heart doses below 30 Gy (39). For a similar group of patients, a radiation dose above 15 Gy is a significant risk factor for congestive heart failure (1). The corresponding dose for myocardial infarction is 35 Gy.

#### 2.3.1.2 Lungs

When studying dose-response data for pulmonary complications, the lungs are usually considered as one single paired organ rather than two separate (41, 42). A large part of the available data comes from adult patients with breast cancer or lung cancer.

Analyzing the lung dose-response is complicated: since the lung volumes vary with breathing, it is difficult to assess the actual dose they receive. Additionally, there can be uncertainties in the delineation, as the choice of CT-image settings such as contrast and brightness can radically change the lung contours.

The lungs are particularly sensitive to radiation and data for radiation pneumonitis support the notion of a large volume effect (see 2.3.4.2 "The LKB-model"). For adult patients, clinically apparent pneumonitis with cough, fever or dyspnea (shortness of breath) usually only occurs when more than 50 % of the lung receives more than 30 Gy in standard 1.8-2 Gy fractions. The majority of the cases become clinically apparent within ten months of radiation therapy (40, 42). The approximate risk of radiation pneumonitis is about 20 % when the mean lung dose is below 23 Gy, provided that the total lung volume receiving more than 20 Gy is less than 30-35 % (42). However, the dose restrictions vary with factors such as fractionation and whether the malignancy treated is located within the lung.

Pulmonary toxicity is a common long-term complication of cancer therapy in childhood and can vary from subclinical to life threatening (40). The risk is more than three times higher in cancer survivors than in their siblings with symptoms such as abnormal chest wall growth, chronic cough, exercise-induced shortness of breath, lung fibrosis, bronchitis and recurrent pneumonia. It is most commonly seen in senior patients, but pneumonitis as well as pulmonary fibroses has been reported in children, with symptoms beginning to show within three months after completing the radiation therapy (40).

#### 2.3.1.3 Esophagus

Acute esophagitis is a common side effect among patients undergoing radiation therapy for thoracic tumors (43). It occurs during the radiation therapy treatment and often persists for several weeks after the last fraction.

Late injury is less commonly reported, but the risk increases with dose escalation and hypofractionation (43). Examples of late esophageal damage are stricture (narrowing or tightening) and dysphagia (difficulties swallowing). These complications normally develop 3-8 months after the radiation therapy.

Dose-response studies of the esophagus have been performed with regards to either esophageal volume, surface-area or circumference. The circumference of the esophagus varies markedly during swallowing, and it has been debated if conventional dose-volume-histograms are able to accurately reflect the partial doses. Additionally, the esophagus is slightly mobile and the position may vary by up to 9 mm in an adult patient (43).

For adult patients, the volumes receiving more than 40-50 Gy correlate significantly with acute esophagitis and it is advised to keep the mean dose to the esophagus below 34 Gy (43).

## 2.3.2 Abdomen & Pelvis

The use of new techniques, such as IMRT, has led to changes in the clinical manifestations of normal tissue morbidity and this might be most apparent among patients receiving abdominal irradiation. For example, severe structural effects, like fistulas or ulcerations, are nowadays rare and instead changes in the organ function have become more common (8).

Manifestations of gastrointestinal toxicity include vomiting, abdominal pain, diarrhea and bleeding. Abdominally irradiated children may develop intolerance to fat, milk, gluten and fiber-containing food – complications that in turn may lead to growth and weight deficits (44).

Childhood cancer survivors treated with abdominal irradiation also have an increased risk of diabetes mellitus, that appears to be unrelated to their body mass index or physical (in)activity (45). However, the underlying mechanisms are several and complicated. For example, it remains unclear whether the most important factor is irradiation of the pancreas or irradiation of adipose tissue.

Radiation therapy to the pelvic area may also result in genitourinary complications. Acute side effects occurring during the course of treatment usually resolve within a few months (46, 47). Long-term symptoms of radiation-induced side effects are dysuria (discomfort or pain while urinating), reduced flow, incontinence and changed frequency or urgency of bladder voiding. Grading of toxicities is difficult and some symptoms attributable to the bladder may actually be caused by the urethra.

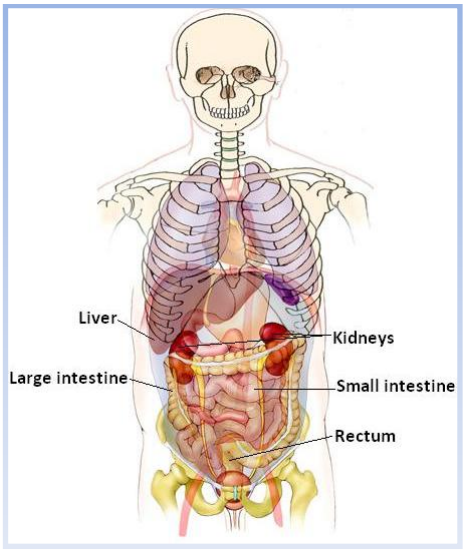


**Figure 10: Basic anatomy of the abdomen and pelvis.**

### 2.3.2.1 Kidneys

The kidneys are vitally important organs, for example responsible for filtering the blood from waste metabolites and electrolytes, stimulating the production of red blood cells and modulating the blood pressure. This makes them the dose-limiting organs for radiation therapy to a large number of cancer diagnoses.

The observed effects of irradiation on renal function depend on total renal dose, irradiated renal volume and whether only one or both of the kidneys have been irradiated (uni- or bilateral kidney irradiation) (44).

Radiation nephritis can be evaluated clinically, i.e. from observations, or subclinically, by measuring the renal clearance (glomerular filtration rate, GFR). Subclinical renal impairment has been observed in patients receiving 20 Gy to both kidneys in combination with a dose above 30 Gy to the upper half of one kidney (44). Acute kidney injury, occurring within 3-18 months, is generally subclinical (48).

Late renal dysfunction is assumed to be mainly attributable to radiation nephropathy and occurs after more than 1.5 years. These chronic injuries are characterized by an increase of serum creatinine, proteinuria (excess of proteins in the urine), anaemia, malignant hypertension (high blood pressure) and renal failure (48, 49).

The long latency of radiation therapy-associated kidney injury, as well has the high prevalence of confounding factors such as chemotherapy, smoking, diabetes, heart disease etc., makes it difficult to estimate the incidence as well as the effects of partial kidney irradiation (48). Additionally, assessments of the actual dose to the kidney are further complicated by the kidney breathing motion and change of shape as well as shifts in kidney position.

Radiation nephropathy is a well-known phenomenon, however for pediatric patients most thoroughly studied for patients undergoing total body irradiation (TBI). These patients have a considerably lower tolerance dose as their renal function often is compromised by other potential nephrotoxic agents in their therapy, preparing them for bone-marrow transplantation (50).
In general, radiation-induced impairment of the kidney function in children is considered to be rare. For children above the age of five, there is no evidence that the kidney tolerance differs from that of adults (48).

Late renal sequelae have been reported in pediatric patients receiving higher doses to both kidneys: bilateral kidney doses below 10-12 Gy do not seem to induce kidney failure in children. For children having undergone nephrectomy, the incidence of reduced creatinine clearance is higher when the remaining kidney receives more than 12 Gy (44). For nephrectomized patients, no cases of renal failure have been reported for kidney doses below 23 Gy (44).

#### 2.3.2.2 Liver

Radiation-induced liver disease (RILD) is the most common liver toxicity after radiation therapy (51). The syndrome includes hepatomegaly (enlargement of the liver), ascites (fluid accumulation) and elevated liver enzymes and the symptoms typically occur between two weeks and three months after completion of the radiation therapy. Pathologically, radiation can cause venous congestion, followed by atrophy adjacent to the congested veins. Some cases of RILD are transient and the patients can recover within a few months, but persistent liver complications can lead to liver failure, a fatal condition that often requires transplantation (44, 51, 52).

RILD in adult patients is a well-known and well-studied phenomenon, is usually evaluated paraclinically with liver function tests, hematological analysis or liver scanning.

Most available dose-response data come from adult patients with malignancies in the liver, either primary tumors or metastases, making it difficult to estimate the corresponding model for patients with healthy livers.
In the adult patient, the whole-liver tolerance to radiation therapy is low: there is an estimated 5 % risk of RILD after whole-liver doses of 30-35 Gy delivered in 2 Gy per fraction (51).

The degree of hepatic damage is strongly related to the liver volume irradiated and the dose delivered. Due to the strong volume-effect of RILD, the mean liver dose may be useful when ranking radiation plans (53). The mean liver dose associated with 5 % risk of RILD appears to be slightly above 30 Gy, and for a mean liver dose of about 40 Gy the estimated risk is about 50 %.
The partial-volume tolerance of the liver shows a strong dependence on the liver function status pre-irradiation (51, 52). Apart from having a different dose-volume relationship for RILD, patients with abnormal liver function, such as cirrhosis or hepatitis are at risk of developing other types of radiation toxicities. The partial-volume tolerance also depends on whether the patient is treated for primary liver malignancies or liver metastases (53).

Despite the lower number of studies based on pediatric patients, several reports confirm a similar dose-effect as well as a volume-effect for this patient group (44). In children and adolescents, radiation doses below 20 Gy to the majority of the liver or higher doses to smaller parts seem to be safe (44).

#### 2.3.2.3 Small intestine

The small intestine is one of the most radiosensitive organs of the digestive system and thus one of the critical organs at risk for abdominal irradiation (8). In adults, the small intestine is about 7 m long and it has a large surface area. It is often incidentally irradiated during radiation therapy of tumors in the upper gastroinstestinal tract, inferior lung or pelvis.

Studies on radiation therapy side effects of the bowel generally focus on acute toxicities, e.g. nausea and vomiting that can occur within hours after radiation therapy to the small bowel (54). Days to weeks after radiation, acute therapy-induced injuries range from transient mucosal inflammations to severe bleeding. Another potential early effect in the irradiated small intestine is epithelial destruction, which later can be accompanied by submucosal changes, vasodilatation (increased diameter of the blood vessels) and edema (8). Eventually, these fibrotic changes in the mucosa can lead to vascular occlusion, but these changes are rare in the small intestine. The duration and severity of the early effects seem to have a large impact on the risk of developing late and long-lasting changes.

Late complications can manifest within weeks or months after radiation therapy, for example as obstructions caused by radiation-induced fibrosis (which limits the mobility of the bowel) (54). Chronic symptoms of post-radiation therapy injury may include long-term dyspepsia (e.g. heartburn and regurgitation), ulceration, fistula and perforation. The majority of symptoms occur within three years, but the patients remain at risk indefinitely.

The early as well as the late mucosal changes result in an impairment of the digestive and absorptive functions of the intestine, manifested as acute or chronic diarrhea. Studies indicate a strong correlation between the irradiated small bowel volume and the occurrence of diarrhea and other acute toxicities (55, 56). There seems to be no such volume effect for irradiation of the large bowel (colon) (55).

Whether any threshold of irradiated small bowel volume exists, below which no toxicity can be seen, is unclear and depends on the severity of the studied endpoint (complication) (54, 57). Some data suggest that the maximum point dose might be an important predictor of toxicity, while most studies emphasizes the relationship between reduced irradiated small bowel volume and decreased toxicity incidence as well as grade (54, 58). For adult patients, the small bowel volume receiving at least 15 Gy seem to be correlated with the degree of toxicity (56). Published dose-volume constraints show large variations, partly because the volume of the small bowel depends on how detailed the structure delineation has been. If individual bowel loops are outlined, the volume receiving 15 Gy or more should be kept below 120 $cm^3$ (54).

#### 2.3.2.4 Rectum

Late rectal bleeding is an important consideration, or even a dose-limiting endpoint, when planning radiation therapy to the pelvis (59). The incidence of late rectal sequelae is strongly correlated with the absorbed dose (60, 61). Apart from rectal bleeding, fibrotic changes in the submucosa that may cause vascular occlusions are frequently observed (8).

Acute rectal effects occur during or shortly after radiation therapy and usually include changed bowel habits, pain, diarrhea or superficial ulceration with bleedings (61). These signs of early responding damage are probably a good indicator for the risk of late rectal damage, usually clinically manifest within three to four years, as some of the late complications are a direct consequence of the early damage (59, 61).
Symptoms of rectal toxicity may for example include fecal incontinence, bowel urgency, stool frequency and rectal bleeding, however – because of its objectivity – the last-mentioned is the most commonly studied (61).
Late rectal bleeding does usually not require medical management, although in rare situations antibiotics and coagulative therapies may be necessary.

Inter-and intra-fractionation variations in rectal filling, intestinal gas and bladder filling change the position of the rectum and makes it difficult to assess the actual rectal dose. Some published data suggests that the relative rectal volume has a stronger correlation with the risk of developing late rectal toxicity, rather than the absolute volume (60, 62). For adult (male) patients, the percentage of rectal volume irradiated to 60 Gy should be limited to below 40 %.

## 2.3.3 Head and neck

The group of patients with tumors in the head and neck may be the one benefiting most from the new treatment techniques as they may enable treatment in traditionally treatment limited situations (due to high risks of complications and unacceptable toxicities). Modern radiation therapy of tumors in the upper aero-digestive tract often provides the ability to preserve sensitive tissues and areas, such as the larynx. However, radiation-induced laryngeal edema, due to inflammation and lymphatic disruption, is a common side effect (63). Progressive edema and associated fibrosis can lead to long-term problems with phonation and swallowing.

### 2.3.3.1 Parotid glands

In normal physiological conditions, the daily saliva production ranges between 0.5 and 1.0 liters. Without stimulation, about two-thirds of the whole saliva volume is produces by the submandibular glands (64). Depending on the type of stimulus, the parotid glands account for at least half of the saliva produced. The sublingual glands only contribute with a few percent to the saliva production.
Saliva is important for the oral health and function, both by its fluid characteristics and its specific components. Cancer patients receiving radiation therapy to the head and neck region often experience reduced salivary production (xerostomia) with severe dry mouth symptoms manifesting as impaired taste perception, difficulties swallowing, eating and speaking as well as deteriorating oral health (64, 65).

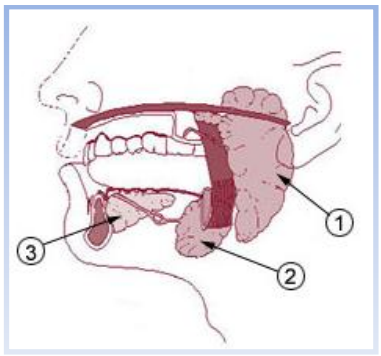


**Figure 11: The salivary glands: 1) Parotid gland, 2) Submandibular gland and 3) Sublingual gland.**

Data for radiation-induced xerostomia, defined as a 25 % reduction in the salivary flow, indicate a large volume effect and that the mean dose to the parotid gland is a useful parameter (41, 66). In general, the parotid glands are analyzed as separate organs when investigating the dose-response, based on indications that the glands respond independently (67). Most studies conclude that there is no threshold dose; however there seem to be less consensus on the $TD_{50}$ (see 2.3.4.2 “The LKB-model”), with reported values varying between 28 Gy and 40 Gy.

The literature on xerostomia in pediatric cancer populations is sparse and the recommended dose-limits mentioned below come from adult patient data. At a mean dose of less than 10-15 Gy, there seem to be a minimal gland function reduction, which then gradually increases with doses up to about 40 Gy (67). The reported $TD_{50}$ increases with longer follow-up times – indicating that there is some recovery of function and reversibility of injury. Severe long-term xerostomia (salivary function <25 % of baseline) is usually avoided if the mean dose to at least one of the parotid glands can be kept below 20 Gy or if the mean dose to both glands is less than 25 Gy (67). Even for relatively low mean doses (<10 Gy) a reduced mean dose to the parotid gland usually results in better function. Similarly, if the mean dose cannot be kept below 25 Gy, there can be a lot to gain from keeping the dose as low as possible.

The pathophysiology behind reduced salivary production is complex. Traditionally, the parotid glands have been the main focus in dose-sparing studies, but it has been suggested that the submandibular as well as the minor salivary glands should be regarded as equally important (5). Within the parotid gland, there may be variations in radiosensitivity and areas where dose-sparing would have a greater impact on the risk of hypofunction (67). This data is rather new, and may to some extend contradict the dose-response levels mentioned above.

### 2.3.3.2 Thyroid gland

Thyroid dysfunction is a common late effect after irradiation of the thyroid gland. The dysfunction may be manifested as hypothyroidism (reduced function of the thyroid), goiter or nodules (38). Transient thyrotoxicosis and thyroid cancer have also been reported (68).

The most frequently reported radiation-induced abnormalities are elevated levels of TSH (thyroid-stimulating hormone), depressed production of T4 (thyroxine) or both (38). High levels of TSH and low levels of T4 is an indication of clinically apparent hypothyroidism, whereas high TSH and normal T4 indicate subclinical hypothyroidism. The symptoms of hypothyroidism can be very unspecific and obscure; often including fatigue, edema, dry skin, depression and/or myalgia (muscle pains.

Among children treated with radiation therapy for Hodgkin's disease, most hypothyroidism cases develop within two to five years post-treatment (median: six years) (68). The actuarial risk of developing hypothyroidism within eleven years after radiation therapy is estimated to be 74 % for a mean thyroid dose above 45 Gy, 65 % for a mean thyroid dose between 30 and 45 Gy, 54 % for thyroid dose < 30 Gy and about 8 % for pediatric patients who do not undergo irradiation of the thyroid gland.
The risk of hypothyroidism among childhood medulloblastoma patients seem to decrease when the dose per fraction is reduced and the number of fractions increased (hyperfractionation) (69).

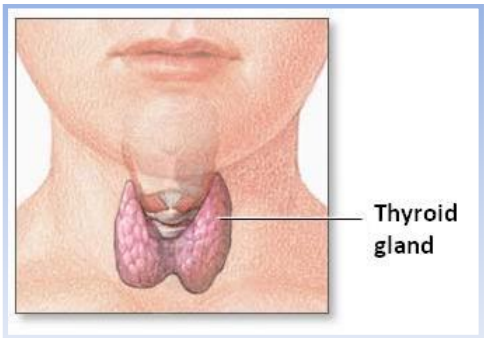


Figure 12: The thyroid gland.


Figure 13: The lacrimal gland.

### 2.3.3.3 Eye

Irradiation of the eyes may cause visual impairment, such as cataract, double vision or blindness (70). The time between treatment and the manifestation of the symptoms can be more than five years.

Cataract formation is one of the most commonly reported late effects following Total Body Irradiation (TBI), with a rather distinct threshold-dose at a biologically effective dose (BED[4]) of 40 Gy (71). However, as TBI-patients often undergo a tough and complicated multimodality treatment regime, with many factors influencing the probability of normal tissue complications, it is difficult to extrapolate dose-effect relationships based on TBI-data to other groups of patients.

The association between radiation dose to the eye and the risk of blindness has been shown to be significant, especially for doses greater than 0.5 Gy (70). Radiation to the posterior fossa[5] or temporal lobe also increases the risk of inducing blindness in one or both eyes.

Another common side effect among patients receiving radiation to the eyes is dry eye syndrome (DES). This complication can be very painful and is mainly caused by irradiation of the main tear secretor of the eye: the lacrimal gland. The lacrimal gland is particular important to the production of the layer of the tear film lubricating the eyes.

[4] BED is an approximate quantity, formulated in various ways with various complexity. In short, calculating the BED allows for comparisons between the biological effect of different fractionation regimes. Some information about the cell kill per Gy and $Gy^2$ is necessary.
[5] The posterior fossa is a region near the base of the skull, close to the brainstem and the cerebellum.

The lacrimal dose distribution and the median dose to the lacrimal gland are factors related to reduced tear production as well as DES (72, 73). A clear dose-volume relationship with regards to the appearance of DES has been reported: a mean dose of 6 Gy per fraction as well as a median dose of 7 Gy per fraction is likely to cause reduced tear production in 50 % of the patients. A mean dose of 8 Gy per fraction and a median dose of 10 Gy per fraction is associated with a 50 % probability of DES.

#### 2.3.3.4 Ear (cochlea)

Radiation therapy may cause damage to the cochlea or the acoustic nerve, which in turn may lead to sensorineural hearing loss, SNHL. Changes in hearing manifesting early on, sometimes during the radiation therapy, can be reversible whereas permanent hearing loss usually appears later and increases with time (74). Persistent hearing impairment can occur as early as three months after the last treatment fraction, although the median latency is two years according to some studies and most common within 3-5 years in others (74, 75). The early occurring and transient hearing impairment is often a conductive hearing loss, whereas the permanent SNHL is caused by irreversible damage to the outer or inner sensory cells in the cochlea (75).
Damage to the hearing apparatus and hearing loss caused by radiation therapy is sometimes referred to as ototoxicity.

The incidence of SNHL depends on factors such as the frequencies studied and the control used for comparison. It is however clear that radiation-induced hearing loss is first and most noticeable in the higher frequencies (74, 76). Although different structures within the cochlea have varying radiosensitivity, the cochlea is usually regarded as a whole organ for dose-response analysis. The small volume of the cochlea as well as the limitations and uncertainties associated with its delineation, makes it difficult to perform a more detailed analysis. For pediatric patients treated without ototoxic chemotherapy, it is recommended to keep the cumulative cochlear dose below 30-35 Gy in order to minimize the risk of hearing loss (75).

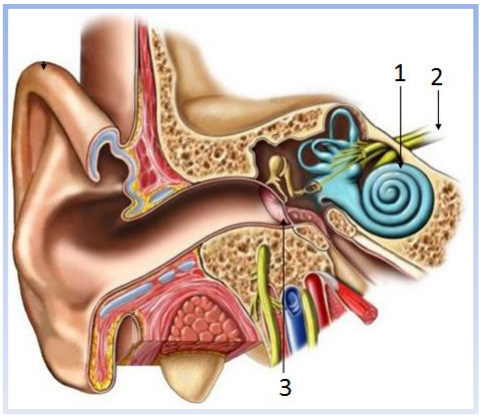


**Figure 14: Parts of the anatomy of the hearing apparatus.
1. Cochlea, 2. Hearing nerve and 3. Eardrum.**

## 2.3.4 NTCP-models

Efforts to describe the normal tissue reactions to radiation and estimate the normal tissue complication probability (NTCP) have been done for several decades. The main purpose of NTCP-models is to balance the need of delivering high dose to the target volume against the risk of causing unacceptable complications in the organs at risk (OARs).

The biological processes of radiation-induced effects are complex and yet not fully understood. Research on radiobiological mechanisms at cellular level is still focused on in vitro experiments with isolated cells and tissues. However, this initial damage is only one small factor for the clinical outcome, which for example also depends on the cellular environment, the structural design of the tissue and the general health of the organ as well as the entire organism.

Most models are based on the assumption that all radiation effects are local effects, i.e. that the tissue reaction depend on the dose to that tissue alone. Non-local effects, such as tissue repair, compensatory mechanisms, functional dependence (e.g. between heart and lung) and compensation between organs (e.g. salivary glands and swallowing structures) are either not enough studied, too complicated or too individual to be included in the model (77).

The models can be of phenomenological nature, based on empirical observations, derived from experiments in vitro or based on theoretical concepts. The fitted mathematical model depends on the particular data set, treatment protocol, choice of endpoints, delineation of organs (77).
As a result, the modeling of risks of normal tissue complications is associated with large uncertainties. Attempting to describe complex biological processes such as the dose-dependence of a particular complication with a mathematical function is bound to include over-simplifications. This gives the existing NTCP-models a limited value for the individual patient and the models are rarely adopted in clinical practice (77). However, the NTCP-models can be a useful tool when comparing different fractionation regimes and developing new fractionation schemes. So, while a certain degree of reservation for NTCP models is legitimate, they can potentially be very useful as more is learned about the underlying biological mechanisms and the predictive power of the models are improved.

When looking at dose-response curves for various complications, it is important to keep in mind that the curves do not show increase in severity of the complication as a function of dose, but how changes in dose affects the estimated incidence of the specific side effect.

The following sections describe the three NTCP-models used in this thesis.

### 2.3.4.1 The linear model

A linear dose-response model describes the normal tissue complication probability (NTCP) as a function of the dose, usually the mean dose, with the equation for a straight line:

$$NTCP = (k \cdot Dose) + m$$

where

k = the slope of the line
m = the intersection of the straight line and the y-axis

### 2.3.4.2 The LKB-model

The Lyman-Kutcher-Burman-model (LKB-model) requires three parameters, $TD_{50}$, m and n, to describe the dose-dependency of the complication.

- $TD_{50}$ is the uniform tolerance dose, i.e. the dose causing a known endpoint to 50 % of the population following whole organ irradiation.
- The parameter m describes the slope of the dose-response curve.
- The parameter n accounts for the volume effect, i.e. the volume dependence of the organ.

- For large values of n, e.g. around 1.0, the organ responds as a parallel structure, where the volume receiving a certain dose is of greatest importance, i.e. there is a large volume effect. An organ responding as a parallel structure is the liver, which can tolerate rather high doses to limited parts of the organ.
- For values of n close to 0, the organ responds as a serial structure where the maximum dose needs to be limited. An organ that traditionally has been regarded as a very serial organ is the medulla, where the maximum dose must be limited, regardless of the volume receiving this dose.
- If n = 1, the model is usually referred to as the mean dose model.

In this model, the probability of normal tissue complication from a dose D is estimated according to:

$$NTCP = \frac{1}{\sqrt{2\pi}} \int_{-\infty}^{t} e^{-\frac{x^2}{2}} dx$$

where

$$t = \frac{(D - TD_{50})}{(m \cdot TD_{50})}$$

For uniform irradiation, Lyman (78) calculated the tolerance dose for each small part *v* of the organ and accounted for the volume effect:

$$TD_{50}(v) = TD_{50} \cdot v^{-n}$$

Kutcher and Burman adapted the Lyman model and made it applicable to non-uniform irradiation of organs (79). They developed a so-called DVH-reducing algorithm, which calculates a partial effective volume, $v_{s,eff}$. Irradiating this volume with a certain dose $d_{ref}$ causes the same NTCP as irradiating the fractional volume $v_s$ with the dose $d_s$. Based on this, a total effective volume $v_{eff}$ can be calculated. Irradiating $v_{eff}$ with $d_{ref}$ gives the same NTCP as the inhomogenous dose-distribution described by the DVH. In other words:

1. For each irradiated sub-volume $v_s$ receiving the absorbed dose $d_s$, there is a corresponding partial effective volume, $v_{s,eff}$:

$$v_{s,eff} = v_s \cdot \left(\frac{d_s}{d_{ref}}\right)^{1/n}$$

   The parameter $d_{ref}$ is usually the maximum dose in the DVH.

2. Irradiating the partial effective volume $v_{s,eff}$ to the absorbed dose $d_{ref}$ yields the same NTCP as irradiating the sub-volume $v_s$ to the dose $d_s$ (provided that $v_{s,eff}$ and $v_s$ have the same volume-dependence, n).

To estimate the NTCP for the entire inhomogeneously irradiated organ, the total effective volume $v_{eff}$ is calculated as the sum of all partial effective volumes $v_{s,eff}$:

$$v_{eff} = \sum_{s=1}^{k} v_{s,eff} = \sum_{s=1}^{k} v_s \cdot \left(\frac{d_s}{d_{ref}}\right)^{1/n}$$

The NTCP for non-uniform irradiation can then be calculated from a DVH with the first formula in this section, with:

$$t = \frac{\left(d_{ref} - TD_{50}\left(v_{eff}\right)\right)}{\left(m \cdot TD_{50}\left(v_{eff}\right)\right)}$$

$$TD_{50}\left(v_{eff}\right) = TD_{50} \cdot {v_{eff}}^{-n}$$

The assumption that a certain dose, when given uniformly to the whole organ, will yield the same NTCP as the inhomogeneous dose distribution in the DVH can be explained by the concept of equivalent uniform dose, EUD

(80). The concept was developed to take into account the inhomogeneity of clinical dose distributions when estimating tumor control probability (TCP). Since the dose distribution is far from uniform in the OARs surrounding the target volume, this concept is useful for estimations of NTCP as well.

The formulation of EUD is based on the following assumptions:

- An irradiated tumor is composed of a large number of independent clonogens[6] (any by-stander effects are omitted).
- Random killing of clonogens is well described by Poisson statistics
- The control or failure to kill an irradiated tumor is determined by the expected number of surviving clonogens (the surviving fraction, SF).
- Two different tumor dose distributions are equivalent if the corresponding SFs are equal.

The most basic formulation of EUD describing TCP is based on the SF for a standard regimen, with the reference dose, $D_{ref}$, of 2 Gy. The formulation can then be expanded to include more details and radiobiological concepts such as non-homogenous distribution of clonogens and proliferation.

Expressing EUD with the variables used in the LKB-model results in the formula below (81):

$$EUD = \left( \sum_{s=1}^{k} v_s \cdot {d_s}^{1/n} \right)^n$$

### 2.3.4.3 The logistic model

A logistic dose-response model describes the NTCP as a function of dose with the formula below:

$$NTCP = \frac{1}{1 + e^{4\gamma_{50}\left(1 - {D}/{TD_{50}}\right)}}$$

where

$TD_{50}$ is the same parameter as in the LKB-model and
$\gamma_{50}$ represents the increase in response at the 50 % dose-response level per 1 % increase in dose.

[6] Tumor cells able to grow and divide (proliferate).

## 2.4 Secondary cancers

With the increasing number of long-time cancer survivors, resulting from improvements in cancer therapy, the issue of therapy-induced secondary malignancies has become increasingly important. The definition of what is meant by a secondary cancer may vary, but the term usually refers to a tumor of new histological type in, or very near, the radiation field appearing about ten years or more after a course of radiation therapy (82).

Ionizing radiation used in radiation therapy is a known mutagen and carcinogen. Regardless of what dose-response function is used to describe the risk, cancer induction is a stochastic process and doses below 6 Gy are known to be sufficient to cause secondary neoplasms in adults (83). As the increased risk is present even at doses below 1 Gy (84), the dose-distributions associated with modern dose-delivery techniques are likely to have an impact on secondary cancer incidence.

The estimated increase in cancer incidence per Gy varies between different types of cancers as well as organs: (female) breast-tissue, bone marrow and thyroid are known to be especially sensitive to radiation and thus prone to develop radiation therapy-induced tumors. Sarcoma, mesothelioma, leukemia and bone cancers have also been reported as secondary cancers (40, 82).

Radiation-induced solid tumors often have a latency period of about ten years or more, while leukemia (one of the most prominent radiogenic cancers) is thought to have a shorter latency time. As secondary cancers need a long time to develop, this is a great concern in childhood cancer patients since many of them will live a long time after being cured of their primary disease.

The risk of secondary malignancies depend on physical and biological variables such as dose, fractionation, size and radioresistancy of the irradiated tissue volume, but one of the most important factors is the age of the irradiated individual (82, 85). Thus, while the number of pediatric cancer patients continues to be rather low, the risk of therapy-induced secondary malignancies is larger among the younger patients.

Extrapolating data from atomic bomb survivors show that the increase of risk is about one order of magnitude greater than that of adults (2). Some age-related models of radiation carcinogenesis estimate that the secondary cancer risk of irradiating a 5-10 years old is at least five to ten times greater compared to a 50-year-old receiving the same dose (86).

Just as for NTCP, a number of models have been proposed for estimating the risk of developing secondary malignancies subsequent to radiation therapy (87). Traditionally, most dose-effect curves for secondary cancers are based on data from the atomic bomb survivors. For radiation doses above one or two Gy, these models are gradually being replaced, or complemented, by dose-response estimations from large clinical series, such as data from Hodgkin's lymphoma patients (88). However, it is still debated which dose-response relationship – e.g. linear, bell-shaped, plateau-shaped, logistic – best describes the risk of secondary cancers induced by fractionated radiation therapy in different organs (89).

# 3. Methodology

## 3.1 Target volumes

### 3.1.1 Delineation

The target volumes were delineated by experienced senior physicians according to the clinical routine at Rigshospitalet.

The PET positive area (the "PET-GTV") was delineated by a physician specialized in nuclear medicine. While delineating, the physician was able to collaborate with any of the radiologists in the clinic. No automatic segmentation technique was used.

The GTV was delineated by a radiologist. As in the clinical situation, the physician could use information from the patient journal (with results from other examinations, e.g. MRI, US or palpation) as well as consulting other doctors.

The CTV was delineated by a specialist in radiation oncology. In general, a margin of 1 cm was added to the GTV and adjusted to fit anatomical structures. However, when necessary the margin was extended to ensure that areas with potential sub-clinical disease were accurately covered, according to the definition of CTV found in ICRU reports number 50 and 62. The CTV was delineated as of the CWS 2002 protocol "Guidelines for Soft Tissue Sarcoma" for the sarcoma as well as for the head and neck cancer patients.

The PTV was delineated by the treatment planner.

### 3.1.2 CTV to PTV margins

Two methods were used to evaluate the appropriate CTV margins for this project.

First, a study of recently published literature regarding set-up uncertainties was performed. A summary of the literature is given in Table 1.

Second, the verification images (CBCT or EPID) of the patients in this study were reviewed:
There are a number of ways to estimate the CTV to PTV margin. ICRU Report 62 suggests the following formula:

$$\sqrt{\Sigma^2 + \sigma^2}$$

$\Sigma$ = the SD of systematic errors
$\sigma$ = the SD of random errors

One of the most accepted methods is the formula below, by Marcel van Herk (90, 91):

$$2{,}5\Sigma + 0{,}7\sigma$$

$\Sigma$ = the SD of systematic errors
$\sigma$ = the SD of random errors

The van Herk formula is derived to include all sources of uncertainty. van Herk defines $\sum$ as the combined standard deviation (SD) of preparation errors (e.g. systematic errors): $\sum^2 = \sum^2_s + \sum^2_m + \sum^2_d$ with $\sum^2_s$ = standard error of set-up, $\sum^2_m$ = standard error of organ motion and $\sum^2_d$ = standard error of delineation.
The σ, the total SD of treatment execution (e.g. random variations) is defined in a similar way: $\sigma^2 = \sigma^2_s + \sigma^2_m + \sigma^2_p$ with $\sigma^2_s$ = random error of set- up, $\sigma^2_m$ = random error of organ motion and $\sigma^2_p$ = standard error of penumbra width.

| | Formula to calculate margins | Pediatric patients | Number of patients | Image modality | | | | | |
|---|---|---|---|---|---|---|---|---|---|
| **Eldebawy et al (92)** | 1 | Yes | 48 | EPID | | **H&N** | **Chest** | **Abdominal and pelvis** | **All patients** |
| | | | | | **Long** | 4.5 mm | 7.5 mm | 5.5 mm | 5.5 mm |
| | | | | | **Lat** | 4.0 mm | 5.5 mm | 4.5 mm | 4.5 mm |
| | | | | | **Vert** | 5.5 mm | 4.5 mm | 7.5 mm | 5.5 mm |
| **Zaghloul et al (93)** | 1 | Yes | 72 | MV-CBCT | | **H&N EPID/CBCT** | | **Not H&N EPID/CBCT** | |
| | | | | | **Long** | 4.6 mm / 3.6 mm | | 6.7 mm / 6.5 mm | |
| | | | | | **Lat** | 3.5 mm / 3.8 mm | | 4.9 mm / 4.1 mm | |
| | | | | | **Vert** | 4.3 mm / 4.6 mm | | 5.7 mm / 5.8 mm | |
| **Li et al (94)** | 2 | No | 152 | MV-CBCT | | **H&N** | **Chest** | **Abdomen** | **Pelvis** |
| | | | | | | 5.6 mm | 8.0 mm | 8.1 mm | 8.3 mm |
| **Gupta et al (95)** | 1,2,3 | No | 25 | EPID | | **H&N[1]** | **H&N[2]** | **H&N[3]** | |
| | | | | | **AP** | 3.76 mm | 3.28 mm | 2.16 mm | |
| | | | | | **ML** | 3.83 mm | 3.34 mm | 2.20 mm | |
| | | | | | **SI** | 4.74 mm | 4.14 mm | 3.76 mm | |

[1] Margins calculated as 2,5∑ + 0,7σ (formula by van Herk). [2] Margins calculated as 2∑ + 0,7σ (formula by Stroom et al).
[3] Margins calculated as $(\sum^2 + \sigma^2)^{0,5}$ (formula in ICRU Report 62). AP = anterio-posterior, ML = medio-lateral and SI = supero-inferior.

**Table 1: Summary of publications on the topic CTV to PTV margins.**

Set-up data and verification images of the patients in this study were found in clinical records. The systematic as well as the random errors in set-up were evaluated and the standard deviations were calculated according to van Herk's descriptions (91). Despite the various anatomic locations of the tumors (see Table 9) the figures presented below are based on data from all patients and represent average values.

The calculations of the standard deviations can be made in different ways. One alternative is to include the set-up information from all verification images, another alternative is to only use information from the first three days of treatment and a third option is to use information from verification images taken once a week.
The first or the third method is often used to estimate σ, whereas the second method often is used to calculate ∑.

The calculated CTV to PTV margins listed in table Table 2 below are those that would be required if no verification images were to be taken:

| | AP (vertical) | ML (lateral) | SI (longitudinal) |
|---|---|---|---|
| ∑ | 2.9 mm | 1.1 mm | 2.6 mm |
| σ | 2.2 mm | 1.8 mm | 2.3 mm |
| ICRU 62 $\sqrt{\Sigma^2 + \sigma^2}$ | 3.6 mm | 2.1 mm | 3.5 mm |
| van Herk $2{,}5\Sigma + 0{,}7\sigma$ | 8.8 mm | 4.0 mm | 8.1 mm |

**Table 2: CTV to PTV margins required if no verification images are taken.**

If verification images are taken, one may choose to apply a so called NAL, No Action Limit. Set-up deviations smaller than the selected NAL-value will not warrant any repositioning of the patient on the treatment table. Assuming a clinical NAL of 3 mm regardless of the anatomical area of the tumor, all set-up deviations below 3 mm can be omitted from the calculations. This alters the margins slightly:

| | AP (vertical) | ML (lateral) | SI (longitudinal) |
|---|---|---|---|
| van Herk $2.5\Sigma + 0.7\sigma$ | 4.6 mm | 4.0 mm | 3.0 mm |

**Table 3: CTV to PTV margins with NAL of 3,0 mm.**

Using only the first three days to calculate the systematic error results in a small decrease of ∑ in two directions, compared to those listed in Table 2, and thereby in the CTV to PTV margin as well:

| | AP (vertical) | ML (lateral) | SI (longitudinal) |
|---|---|---|---|
| ∑ | 2.4 mm | 0.9 mm | 2.6 mm |
| σ | 2.2 mm | 1.8 mm | 2.3 mm |
| van Herk $2.5\Sigma + 0.7\sigma$ | 7.6 mm | 3.6 mm | 8.1 mm |

**Table 4: CTV to PTV margins required if no verification images are taken. ∑ derived from the first three days only.**

Combining NAL of 3 mm with ∑ from the initial three treatment verifications:

| | AP (vert) | ML (lat) | SI (long) |
|---|---|---|---|
| van Herk $2.5\Sigma + 0.7\sigma$ | 3.8 mm | 3.6 mm | 5.5 mm |

**Table 5: CTV to PTV margins with NAL of 3.0 mm. ∑ derived from the first three days only.**

It must be emphasized that the calculated SD:s of the systematic and random errors in this study only include the set-up errors. The verification images merely give information about $\sum^2_s$ and $\sigma^2_s$. The margins do not include any other uncertainties, such as delineation variations, e.g. $\sum^2_m$, $\sum^2_d$, $\sigma^2_m$ and $\sigma^2_p$ are assumed to be zero. This will lead to an underestimation of $\sum$ and $\sigma$.
The calculated margins are crude and suffer from large uncertainties. They are based on a limited number of patients and on verification images with various treatment areas and images from both EPID and CBCT have been used.
The reviewed articles as well as these simple calculations imply that a margin of about 10 mm will be acceptable.

A majority of the patients in this study have been diagnosed with sarcoma. Hence, the recommendations in CWS 2002 protocol influenced the final choice of CTV to PTV margins. The CWS recommend adding 5-10 mm to the CTV when defining the PTV, and this – combined with the shallow study and literature – led to the decision of using a CTV to PTV margin of 6 mm.

One may argue that the chosen margin is too small for treatment areas in the abdomen or pelvis. However, assuming daily verification imaging, this margin might very well be sufficient for abdomino-pelvic radiation therapy, especially in small children. For the head and neck area, this margin is likely to be more than enough.

The same margin was used in every direction and on all patients, regardless of the anatomical location of the CTV or the immobilization device used for the patient. Young patients are often treated under general anesthesia and generally, this reduces the set-up uncertainties and the required margins (96). This factor was omitted when selecting the margin.

The same CTV to PTV margins were used for the proton therapy as for the photon modalities. Whether this approach is correct can be debated. For proton therapy, it has been proposed that a smaller margin can be used in the direction of the incident beam (97). Also, the use of a CTV to PTV margin may depend on the number of fields as well as the steepness of the in-field dose gradients (98, 99). It may also differ between static beam techniques and scanning proton beams (100). The number of incident beams and the field configuration may also affect the margin width required for photon therapy such as IMRT (101).

### 3.1.3 Skeletal growth retardation

Irradiating bone tissues in growing individuals may result in severe inhibition or impairment of skeletal growth. This is an important dose limiting toxicity as it may lead to deformed craniofacial structures, scoliosis, hip joint problems and disproportions of the body such as leg length discrepancies.
Radiation parameters such as total dose and dose per fraction influence the severity of the radiation-induced growth arrest, as do the size and site of the treatment volume and the age of the patient (102, 103). Some studies indicate a steep dose- effect relationship between total doses of 15-30 Gy, whereas other suggests that 25 Gy is the lowest dose to cause growth abnormalities. Doses above 50 Gy may cause avascular necrosis and radiation-induced fractures.

In some cases, attention to the anatomy of the epiphyseal bone can reduce the risks of serious late effects and actively growing parts should be excluded from the radiation field, if possible. If, however, a portion of a growth plate must be treated to ensure tumor coverage, it is usually better to treat the entire growth plate and ensure symmetrical irradiation in order to avoid asymmetric bone growth and severe scoliosis (102-104).

Some of the patients in this study have treatment volumes located nearby or overlapping vertebral bodies. To avoid (hypothetical) severe deformities of the spine, an additional target volume was added to ensure symmetrical irradiation. This additional target volume surrounded the bone tissue, with a margin of approximately 6 mm, and the PTV, with no additional margin. Regardless of the treatment modality, this additional target volume was planned to receive a total dose of 20 Gy, as this should result in a symmetric and total growth inhibition. The remainder of the prescribed dose was delivered to the PTV only, as the bone growth is assumed not to be worsened by doses above 20 Gy.

## 3.1.4 Evaluation of the target volumes

Whether the target volumes were altered by including PET scan information in the delineation process was evaluated with respect to size as well as shape.

### 3.1.4.1 Size

The Wilcoxon signed rank test (Wilcoxon matched pairs test) was used to evaluate if the size of the CTV:s was significantly altered. The test was conducted with IBM SPSS Statistics version 20 with the null-hypothesis stating that there was no alteration of the volume size.

The Wilcoxon Sign test is a statistical comparison of the average of two dependent samples. The samples in this study must be regarded as paired, e.g. dependent, since the targets are delineated on CT- slices from the same CT scan and the only difference whether there is a PET-GTV or not.

Unlike the t-test, the Wilcoxon Sign Test does not assume any properties regarding the distribution of the underlying variables in the analysis. This makes the Wilcoxon Sign Test suitable to compare mean scores when the dependent variable is not normally distributed.
Dependence tests analyze whether there is a significant difference between the factor levels. The t-test family uses mean scores as the average to compare the differences, the Mann-Whitney U-test uses mean ranks as the average, and the Wilcoxon Sign test uses signed ranks.
The Wilcoxon signed rank test pools all differences, ranks them and applies a negative sign to all the ranks where the difference between the two observations is negative (the signed rank).

### 3.1.4.2 Shape

#### 3.1.4.2.1 Dice coefficient

The Dice coefficient is a measure of set agreement. For the two sets A and B, the measure is given by the formula:

$$D(A,B) = \frac{2|A \text{ and } B|}{|A| + |B|}$$

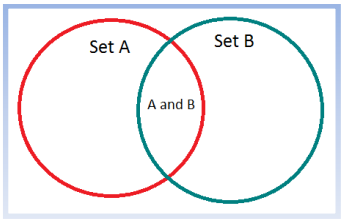


Figure 15: Visualization of the Dice coefficient.

In other words, the Dice coefficient is calculated by dividing the size of the union of the two sets by the average size of the two sets. Thus, the Dice coefficient in this study is calculated by dividing the volume shared by CTV(-PET) and CTV(+PET) by the sum of the two individual volumes.

$$D(A,B) = \frac{2|CTV(noPET) \cup CTV(withPET)|}{|CTV(noPET)| + |CTV(withPET)|}$$

A Dice coefficient value of 0 indicates no overlap; a value of 1 indicates perfect agreement.
Whether the Dice coefficients indicate a significance change of the CTV:s is preferably evaluated with the Wilcoxon Signed Rank Test or a paired t-test.

#### 3.1.4.2.2 Mismatch

The Dice coefficient gives information about whether the volumes overlap or not, but it says nothing about *how* they overlap.
To be able to compare the differences in both directions, the concept of mismatch was used (105). The mismatch between the two sets A and B (e.g the mismatch A to B) is defined as the volume of A expressed as a percentage of the total volume of B.

In this study, the mismatch of CTV(+PET) to CTV(-PET) is the volume of CTV(+PET) as percentage of the volume of CTV(-PET). The result expresses the fraction of the CTV(+PET) volume that is additionally included in the CTV(-PET). In other words, it describes by which percentage the volume of the CTV(+PET) would have to increase in order to cover the CTV(-PET) volume.

The mismatch will show if adding the PET scan information causes unanimous change of the target volumes.

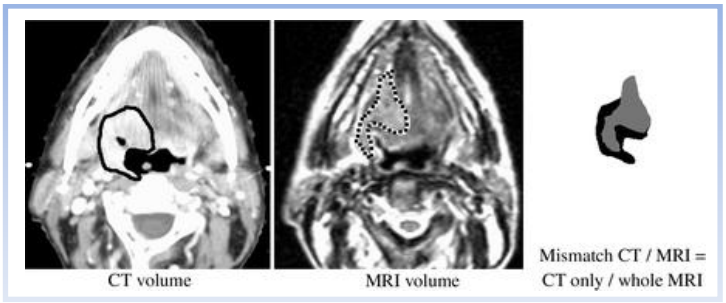


**Figure 16: The mismatch of CT to MRI is calculated by dividing the CT volume by the MRI volume (105). This describes what fraction of the MRI volume that would have to be added in order to cover the CT volume**

# 3.2 Treatment planning

Radiation therapy treatment plans with curative, or locally curative, intent were made with the ambition to make plans useful in clinical practice. All treatment plans were generated using Eclipse external beam dose planning software, version 11.0, from Varian Medical Systems. Published organ-specific dose objectives relevant for pediatric radiation therapy patients were used. A neat summary by Brodin et al (Table 1 in (106)) was used extensively, however compared and validated with recommendations in other publications (107, 108). Individual adjustments of the priorities were made, for example: for a patient with one kidney entirely within the CTV, the dose-restrictions to the remaining kidney was given a very high priority. To be more precise: the main priority of the treatment planning was target coverage, unless the organ was considered to be vital and the doses to the organ would seriously compromise the survival of the patient.

All plans have been normalized to the mean dose delivered to the PTV minus any dose limiting OAR:s or PRV:s when these overlap with the target. In general, the distance between the PTV and the body contour was 3-5 mm. The same field set-up was used for the plans with and without PET.

To account for the degree of conformity, which in some aspects may give a hint of the quality of the plan, a radiation conformity index was calculated (109). This conformity index, CI, is defined as the ratio between the target volume (PTV) and the volume receiving 95 % of the prescription dose:

$$CI = \frac{V_{PTV}}{V_{95\%}}$$

$V_{PTV}$ = the volume of the PTV
$V_{95\%}$ = the volume enclosed by the 95% isodose

To complement the Conformity Index, which is not affected by overdose, the volumes receiving 95 % and 107 % of the prescribed dose were also calculated ($V_{95\%}$ and $V_{107\%}$).

### 3.2.1 3DCRT

The field set-up was manually selected. The number of fields, angle of table, gantry and collimators as well as any wedges and blocks were chosen by the dose-planner and adjusted to give the best dose-distribution possible. No rigorous limitations were applied, for example regarding the number of fields, but for most patients, the 3D-CRT plans were made with five fields or less.

The dose-planner's lack of planning experience was a limiting factor for all treatment modalities, but prehaps most evident for the 3D-CRT and the head-and-neck patients.

### 3.2.2 IMRT

Since the aspiration was to generate clinically useful plans, the number of fields in the IMRT-plans was limited to nine. but most IMRT-plans were made using five or seven fields. The angle of table and gantry were chosen by the treatment planner.
The collimator angle was set to $2^{o}$ for all fields in every IMRT plan, as this is how the potential disturbance of the dose-distribution caused by the so called tongue-and groove effect is adressed at Rigshospitalet (110).

### 3.2.3 IMAT

The rotational therapy-plans were made from two full gantry rotations (two arcs). The collimator angles were optimized by the treatment-planning system and any rotation of the treatment table was set by the treatment planner.

### 3.2.4 IMPT

To fully benefit from the dose-sparing potential of proton beams, the number of fields were in general not more than three. However, in some head-and-neck plans as many as five fields were required, in order to generate an acceptable dose distribution.

# 3.3 Normal tissue complications

Based on published literature and the normal tissues relevant for the patients in this study, models estimating the risks of NTC in eleven organs were used. Some models and parameters were found directly in publications while others have been derived from published studies. Reliable studies on pediatric patients were unfortunately not found for all organs.
The statistical uncertainties of the models were estimated when feasible (Appendix C).

## 3.3.1 Heart

Data from the CCSS was used to derive linear functions describing the hazard ration (HR) of four heart complications as a function of the average cardiac dose (1). For each complication, a linear regression weighted by the (inverse of the) variance was performed with the curve-fitting tool in MATLAB. This tool also provides a 95 % confidence interval (CI) based on the variance. The red and green lines in the plots below are fitted to the error bars (derived from the variance) and can be used to estimate the 95 % CI.
The hazard ratio describes the risk of developing the complication relative a pediatric cancer patient in the same age, with the same diagnosis, who has not received any cardiac irradiation. Since the models should not indicate any protective effects from cardiac irradiation, a cut-off for the lower bound of the CI was set to 1.0.

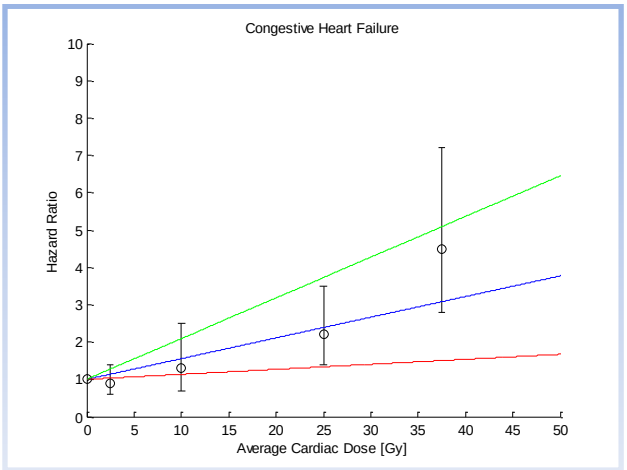


Figure 17: Dose-response relationship for congestive heart failure. The error-bars represent the 95% CI.

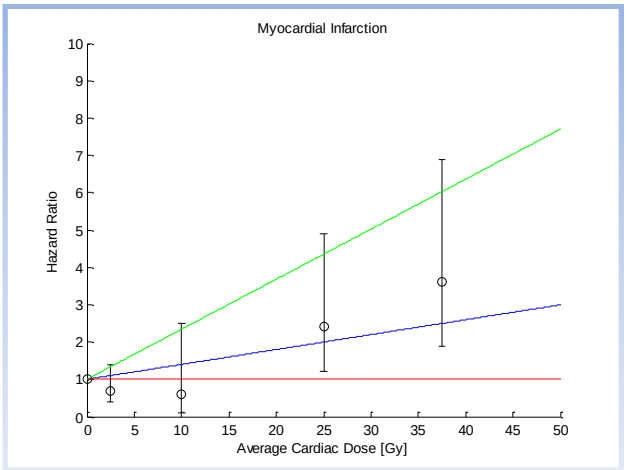


Figure 18: Dose-response relationship for myocardial infarction. The error-bars represent the 95% CI.

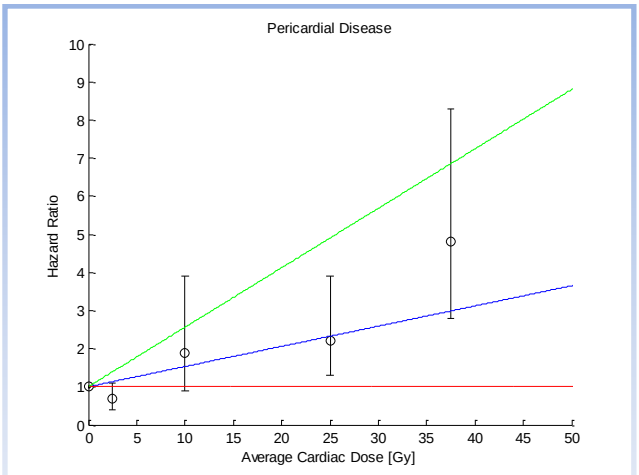


Figure 19: Dose-response relationship for pericardial disease. The error-bars represent the 95% CI.

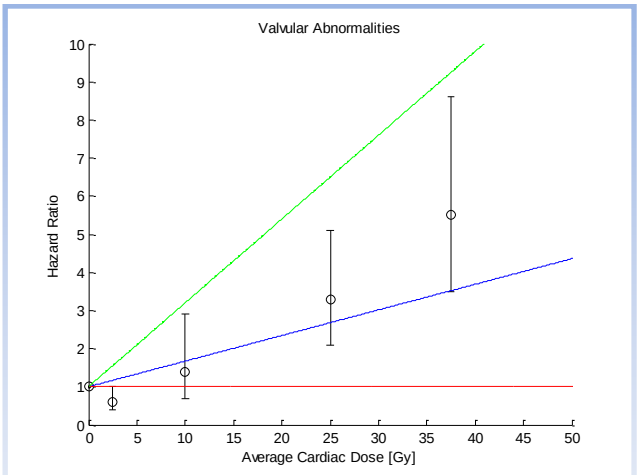


Figure 20: Dose-response relationship for valvular abnormalities. The error-bars represent the 95% CI.

At first glance, a linear fit might appear not to be the best function to describe these dose- effect relationships. However, the linear regression for each complication is significant (p-values ≤ 0.001).
Due to the low number of data points, choosing a more complicated model with more parameters would increase the uncertainty of the model. Hence, the linear model, with only one parameter, was chosen.

## 3.3.2 Lungs

To describe the association between radiation pneumonitis (RP) and the mean lung dose, a logistic function with parameters from QUANTEC was chosen (42). The model uses the mean lung dose for both lungs, e.g. the two lungs are considered to be one organ and the risk of RP cannot be estimated for one lung separately.

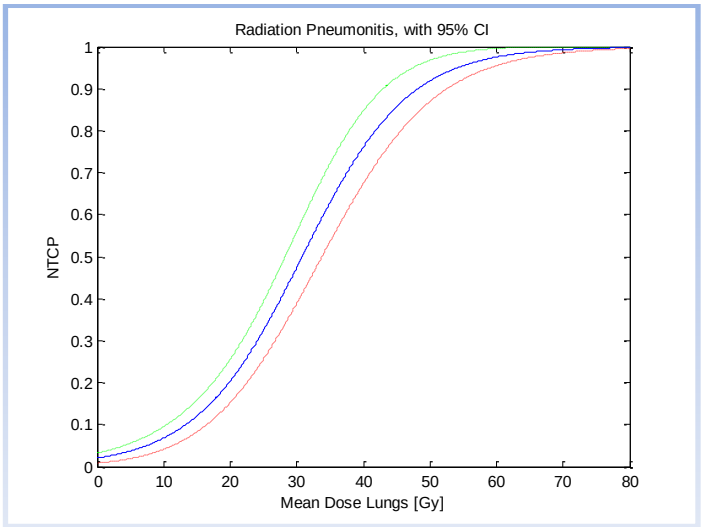


**Figure 21: Dose-response relationship for radiation pneumonitis.**
**The green and the red curve represent the 95% CI, estimated from the Gaussian error propagation formula.**

## 3.3.3 Esophagus

QUANTEC refers to two LKB-models describing the relationship between the mean dose to esophagus and the risk of esophageal complications, such as acute esophagitis of WHO Grade≥2 (43). The parameters from Belderbos et al were chosen, mainly because of the very large confidence interval in the other model.

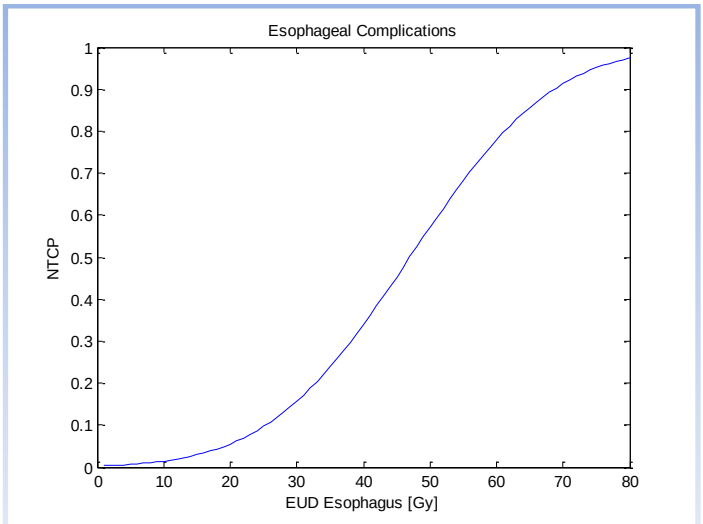


**Figure 22: Dose-response relationship for esophageal complications.**

## 3.3.4 Kidneys

Dose-response data published in 1995 was used to extract a logistic function (111). The function describes the risk of kidney injury from non-total body irradiation of bilateral whole kidneys. In other words, the mean dose to both kidneys is the covariate and the risk of injuries on one of the kidneys cannot be predicted by this model. A recent report from QUANTEC concludes that greater doses than suggested by this model can safely be delivered to partial kidney volumes (48).

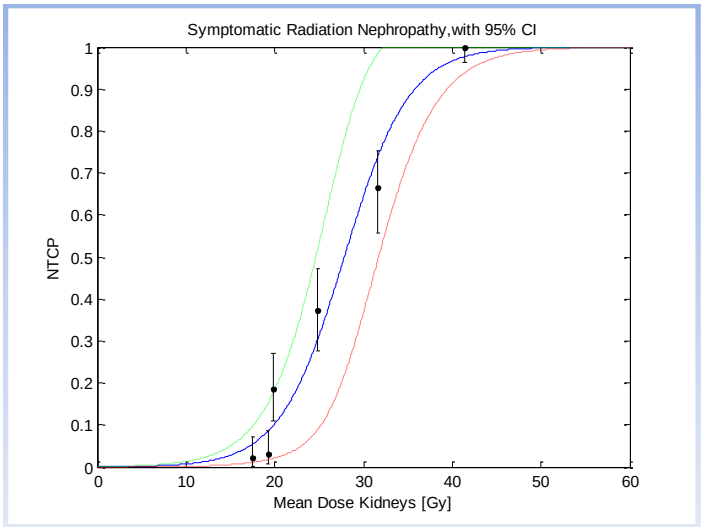


**Figure 23: Dose-response relationship for symptomatic radiation nephropathy.**
**The green and the red curve represent the 95% CI, estimated from the Gaussian error propagation formula.**
**The data points, to which the function was fitted as well as the uncertainty of each point are also in the figure.**

## 3.3.5 Liver

LKB- model parameters for patients with liver function of Child- Pugh A[7] or better were used to estimate the risk of radiation induced liver disease (RILD) (52) . Since the range of parameters summarized by QUANTEC is based on adult patients, the parameters rendering the most sensitive dose-response curve were chosen.

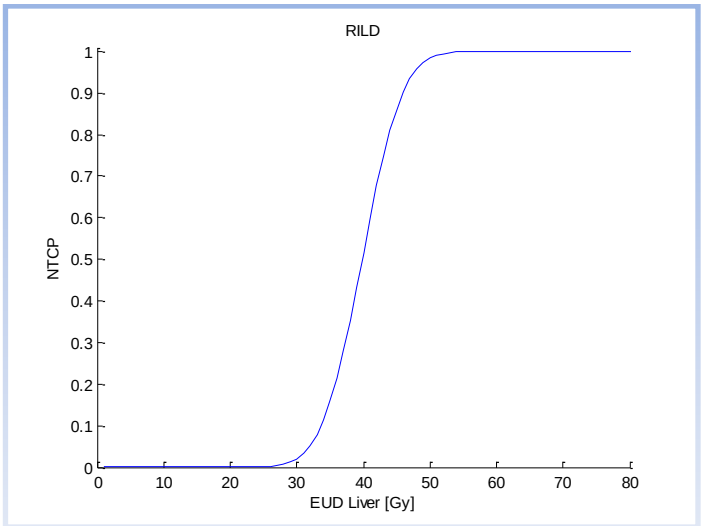


**Figure 24: Dose-response relationship for radiation-induced liver disease (RILD).**

[7] Child- Pugh is a scoring system used to assess liver dysfunction based on clinical and laboratory parameters.

## 3.3.6 Small intestine

A LKB- model derived from German patients with Hodgkin's lymphoma was used to describe the probability of acute gastrointestinal side effects such as nausea, vomiting, diarrhea, infections and bleeding (WHO Grade 1-4) (58).

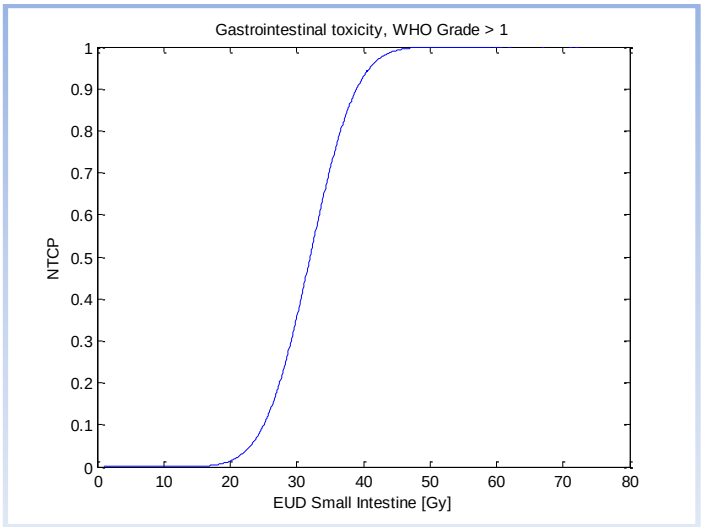


**Figure 25: Dose-response relationship for gastrointestinal toxicity.**

## 3.3.7 Rectum

The LKB-model recommended by QUANTEC was used to estimate the risk of RTOG Grade ≥ 2 rectal toxicity or rectal bleeding (61). These observed complications along with the best-fit parameters in this model have been supported by an independent study (112).

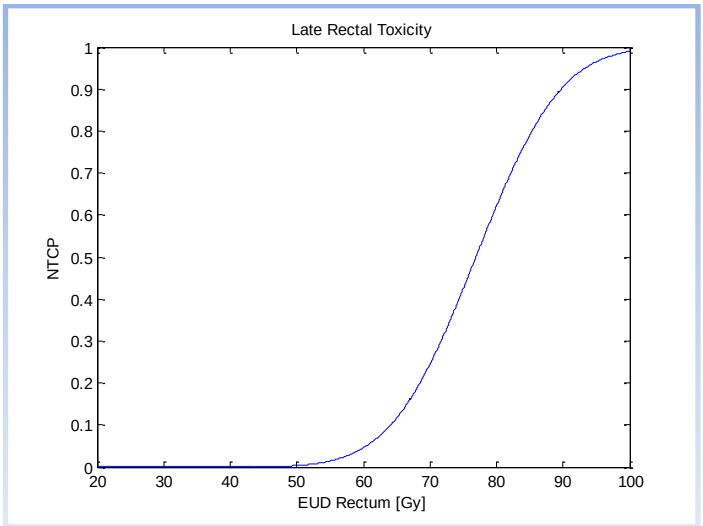


**Figure 26: Dose-response relationship for late rectal toxicity.**

## 3.3.8 Parotid glands

A LKB-model with n=1 (i.e. a mean-dose model) depicting the risk of xerostomia, defined as 25 % of the original saliva flow, as a function of the mean parotid dose was chosen (65). The function is well suited to be used for each parotid gland separately, since the glands seem to respond independently.

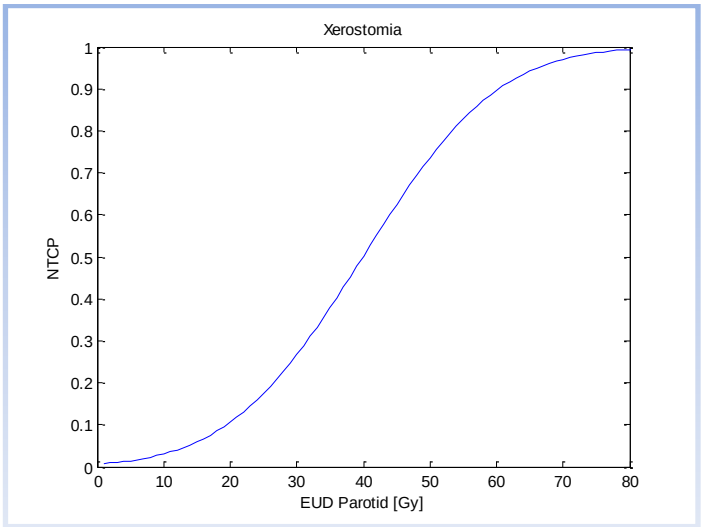


**Figure 27: Dose-response relationship for radiation- induced xerostomia.**

## 3.3.9 Thyroid gland

A comprehensive study on pediatric patients was used to derive a logistic function describing the risk of hypothyroidism as a function of the mean dose to the thyroid gland (68). Note that the function is based on data of the incidence of hypothyroidism and that the risk is not zero for 0 Gy.

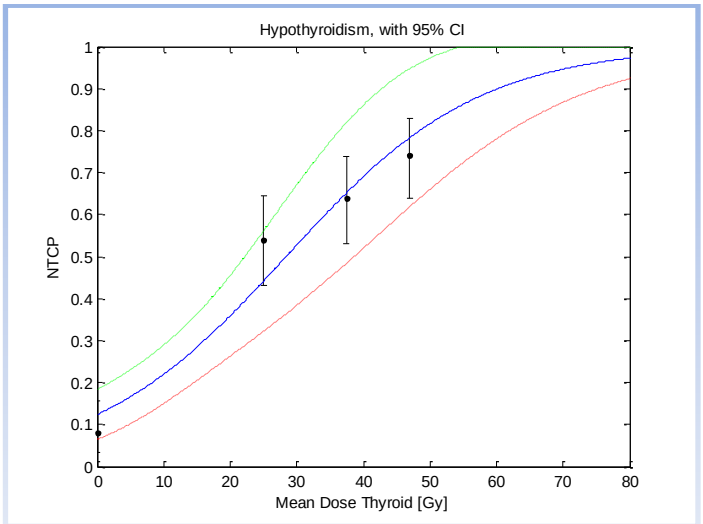


**Figure 28: Dose-response relationship for radiation-induced hypothyroidism.**
**The green and the red curve represent the 95% CI, estimated from the Gaussian error propagation formula.**
**The data points, to which the function was fitted as well as the uncertainty of each point are also shown in the figure.**

## 3.3.10 Eye

Data from the CCSS was used to attain a function describing the relative risk of radiation-induced blindness as a function of maximum dose to the eye (70). An invariance-weighted linear regression was performed with the curve-fitting tool in MATLAB.

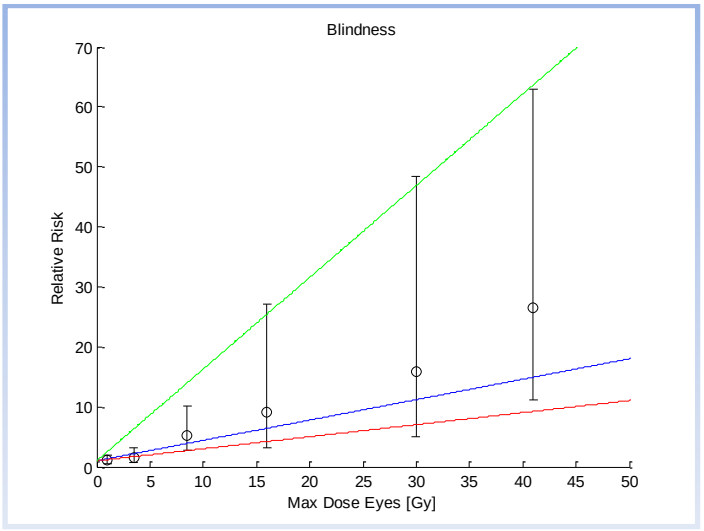


**Figure 29: Dose-response relationship for radiation-induced hypothyroidism. The error-bars as well as the red and the green curves represent the 95% CI.**

The CCSS provides data to estimate the incidence of blindness in the sibling cohort (see Appendix D). Multiplying this percentage with the relative risk from the model yields the incidence among the patients, i.e. the risk of blindness among childhood cancer survivors.

## 3.3.11 Ear (cochlea)

Data from pediatric medulloblastoma patients was used to derive a logistic function describing the probability of developing bilateral and irreversible ototoxicity (76). Unfortunately, the uncertainties of the model were too large to provide a useful confidence interval.

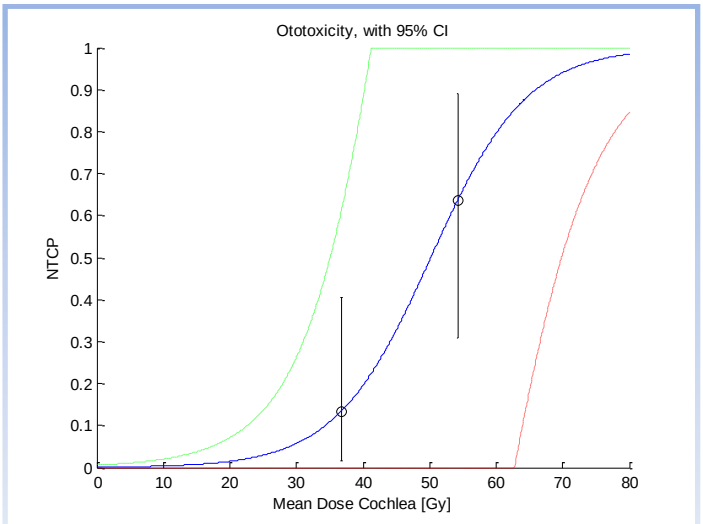


**Figure 30: Dose-response relationship for radiation-induced ototoxicity. The green and the red curve represent the 95% CI, estimated from the Gaussian error propagation formula.**

| Organ | Reference | Pediatric patients | Endpoint | Model | Parameters |
|---|---|---|---|---|---|
| **Heart** | Mulrooney et al (1) | Yes | Congestive heart failure | Linear model $HR = 1 + k \cdot D_{mean,heart}$ | k = 0.0554 |
| | | | Myocardial infarction | | k = 0.0399 |
| | | | Pericardial disease | | k = 0.0530 |
| | | | Valvular abnormalities | | k = 0.0672 |
| **Lung** | Marks et al (42) | No | Radiation pneumonitis | Logistic model | $\gamma_{50}$ = 0.97<br>$TD_{50}$ = 30.8 |
| **Esophagus** | Werner-Wasik et al (43) | No | Esophageal complications (Acute esophagitis) | LKB-model | n = 0.69<br>m = 0.36<br>$TD_{50}$ = 47 |
| **Kidney** | Cassady (111) | No | Symptomatic radiation nephropathy | Logistic model | $\gamma_{50}$ = 1.924<br>$TD_{50}$ = 27.84 |
| **Liver** | Pan et al (52) | No | RILD | LKB-model | n = 1<br>m = 0.12<br>$TD_{50}$ = 39.8 |
| **Small intestine** | Eich et al (58) | No | Gastrointestinal toxicity | LKB-model | n = 0.09<br>m = 0.17<br>$TD_{50}$ = 32 |
| **Rectum** | Michalski et al (61) | No | RTOG Grade ≥ 2 | LKB-model | n = 0.09<br>m = 0.13<br>$TD_{50}$ = 76.9 |
| **Parotids** | Houweling et al (65) | No | Xerostomia | LKB-model | n = 1<br>m = 0.4<br>$TD_{50}$ = 39.9 |
| **Thyroid** | Bhatia et al (68) | Yes | Hypothyroidism | Logistic model | $\gamma_{50}$ = 0.49<br>$D_{50}$ = 28.41 |
| **Eye** | Whelan et al (70) | Yes | Blindness | Linear model $RR = 1 + k \cdot D_{mean,eye}$ | k = 0.34 |
| **Ear** | Huang et al (76) | Yes | Ototoxicity | Logistic model | $\gamma_{50}$ = 1.74<br>$D_{50}$ = 50.17 |

**Table 6: The selected NTCP-models.**

# 3.4 Secondary cancers

Prior to this study, models describing the excess hazard ratios (EHR) for solid secondary cancers in breast, lung, stomach and thyroid had been derived and published by Brodin et al at Rigshospitalet (88).

The models are based on data from large published clinical series with young patients (children and adolescents) receiving fractionated external radiation therapy. At Rigshospitalet, the models had already been thoroughly and carefully refined, and take into consideration parameters such as age at exposure and gender (88). Minor modifications of the published models were done in the writing of this thesis.

The finished models have been used in this work to calculate the cumulative lifetime risk of radiation therapy induced malignancies (Table 7).

| Studied Endpoint | Risk ratio Male:Female | Dose-response function Excess Hazard Ratio per Gy | Parameters |
|---|---|---|---|
| Breast cancer | - | Linear model $k \cdot D_{mean,breast}$ | k = 0.15 |
| Lung cancer | 1:1.7 | Linear model $k \cdot D_{mean,lung}$ | k = 0.141 |
| Thyroid cancer | 1:1.7 | Bell-shaped model $\beta_1 \cdot D_{mean,thyroid} \cdot e^{-\beta_4 D^2_{thyroid}}$ | $\beta_1 = 2.81\text{-}0{,}15e$ $\beta_4 = 0.00164$ |
| Ventricle cancer | 1:3.7 | Linear model $k \cdot D_{mean,stomach}$ | k = 0.84 |

**Table 7: Models used for estimating the risk of secondary cancers (88).**

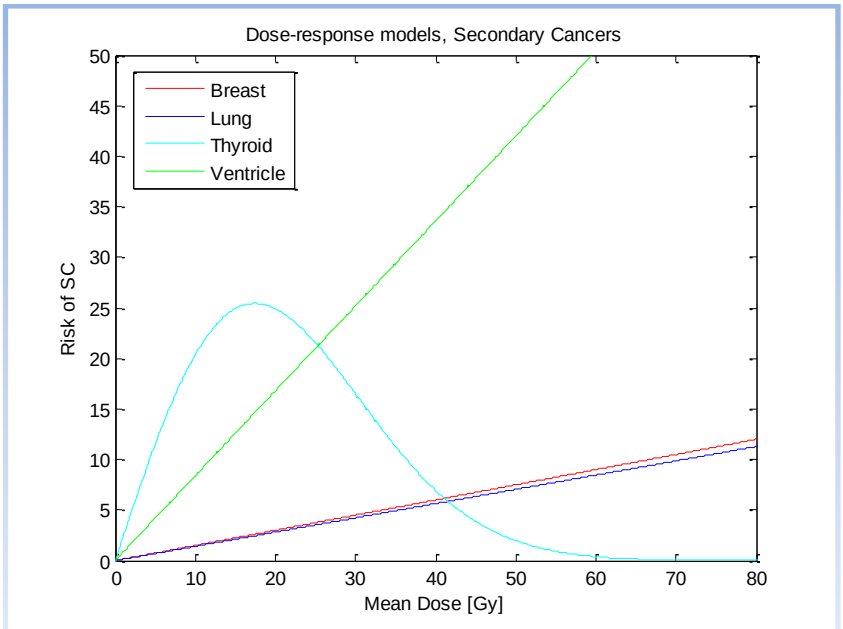


**Figure 31: Dose-response, secondary cancers.**

# 3.5 PET/CT doses

When evaluating the impact of PET on radiation therapy treatment planning, the doses and the associated risks of the PET/CT scan is also of interest.

The effective doses from the PET scans were estimated from the ICRP publication 106 dose data.
For each patient, the value of the absorbed dose per unit activity administered (mGy/MBq) for the phantom with similar weight was used. Information about the administered activity was found in clinical records.

The CT doses for each patient were been calculated with ImPACT Scan, CTDosimetry version 1.0.4. The scanning length was approximated from the treatment planning system and roughly transferred onto the phantom in the Excel sheet. Scan parameters were found in the clinical record of each patient.

The phantom used by ImPACT Scan is based on a mathematical representation of an "average adult". To correct the effective doses to be more representative of pediatric patients, it is recommended to use correction factors (see Table 8 below) (113). Multiplying the calculated adult effective doses by these factors provide a broad estimate of the corresponding doses to children under similar conditions of exposure.

| Age of patient | Head and Neck | Chest | Abdomen & Pelvis |
|---|---|---|---|
| Adult | 1.0 | 1.0 | 1.0 |
| 15 years | 1.1 | 1.0-1.1 | 1.0-1.1 |
| 10 years | 1.2-1.3 | 1.1-1.4 | 1.2-1.5 |
| 5 years | 1.6-1.7 | 1.2-1.6 | 1.2-1.6 |
| 1 years | 2.2 | 1.3-1.9 | 1.3-2.0 |
| Newborn | 2.3-2.6 | 1.4-2.2 | 1.4-2.4 |

**Table 8: Factors to estimate corresponding pediatric doses from calculated adult doses.**

When estimating the risks attributable to doses from a PET/CT scan, the models described previously in this thesis cannot be used, neither for normal tissue toxicities nor for secondary cancers, as the doses associated with a PET/CT scan are much lower than the doses used for radiation therapy.

The risks of health effects other than cancer, cardiovascular disease in particular, have been demonstrated to increase with high therapeutic doses as well as with more modest doses from in atomic bomb exposure (114). However, there is no direct evidence of increased risk of non-cancer diseases at low doses and if the risk exists, there is not enough adequate data to quantify it.

Estimating the risk of cancer from exposure to low-level ionizing radiation, i.e. in the dose range <100 mSv, is associated with large statistical limitations. However debated – and associated with great uncertainties – it is more or less agreed upon that a linear model without a threshold of low doses is the most credible choice (115-117). This LNT-model (linear-no-threshold) assumed that even the smallest dose has the potential to cause a small increase in cancer risk to humans. There are two major competitors to the LNT-model: one assumes that low doses are more harmful than the LNT-model suggests and the other proposes that the risks are lower and that low doses of radiation even may be beneficial (115).

In this work, the method described in the BEIR VII report was used to estimate the risk of radiation- induced cancers from the PET/CT scans (114). It is based on data from studies of the atomic bomb survivors in Hiroshima and Nagasaki as well as data from medical exposure. Data from epidemiologic studies is used to account for the dependence of risk on gender and age at exposure

The BEIR VII model allows for estimation of the EAR (Excess Absolute Risk[8]) of incidence of all solid cancers , (excluding thyroid and non-melanoma) and mortality from all solid cancers at a specific attained age.

$$EAR = \beta \cdot D \cdot e^{\gamma e^*} \cdot \left(\frac{a}{60}\right)^{\eta}$$

ERR = the rate of the disease in an exposed population divided by the rate of the disease in an unexposed population minus 1,0.
$\beta =$ ERR per Sv at age 30 and attained age 60 (from table 12-1 in (114)).
$D =$ effective dose ([Sv]).
$e =$ age at exposure.
$e^* = (e - 30)/10$ for e < 30.
$a =$ attained age.
$\gamma =$ a parameter quantifying the dependence on age at exposure. Increase per decade in age at exposure over the range 0-30 years (from table 12-1 in (114)).
$\eta =$ a parameter quantifying the dependence on attained age (from table 12-1 in (114)).

Integrating the expression from one year after exposure up to the attained age of 90, allows for a rough estimation of the cumulative lifetime risk of solid cancer incidence, caused by the PET/CT scan.

The BEIR VII report contains models for site-specific solid cancers, but emphasizes that they suffer from considerably uncertainties. For that reason, they are not used here.

Naturally, PET- imaging of children involves certain challenges as it requires the patient to lie still and quietly before and during the scan, to minimize FDG-uptake that is unrelated to tumor activity. The expense and risks of sedating the patients who cannot cooperate is beyond the scope of this essay.

[8] EAR = the rate of disease in an exposed population minus the rate of disease in an unexposed population (113).

# 3.6 Patient material

Eleven patients, aged 2-18 years old and PET/CT scanned at Rigshospitalet between 2005 and 2011 were included in this study: six sarcoma patients, four patients with malignancies in the head and neck region and one patient with a lung tumor.

Two of the patients were PET-negative, which means that the accumulation of activity was not higher than what could normally be expected. The motivation for keeping them in the study despite this was to reveal any potential falseness in apparent PET effects.

| Patient number | Patient denotation | Year of treatment | Age at the time of treatment [years] | Gender | Tumor | PET positive | Prescribed dose |
|---|---|---|---|---|---|---|---|
| 1 | PETped01 | 2011 | 4 | F | Abdominal sarcoma | Yes | **55 Gy** |
| 2 | PETped09 | 2009 | 16 | F | Abdominal sarcoma | No | **50.4 Gy** |
| 3 | PETped03 | 2009 | 7 | F | Angiosarcoma (Head and Neck) | Yes | **63 Gy** |
| 4 | PETped10 | 2007 | 16 | M | Abdominal sarcoma | Yes | **30 Gy** |
| 5 | PETped04 | 2006 | 6 | F | Ewing's sarcoma (Spinal canal) | No | **18 Gy (boost)** |
| 6 | PETped20 | 2005 | 2 | F | Rhabdomyosarcoma (Head and Neck) | Yes | **58 Gy** |
| 7 | PETped06 | 2008 | 10 | M | Hodgkin lymphoma (Head and Neck) | Yes | **19.8 Gy** |
| 8 | PETped07 | 2011 | 16 | M | NSCLC (Lung) | Yes | **66 Gy** |
| 9 | PETped08 | 2011 | 18 | M | B-cell lymphoma (Head and Neck) | Yes | **36 Gy** |
| 10 | PETped11 | 2007 | 18 | M | (Head and Neck) | Yes | **66 Gy** |
| 11 | PETped12 | 2006 | 17 | M | (Head and Neck) | Yes | **68 Gy** |

**Table 9: Short summary of the patients in this study.**

# 4. Results

## 4.1 Target volumes

### 4.1.1 Size

| Patient number | Tumor site | PET positive | GTV(-PET) [$cm^3$] | GTV(+PET) [$cm^3$] | CTV(-PET) [$cm^3$] | CTV(+PET) [$cm^3$] |
|---|---|---|---|---|---|---|
| 1 | Abdomen | Yes | 71.94 | 67.95 | 288.46 | 273.66 |
| 2 | Abdomen/ Pelvis | No | 43.86 | 43.60 | 200.86 | 204.64 |
| 3 | Head/Neck | Yes | 28.44 | 25.42 | 97.71 | 101.75 |
| 4 | Abdomen/ Pelvis | Yes | 143.42 | 126.28 | 462.40 | 435.93 |
| 5 | Head/Neck and Pelvis | No | 18.96 | 19.95 | 146.94 | 150.07 |
| 6 | Head/Neck | Yes | 16.88 | 16.69 | 71.10[1] *137.89*[2] | 63.43[1] *129.78*[2] |
| 7 | Head/Neck | Yes | 96.82 | 84.98 | 395.83 | 378.63 |
| 8 | Thorax | Yes | 22.67 | 20.91 | 259.60 | 211.90 |
| 9 | Head/Neck | Yes | 12.85 | 13.65 | 165.53 | 150.67 |
| 10 | Head/Neck | Yes | 126.15 | 152.07 | 433.61[1] *623.67*[3] *780.02*[4] | 497.30[1] *674.27*[3] *814.29*[4] |
| 11 | Head/Neck | Yes | 56.65 | 64.48 | 304.57[1] *555.28*[3] *757.50*[4] | 325.99[1] *586.18*[3] *725.04*[4] |
| | | **Mean:** | **58.06** | **57.82** | **256.96*** *355.06*** | **254.00*** *357.72*** |

[1]CTV-T, [2]CTV-E, [3]CTV-E High-risk, [4]CTV-E Low-risk. *Only CTV-T. **All CTV:s.

**Table 10: The size of the target volumes.**

Null-hypothesis: There is no alteration of the target volume.
The Wilcoxon signed-rank test results in a p-value of 0.477 for the CTV-T:s (0.918 for all of the CTV:s and 0.534 for the GTV:s). With a chosen significance level α of 0.05, the null-hypothesis is retained; including PET causes no significant alteration of the target volume.

## 4.1.2 Shape

### 4.1.2.1 Dice coefficient

| Patient number: | 1 | 2 | 3 | 4 | 5 | 6 | 7 | 8 | 9 | 10 | 11 | Mean: |
|---|---|---|---|---|---|---|---|---|---|---|---|---|
| Dice coefficient: | 0.95 | 0.95 | 0.88 | 0.91 | 0.93 | 0.90 | 0.93 | 0.87 | 0.91 | 0.86 | 0.88 | **0.91** |

Table 11: Dice coefficients for the CTV:s with and without PET.

Null-hypothesis: there is no change of the shape of the target volume, i.e. they will overlap perfectly with Dice coefficients of 1.0.
The Wilcoxon signed-rank test gives a p-value of 0.003. With a chosen significance level α of 0.05, the null-hypothesis is rejected; including PET causes a significant alteration of the shape of the target volumes.

### 4.1.2.2 Mismatch

| Patient number | Pair | Mismatched volume |
|---|---|---|
| 1 | CTV(+PET) to CTV(-PET) | 2.7 % |
| | CTV(-PET) to CTV(+PET) | 8.0 % |
| 2 | CTV(+PET) to CTV(-PET) | 5.9 % |
| | CTV(-PET) to CTV(+PET) | 4.2 % |
| 3 | CTV(+PET) to CTV(-PET) | 14.1 % |
| | CTV(-PET) to CTV(+PET) | 9.7 % |
| 4 | CTV(+PET) to CTV(-PET) | 5.9 % |
| | CTV(-PET) to CTV(+PET) | 12.2 % |
| 5 | CTV(+PET) to CTV(-PET) | 8.5 % |
| | CTV(-PET) to CTV(+PET) | 6.1 % |
| 6 | CTV(+PET) to CTV(-PET) | 4.3 % |
| | CTV(-PET) to CTV(+PET) | 17.1 % |
| 7 | CTV(+PET) to CTV(-PET) | 9.9 % |
| | CTV(-PET) to CTV(+PET) | 5.0 % |
| 8 | CTV(+PET) to CTV(-PET) | 25.4 % |
| | CTV(-PET) to CTV(+PET) | 3.0 % |
| 9 | CTV(+PET) to CTV(-PET) | 13.4 % |
| | CTV(-PET) to CTV(+PET) | 5.0 % |
| 10 | CTV(+PET) to CTV(-PET) | 7.0 % |
| | CTV(-PET) to CTV(+PET) | 22.9 % |
| 11 | CTV(+PET) to CTV(-PET) | 8.2 % |
| | CTV(-PET) to CTV(+PET) | 16.0 % |
| Mean: | CTV(+PET) to CTV(-PET) | **9.6 %** |
| | CTV(-PET) to CTV(+PET) | **9.9 %** |

Table 12: Mismatch for CTV:s with and without PET.
The mismatch of CTV(-PET) to CTV(+PET) describes the fraction of the CTV(-PET) that is additionally included in the CTV(+PET).

## 4.2 Treatment planning

The used measure of objective fulfillment, conformity index (CI), is presented below.

| Abdominal Pelvic & Thoracic (5 PTV:s) | CI PTV |
|---|---|
| CRT noPET | 0.95 |
| CRT wPET | 0.95 |
| IMRT noPET | 0.94 |
| IMRT wPET | 0.95 |
| IMPT noPET | 0.98 |
| IMPT wPET | 0.98 |
| IMAT noPET | 0.94 |
| IMAT wPET | 0.94 |

Table 13: Target coverage, mean values.

| Abdominal Pelvic & Thoracic (5 PTV:s) | CI PTV |
|---|---|
| CRT noPET | 0.95 |
| CRT wPET | 0.95 |
| IMRT noPET | 0.94 |
| IMRT wPET | 0.94 |
| IMPT noPET | 0.98 |
| IMPT wPET | 0.99 |
| IMAT noPET | 0.97 |
| IMAT wPET | 0.97 |

Table 14: Target coverage, median values (range).

| Head and Neck (7 PTV:s) | CI PTV |
|---|---|
| CRT noPET | 0.90 |
| CRT wPET | 0.90 |
| IMRT noPET | 0.96 |
| IMRT wPET | 0.98 |
| IMPT noPET | 0.97 |
| IMPT wPET | 0.96 |
| IMAT noPET | 0.92 |
| IMAT wPET | 0.90 |

Table 15: Target coverage, mean values.

| Head and Neck (7 PTV:s) | CI PTV |
|---|---|
| CRT noPET | 0.93 |
| CRT wPET | 0.91 |
| IMRT noPET | 0.94 |
| IMRT wPET | 0.97 |
| IMPT noPET | 0.97 |
| IMPT wPET | 0.96 |
| IMAT noPET | 0.93 |
| IMAT wPET | 0.91 |

Table 16: Target coverage, median values (range)

The significance was evaluated with a related-samples Wilcoxon signed rank test:
For the patients with PTV in the abdominal-pelvic or thoracic region, there was no significant difference between the mean conformity index without and with PET ($p = 0.180$).
For the patients with PTV in the head and neck region, there was no significant difference between the mean CI-values without and with PET ($p = 0.785$).

The volumes receiving 95 % and 107 % of the prescribed dose ($V_{95\%}$ and $V_{107\%}$) were not significantly different for the PET and the noPET plans.

# 4.3 Normal tissue complications

The results for each patient separately can be found in Appendix A.

| Abdomen Pelvis & Thorax (5 PTV:s) | Heart Failure HR | Myoc. Infarction HR | Peric. Disease HR | Valvular Abnorm. HR | Pneum.* P | Radiation nephropathy bilateral P | Liver disease P | GI toxicity P | Late rectal toxicity P |
|---|---|---|---|---|---|---|---|---|---|
| **CRT noPET** | 1.37 (1.09-1.72) | 1.26 (0.64-1.89) | 1.35 (0.67-2.03) | 1.44 (0.43-2.46) | 13.43% (11.58-15.28) | 18.32% (15.95-20.68) | 0.00% | 32.80% | 0.05% |
| **CRT wPET** | 1.36 (1.09-1.71) | 1.26 (0.65-1.87) | 1.34 (0.67-2.01) | 1.44 (0.44-2.43) | 12.55% (10.79-14.31) | 17.99% (15.29-20.69) | 0.00% | 33.44% | 0.05% |
| **IMRT noPET** | 1.19 (1.05-1.38) | 1.14 (0.81-1.47) | 1.18 (0.83-1.54) | 1.23 (0.70-1.77) | 10.80% (9.23-12.37) | 18.20% (15.71-20.69) | 0.00% | 31.47% | 0.04% |
| **IMRT wPET** | 1.22 (1.05-1.44) | 1.16 (0.78-1.54) | 1.21 (0.80-1.63) | 1.27 (0.65-1.89) | 10.39% (8.87-11.91) | 18.14% (15.59-20.69) | 0.00% | 31.08% | 0.04% |
| **IMPT noPET** | 1.13 (1.03-1.25) | 1.09 (0.88-1.30) | 1.12 (0.89-1.35) | 1.15 (0.81-1.50) | 6.78% (5.75-7.80) | 14.66% (10.99-20.12) | 0.00% | 29.37% | 0.03% |
| **IMPT wPET** | 1.11 (1.03-1.22) | 1.08 (0.89-1.28) | 1.11 (0.90-1.32) | 1.14 (0.82-1.45) | 6.74% (5.72-7.76) | 14.76% (9.80-19.73) | 0.00% | 29.49% | 0.03% |
| **IMAT noPET** | 1.14 (1.03-1.27) | 1.10 (0.87-1.33) | 1.13 (0.88-1.38) | 1.16 (0.79-1.54) | 11.37% (9.74-13.01) | 16.22% (12.06-20.38) | 0.00% | 29.37% | 0.02% |
| **IMAT wPET** | 1.15 (1.04-1.30) | 1.11 (0.85-1.37) | 1.15 (0.86-1.43) | 1.19 (0.76-1.61) | 9.77% (8.33-11.21) | 16.24% (12.09-20.38) | 0.00% | 29.40% | 0.02% |

*Patient nr 1 (PETped01) not included.

**Table 17: NTCP, patients treated in the abdominal, pelvic or thoracic region. Mean values (95% CI).**

| Abdomen Pelvis & Thorax (5 PTV:s) | Heart Failure HR | Myoc. Infarction HR | Peric. Disease HR | Valvular Abnorm. HR | Pneum.* P | Radiation nephropathy bilateral P | Liver disease P | GI toxicity P | Late rectal toxicity P |
|---|---|---|---|---|---|---|---|---|---|
| **CRT noPET** | 1.00 (1.00-2.74) | 1.00 (1.00-2.25) | 1.00 (1.00-2.66) | 1.00 (1.00-3.10) | 2.05% (2.03-47.61) | 0.05% (0.05-91.40) | 0.00% (0.00-0.00) | 0.84% (0.00-100) | 0.00% (0.00-0.26) |
| **CRT wPET** | 1.00 (1.00-2.71) | 1.00 (1.00-2.23) | 1.00 (1.00-2.63) | 1.00 (1.00-3.07) | 2.05% (2.03-44.08) | 0.05% (0.05-89.75) | 0.00% (0.00-0.00) | 0.90% (0.00-100) | 0.00% (0.00-0.26) |
| **IMRT noPET** | 1.00 (1.00-1.89) | 1.00 (1.00-1.64) | 1.00 (1.00-1.85) | 1.00 (1.00-2.08) | 2.04% (2.03-37.09) | 0.05% (0.05-90.79) | 0.00% (0.00-0.00) | 0.72% (0.00-100) | 0.00% (0.00-0.20) |
| **IMRT wPET** | 1.00 (1.00-2.04) | 1.00 (1.00-1.75) | 1.00 (1.00-1.99) | 1.00 (1.00-2.26) | 2.04% (2.03-35.46) | 0.05% (0.05-90.51) | 0.00% (0.00-0.00) | 0.59% (0.00-100) | 0.00% (0.00-0.22) |
| **IMPT noPET** | 1.00 (1.00-1.62) | 1.00 (1.00-1.45) | 1.00 (1.00-1.60) | 1.00 (1.00-1.76) | 2.03% (2.03-21.02) | 0.05% (0.05-73.10) | 0.00% (0.00-0.00) | 0.46% (0.00-100) | 0.00% (0.00-0.15) |
| **IMPT wPET** | 1.00 (1.00-1.57) | 1.00 (1.00-1.41) | 1.00 (1.00-1.54) | 1.00 (1.00-1.69) | 2.03% (2.03-20.87) | 0.05% (0.05-73.63) | 0.00% (0.00-0.00) | 0.44% (0.00-99.99) | 0.00% (0.00-0.14) |
| **IMAT noPET** | 1.00 (1.00-1.59) | 1.00 (1.00-1.43) | 1.00 (1.00-1.57) | 1.00 (1.00-1.72) | 2.04% (2.03-39.39) | 0.05% (0.05-80.90) | 0.00% (0.00-0.00) | 0.45% (0.00-100) | 0.00% (0.00-0.09) |
| **IMAT wPET** | 1.00 (1.00-1.69) | 1.00 (1.00-1.49) | 1.00 (1.00-1.66) | 1.00 (1.00-1.83) | 2.04% (2.03-32.97) | 0.05% (0.05-81.00) | 0.00% (0.00-0.00) | 0.46% (0.00-100) | 0.00% (0.00-0.10) |

*Patient nr 1 (PETped01) not included.

**Table 18: NTCP, patients treated in the abdominal, pelvic or thoracic region. Median values (range).**

| Head & Neck (7 PTV:s) | Heart Failure* HR | Myocar. Infarction* HR | Peric. Disease* HR | Valvular Abnorm.* HR | Pneum.* P | Esoph. Comp. P | Xero. Bilateral P | Hypothyr. P | Blindness p | Ototox. P |
|---|---|---|---|---|---|---|---|---|---|---|
| **CRT noPET** | 1.03 (1.01-1.06) | 1.02 (1.00-1.07) | 1.03 (1.00-1.09) | 1.04 (1.00-1.12) | 2.66% (2.16-3.15) | 3.73% | 42.63% | 48.86% (41.39-56.33) | 2.28% (1.55-8.44) | 25.45% |
| **CRT wPET** | 1.03 (1.01-1.05) | 1.02 (1.00-1.07) | 1.03 (1.00-1.08) | 1.03 (1.00-1.11) | 2.63% (2.13-3.14) | 3.40% | 42.27% | 46.99% (39.94-54.05) | 2.38% (1.61-8.86) | 25.99% |
| **IMRT noPET** | 1.02 (1.00-1.03) | 1.01 (1.00-1.04) | 1.01 (1.00-1.04) | 1.02 (1.00-1.06) | 2.58% (2.23-2.93) | 2.81% | 34.42% | 51.64% (44.98-58.29) | 3.03% (1.99-11.79) | 18.16% |
| **IMRT wPET** | 1.02 (1.00-1.03) | 1.01 (1.00-1.04) | 1.02 (1.00-1.04) | 1.02 (1.00-1.06) | 2.63% (2.27-2.99) | 2.63% | 34.21% | 51.11% (44.04-58.19) | 3.15% (2.07-12.36) | 20.01% |
| **IMPT noPET** | 1.00 (1.00-1.00) | 1.00 (1.00-1.00) | 1.00 (1.00-1.00) | 1.00 (1.00-1.00) | 2.20% (1.83-2.58) | 2.72% | 29.98% | 50.79% (43.83-57.75) | 2.06% (1.34-7.47) | 12.60% |
| **IMPT wPET** | 1.00 (1.00-1.00) | 1.00 (1.00-1.00) | 1.00 (1.00-1.00) | 1.00 (1.00-1.00) | 2.20% (1.82-2.58) | 2.55% | 28.85% | 50.90% (43.97-57.83) | 2.07% (1.37-7.50) | 14.23% |
| **IMAT noPET** | 1.03 (1.01-1.07) | 1.02 (1.00-1.08) | 1.03 (1.00-1.10) | 1.04 (1.00-1.13) | 2.91% (2.60-3.23) | 2.70% | 28.83% | 49.69% (42.62-56.77) | 3.14% (1.98-12.33) | 16.85% |
| **IMAT wPET** | 1.03 (1.01-1.05) | 1.02 (1.00-1.07) | 1.03 (1.00-1.08) | 1.03 (1.00-1.11) | 2.81% (2.47-3.14) | 2.65% | 28.21% | 47.98% (40.69-55.27) | 3.21% (2.04-12.65) | 18.46% |

*Patient nr 9 (PETped08) not included.

**Table 19: NTCP, patients treated in the head and neck region. Mean values (95% CI).**

| Head & Neck (7 PTV:s) | Heart Failure* HR | Myocar. Infarction* HR | Peric. Disease* HR | Valvular Abnorm.* HR | Pneum.* P | Esoph. Comp. P | Xero. Bilateral P | Hypothyr. P | Blindness p | Ototox. P |
|---|---|---|---|---|---|---|---|---|---|---|
| **CRT noPET** | 1.01 (1.00-1.08) | 1.01 (1.00-1.06) | 1.01 (1.00-1.08) | 1.02 (1.00-1.10) | 2.65% (2.06-3.36) | 1.24% (0.28-20.00) | 13.46% (4.20-96.77) | 37.43% (16.90-92.99) | 0.85% (0.66-6.22) | 0.85% (0.12-89.41) |
| **CRT wPET** | 1.01 (1.00-1.08) | 1.01 (1.00-1.06) | 1.01 (1.00-1.08) | 1.02 (1.00-1.10) | 2.54% (2.07-3.41) | 1.21% (0.28-18.22) | 12.70% (4.20-97.15) | 37.40% (16.88-92.90) | 0.85% (0.65-6.51) | 0.76% (0.12-90.36) |
| **IMRT noPET** | 1.01 (1.00-1.04) | 1.01 (1.00-1.03) | 1.01 (1.00-1.04) | 1.01 (1.00-1.05) | 2.35% (2.05-4.00) | 1.06% (0.28-14.12) | 7.29% (1.94-92.15) | 29.11% (13.34-92.26) | 0.96% (0.67-9.65) | 0.40% (0.10-80.00) |
| **IMRT wPET** | 1.01 (1.00-1.04) | 1.01 (1.00-1.03) | 1.01 (1.00-1.04) | 1.01 (1.00-1.05) | 2.33% (2.06-4.12) | 0.99% (0.28-13.62) | 5.62% (1.91-90.84) | 29.05% (13.43-92.27) | 0.88% (0.64-10.11) | 0.33% (0.10-86.46) |
| **IMPT noPET** | 1.00 (1.00-1.00) | 1.00 (1.00-1.00) | 1.00 (1.00-1.00) | 1.00 (1.00-1.00) | 2.13% (2.02-2.71) | 0.97% (0.27-14.14) | 7.31% (1.21-77.96) | 30.20% (12.43-91.07) | 0.53% (0.53-5.43) | 0.23% (0.09-61.67) |
| **IMPT wPET** | 1.00 (1.00-1.00) | 1.00 (1.00-1.00) | 1.00 (1.00-1.00) | 1.00 (1.00-1.00) | 2.13% (2.02-2.66) | 0.95% (0.27-13.67) | 6.14% (1.31-73.59) | 34.76% (12.48-90.72) | 0.55% (0.53-5.96) | 0.24% (0.09-67.31) |
| **IMAT noPET** | 1.02 (1.00-1.12) | 1.01 (1.00-1.09) | 1.01 (1.00-1.12) | 1.02 (1.00-1.15) | 2.54% (2.05-5.11) | 0.95% (0.28-14.51) | 5.48% (1.45-74.24) | 26.82% (13.31-91.71) | 1.10% (0.66-8.80) | 0.62% (0.11-58.10) |
| **IMAT wPET** | 1.02 (1.00-1.09) | 1.01 (1.00-1.06) | 1.02 (1.00-1.08) | 1.02 (1.00-1.10) | 2.53% (2.06-4.67) | 0.94% (0.28-14.43) | 5.59% (1.50-75.84) | 26.99% (13.37-92.68) | 1.20% (0.64-9.10) | 0.60% (0.12-65.62) |

*Patient nr 9 (PETped08) not included.

**Table 20: NTCP, patients treated in the head and neck region. Median values (range).**

The significance was evaluated with the related-samples Wilcoxon signed rank test.
Primarily, the general impact of PET on all treatment modalities was studied: the estimated NTCP-values were grouped in two halves - one without and the other with PET.
For the patients with PTV in the abdominal, pelvic or thoracic region, there was no significant difference between the mean values without and with PET ($p = 0.889$).
For the patients with PTV in the head and neck region, there was no significant difference between the mean NTCP values without and with PET ($p = 0.381$).

The impact of PET was then investigated on each modality separately.
For the patients with PTV in the abdominal, pelvic or thoracic region, this revealed that PET caused no significant difference of the mean estimated NTCP:s between the 3DCRT-plans ($p = 0.343$), IMRT-plans ($p = 0.498$), IMPT-plans ($p = 0.865$) or the IMAT-plans ($p = 0.234$).
Neither for the patients with PTV in the head and neck region, did PET cause any significant difference of the mean estimated NTCP:s between the 3DCRT-plans ($p = 0.398$), IMRT-plans ($p = 0.866$), IMPT-plans ($p = 0.893$) or the IMAT-plans ($p = 0.398$).

# 4.4 Secondary cancers

The result for each patient separately can be found in Appendix A.

| Abdominal Pelvic & Thoracic (5 PTV:s) | Breast cancer* | Lung cancer** | Stomach cancer |
|---|---|---|---|
| **CRT noPET** | 0.12% | 16.14% | 11.06% |
| **CRT wPET** | 0.13% | 15.55% | 10.86% |
| **IMRT noPET** | 0.10% | 14.28% | 9.13% |
| **IMRT wPET** | 0.10% | 13.99% | 10.24% |
| **IMPTnoPET** | 0.04% | 10.85% | 4.50% |
| **IMPT wPET** | 0.04% | 10.82% | 4.54% |
| **IMAT noPET** | 0.06% | 14.69% | 8.32% |
| **IMAT wPET** | 0.09% | 13.52% | 8.67% |

*Patient nr 1 (PETped01) and Patient nr 4 (PETped10) not included.
** Patient nr 1 (PETped01) not included.

**Table 21: Cumulative lifetime risk of secondary cancer for patients treated in the abdominal, pelvic or thoracic region (*only female patients). Mean values.**

| Abdominal Pelvic & Thoracic (5 PTV:s) | Breast cancer* | Lung cancer** | Stomach cancer |
|---|---|---|---|
| **CRT noPET** | 0.12% (0.04-0.20) | 0.18% (0.03-64.17) | 0.16% (0.03-52.67) |
| **CRT wPET** | 0.13%) (0.04-0.21) | 0.21% (0.03-61.76) | 0.72% (0.03-51.45) |
| **IMRT noPET** | 0.10% (0.04-0.16) | 0.14% (0.03-58.83) | 0.01% (0.00-44.77) |
| **IMRT wPET** | 0.10% (0.04-0.17) | 0.16% (0.03-55.64) | 0.21% (0.01-49.99) |
| **IMPTnoPET** | 0.04% (0.04-0.04) | 0.03% (0.01-43.35) | 0.03% (0.02-22.43) |
| **IMPT wPET** | 0.04% (0.04-0.04) | 0.03% (0.02-43.19) | 0.03% (0.02-22.61) |
| **IMAT noPET** | 0.06% (0.04-0.08) | 0.12% (0.03-58.48) | 0.06% (0.02-40.41) |
| **IMAT wPET** | 0.09% (0.04-0.14) | 0.15% (0.03-53.76) | 0.17% (0.03-42.09) |

*Patient nr 1 (PETped01) and Patient nr 4 (PETped10) not included.
** Patient nr 1 (PETped01) not included.

**Table 22: Cumulative lifetime risk of secondary cancer for patients treated in the abdominal, pelvic or thoracic region (*only female patients). Median values (range).**

| Head and Neck (7 PTV:s) | Breast cancer* | Lung cancer** | Thyroid cancer |
|---|---|---|---|
| **CRT noPET** | 0.74% | 4.34% | 14.87 |
| **CRT wPET** | 0.70% | 4.20% | 14.48 |
| **IMRT noPET** | 0.47% | 3.70% | 11.25 |
| **IMRT wPET** | 0.48% | 3.98% | 11.82 |
| **IMPT noPET** | 0.04% | 1.38% | 9.85 |
| **IMPT wPET** | 0.04% | 1.35% | 11.02 |
| **IMAT noPET** | 0.73% | 5.42% | 11.31 |
| **IMAT wPET** | 0.64% | 4.93% | 11.90 |

*Only female patients. **Patient nr 9 (PETped08) not included.

**Table 23: Cumulative lifetime risk of secondary cancer for patients treated in the head and neck region. Mean values.**

| Head and Neck (7 PTV:s) | Breast cancer* | Lung cancer** | Thyroid cancer |
|---|---|---|---|
| **CRT noPET** | 0.20% (0.04-1.99) | 4.37% (0.33-8.85) | 15.19% (0.15-30.78) |
| **CRT wPET** | 0.21% (0.03-1.85) | 3.73% (0.40-9.10) | 13.23% (0.16-30.89) |
| **IMRT noPET** | 0.62% (0.16-0.63) | 2.59% (0.25-11.61) | 3.36% (0.21-27.37) |
| **IMRT wPET** | 0.61% (0.17-0.66) | 2.45% (0.29-12.12) | 3.64% (0.19-26.40) |
| **IMPTnoPET** | 0.04% (0.04-0.04) | 0.87% (0.00-4.92) | 3.02% (0.28-25.77) |
| **IMPT wPET** | 0.04% (0.04-0.04) | 0.86% (0.00-4.65) | 3.57% (0.39-31.40) |
| **IMAT noPET** | 0.68% (0.08-1.44) | 3.91% (0.22-15.86) | 5.77% (0.27-27.14) |
| **IMAT wPET** | 0.58% (0.14-1.21) | 3.80% (0.28-14.31) | 10.44% (0.17-26.04) |

*Only female patients. **Patient nr 9 (PETped08) not included.

**Table 24: Cumulative lifetime risk of secondary cancer for patients treated in the head and neck region (*only female patients). Median values (range).**

The significance was evaluated with a related-samples Wilcoxon signed rank test:
For the patients with PTV in the abdominal, pelvic or thoracic region there was no significant difference between the mean SC-risk without and with PET ($p = 0.722$).
For the patients with PTV in the head and neck region, there was no significant difference between the mean values without and with PET ($p = 0.722$).

# 4.5 PET/CT doses

| Patient number | Tumor site | Administered activity | Effective Dose PET | Age corrected Effective Dose CT [mSv] | Total Effective Dose PET/CT | Incidence All Solid Cancers* Cumulative EAR** |
|---|---|---|---|---|---|---|
| 1 | Abdomen | 62 MBq | 4 mSv | 16 mSv | 20 mSv | 1.22 % |
| 2 | Abdomen/ Pelvis | 283 MBq | 11 mSv | 28 mSv | 39 mSv | 1.46 % |
| 3 | Head/Neck | 89 MBq | 5 mSv | 6 mSv | 11 mSv | 0.60 % |
| 4 | Abdomen/ Pelvis | 413 MBq | 10 mSv | 29 mSv | 39 mSv | 1.14 % |
| 5 | Head/Neck and Pelvis | 190 MBq | 11 mSv | 7 mSv | 18 mSv | 1.01 % |
| 6 | Head/Neck | 86 MBq | 8 mSv | 5 mSv | 13 mSv | 0.86 % |
| 7 | Head/Neck | 114 MBq | 4 mSv | 37 mSv | 41 mSv | 1.54 % |
| 8 | Thorax/Lungs | 226 MBq | 5 mSv | 21 mSv | 26 mSv | 0.76 % |
| 9 | Head/Neck | 407 MBq | 8 mSv | 63 mSv | 71 mSv | 1.91 % |
| 10 | Head/Neck | 382 MBq | 9 mSv | 28 mSv | 37 mSv | 1.00 % |
| 11 | Head/Neck | 426 MBq | 10 mSv | 8 mSv | 18 mSv | 0.51 % |
| | **Mean values:** | | **7.7 mSv** | **22.5 mSv** | **30.3 mSv** | **1.01 %** |

*Incidence of all solid cancers, excluding thyroid and non-melanoma skin cancers.
** EAR, summed from age at exposure+1 through the attained age of 90.

**Table 25: Effective doses from the PET/CT scan and the attributable EAR for solid cancer incidence.**

# 5. Discussion

## Treatment planning

The ambition to accomplish clinically useful plans was not always feasible. Due to the limited experience of the treatment planner, some of the 3DCRT plans were far from a realistic choice compared to the other modalities. Then again, for other patients this modality turned out to provide one of the better alternatives when comparing the low-dose volumes, see Figure 32 and Figure 33 below. The DVH:s for each patient can be viewed in Appendix B.

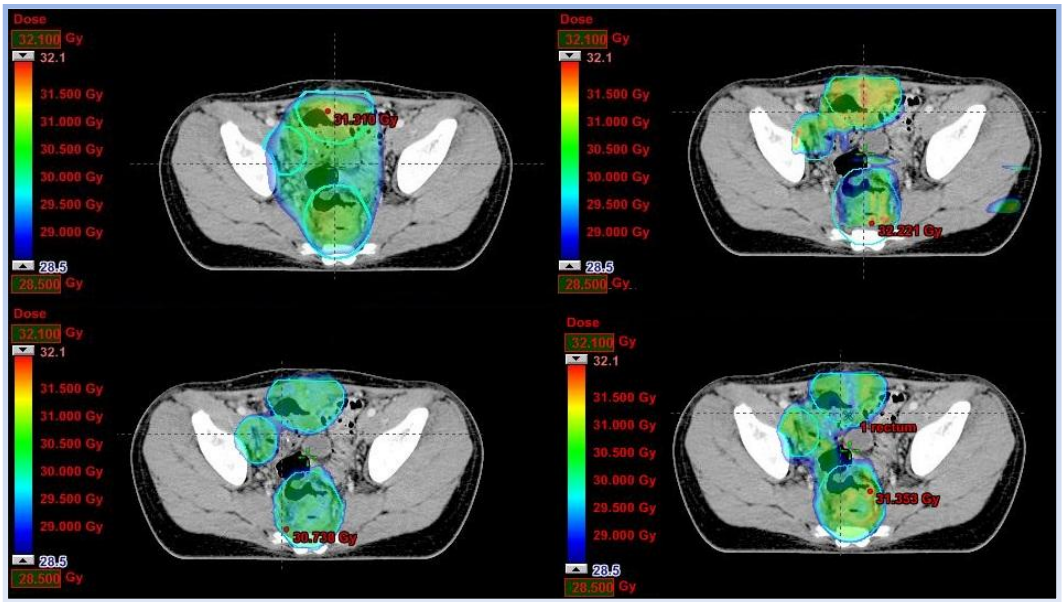


**Figure 32: Patient nr 4, dose-cut off at 107% and 95% of the prescribed dose (30 Gy). Upper row from left: 3DCRT and IMRT. Lower row from left: IMPT and IMAT.**

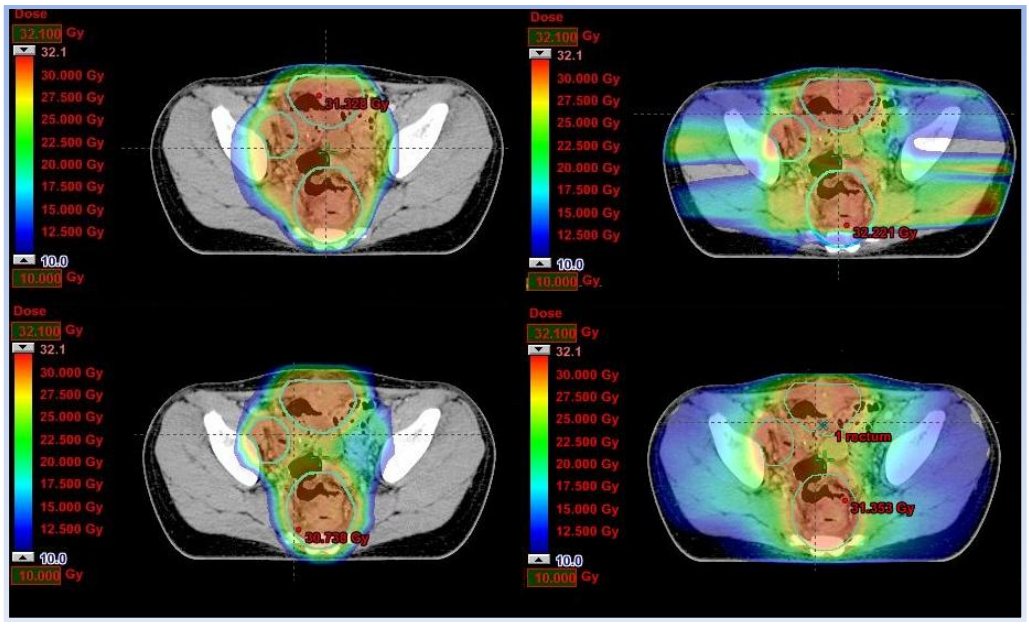


**Figure 33: Patient nr 4, dose-cut off at 107% and 33% of the prescribed dose (30 Gy). Upper row from left: 3DCRT and IMRT. Lower row from left: IMPT and IMAT.**

## Target volumes

Including PET into the delineation process increased the size of five out of the eleven target volumes (CTV-T).

The mean size of the GTV was 58.06 $cm^3$ (range: 12.85-143.42 $cm^3$, median 43.86 $cm^3$) and 57.82 $cm^3$ (range: 13.65-152.07 $cm^3$, median 43.60 $cm^3$) without and with PET respectively. Corresponding figures for the CTV-T were 256.96 $cm^3$ (range: 71.10-462.40 $cm^3$, median 259.60 $cm^3$) and 254.00 $cm^3$ (range: 63.43-497.30 $cm^3$, median 211.90 $cm^3$). On average, the size of CTV-T(+PET) was 98% of the CTV-T(-PET) size.
In the two PET-negative patients, the CTV-T(+PET) was about 2% larger than the CTV-T(-PET). Excluding these patients, the average size difference between CTV-T(+PET) and CTV-T(-PET) was 97%.

For most patients with additional CTV:s, the change of the CTV-T was reflected by the CTV-E. However, for patient number 11, CTV-T and CTV-Eh became larger with PET, while CTV-El was smaller with than without PET.

The p-values from the Wilcoxon sign test indicate that PET causes no significant change of the size of the target volumes, neither the GTV:s nor the CTV-T:s. Including the additional CTV:s (CTV-E) does not change the results.

Whether the Dice coefficients indicate a significant change of the CTV:s was evaluated with a Wilcoxon signed-rank test. The null-hypothesis was that there would be no change, i.e. a perfect overlap with Dice coefficients of 1.0. The resulting p-value indicates that the shapes are changed significantly. However, expecting a perfect overlap is not a just comparison method. In fact, the values of the obtained Dice-coefficients are high and within the expected normal intra-observer variability, with a mean value of 0.91 (range: 0.86-0.95).

The mismatch shows that the PET scan information gives no unanimous increase or decrease of the CTV. If all the CTV(+PET) would be extending outside of the CTV(-PET), then the mismatch CTV(-PET)/CT(+PET) would be zero. Since neither this nor the opposite is the case, the results indicate that the PET scan can in fact result in removing as well as including some areas of suspicion. The impact of PET on the shape of the target volumes is most visible in cases where PET gives useful information regarding lymph nodes. Two patients where PET rendered some of the smallest and the largest changes of shape as well as size are shown in Figure 34 and Figure 35 below.

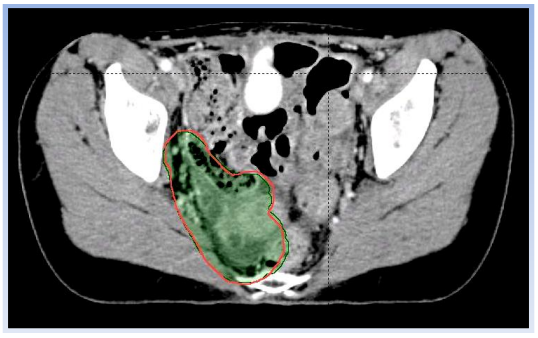

**Figure 34: Patient nr 2.**
**The green CTV is without and the red CTV is with PET.**

**Figure 35: Patient nr 6.**
**The green CTV is without and the red CTV is with PET.**

## NTCP & SC

The calculated risks for normal tissue complications and secondary cancers shall not be used as absolute risk values, due to the large uncertainties in the models. Even so, the risk estimations do allow for rough relative comparisons between the treatment modalities, but still with reservations for the large confidence intervals.

Even though the results are unsuited for absolute risk comparisons, they may come across as remarkably and unexpectedly high. However, the risk of late complications for childhood cancer survivors is indeed very high and their life expectancy is significantly reduced. It has been estimated that 5-year survivors, diagnosed with cancer at the age of 10, will lose about 10 years (118). Not taking the risk of dying from relapses into account, the loss in life expectancy is about 6 years.

A probable assumption is that larger treatment volumes general will result in elevated risks of secondary cancers as well as normal tissue complications. This work on pediatric sarcomas and head and neck cancers does not reveal any correlation between the use of PET in pediatric radiation therapy treatment planning and the size of the treatment volumes, and no distinct increase or decrease in the estimated risks. A plausible reason for this is the small number of patients in the study: in a different and larger group of patients there might be more distinct differences between the target volumes with and without PET. It is also possible that any distinct differences are lost as a result of generous target-delineation or too wide collimator openings, possibly extinguishing any differences for the photon modalities.

All of the NTCP-models used are derived from photon therapy data and the relative biological effectiveness (RBE) is slightly higher for proton radiation than photons. This might increase the uncertainties of the risks estimated for the IMPT-plans, but will probably be negligible compared to other uncertainties in the models.

## PET/CT

The mean dose of 30.3 mSv (range: 11 to 71 mSv) is slightly higher than the values found for pediatric patients in up-to-date publications: 24.8 mSv (range: 6.2 to 60.7 mSv) (2) and 19.8 mSv (range: 12.1 to 27.8 mSv) (119). For the eleven patients in this work, the FDG-PET caused approximately 64% of the total effective PET/CT dose (range: 11% to 160%). However, it must be pointed out that the patients in this study have been scanned between the years 2005 and 2011. The current clinical routine at Rigshospitalet is to administer 3.0 MBq FDG per kg body weight for PET scanning of pediatric patients, to compare with the average of 5.3 MBq per kg for the patients in this study (range: 3.1 to 7.3).

Despite the increasing use of PET/CT, with FDG as the most commonly used tracer, there are large uncertainties in the internal dose estimates. There is a large need for studies and data to refine them, especially for pediatric patients. The dose-data from ICRP has been accused of relying on outdated studies and recently published articles show absorbed dose estimates that differ significantly from those in ICRP reports (120).

The calculated doses and the risks from the PET/CT scan are probably the part associated with largest uncertainties in this study. Improved methods to estimate the risks of PET/CT scanning of pediatric patients would be desirable. The estimated cumulative EAR of developing a solid cancer from this exposure ranges from 0.43 % to 2.93 %, with a mean value of 1.04 %. These estimations are most likely overestimated, since the model is not designed for calculations of the cumulative lifetime risk.

This study and the models used do not allow for any detailed comparisons between the risks associated with a PET/CT scan and the risks of the radiation therapy treatment. As mentioned above, the PET/CT scan on average increases the cumulative lifetime risk of any solid cancer about 1% whereas the risk of acquiring the specific therapy-induced secondary cancers included in the study is much higher: for abdomino-pelvic-thoracic patients the mean cumulative lifetime risk of developing secondary cancer in the ventricle and lungs is about 8.4 % and 13.7 % respectively. For head and neck patients, the mean cumulative lifetime risk of developing thyroid cancer due to their radiation therapy is approximately 12 %.

The BEIR VII lifetime risk model predicts that approximately one individual (adult) in 100 persons would be expected to develop solid cancer or leukemia from a dose of 100 mSv, to compare with 42 out of 100 persons that would be expected to develop the same diseases from other causes (114). Lower doses produce proportionally lower risks, and exposure of 10 mSv is predicted to induce cancer in one individual in 1000.

This study only includes the doses from the radiation therapy planning PET/CT scan. It is however common for pediatric cancer patients to go through more than one PET/CT scan; for some patients the therapeutic PET/CT scan is done a short time after a diagnostic CT or PET/CT, and the post-treatment status is usually evaluated by a scan a couple of months after the last fractionation. Additionally, the use of real-time imaging techniques at the linear accelerator to ensure the accuracy of the treatment is increasing. Although the radiation dose from each single scan is small compared with the therapeutic dose, this repeated – often daily – imaging can lead to non-negligible cumulative exposures and possibly an increased risk of complications including secondary malignancies.
The importance of applying the ALARA principle as well as establishing standards of frequency, interval and number of needed PET/CT scans is of outmost importance in the management of pediatric malignancies. The improvement in detector materials and CT technique has reduced the doses and they might decrease somewhat further. Hopefully, the clinical implementation of PET/MR will result in fewer CT scans, without compromising the diagnostic information.

# 6. Conclusion

Looking back at the questions this thesis was hoping to answer:

1. Does PET change the size of the target volumes?
2. Does PET change the shape of the target volumes?
3. Does PET improve the outcome of radiation therapy in terms of reduced normal tissue toxicity and/or secondary cancer risk?
4. If there are any benefits from using PET in radiation therapy planning, do they depend on the choice of treatment technique?

According to the results in this work the answers are as following:

1. No, not significantly.
2. For some patients, yes.
3. No, not for the limited number of patients included in this study.
4. No, not for the limited number of patients included in this study.

The risk of radiation-induced side effects from the PET/CT scan is very low compared to the risks associated with the radiation therapy as well as other treatments for pediatric cancer. The risks associated with irradiating large volumes of healthy tissues as well as the risks evolving from failed local control of the primary disease are also much more prominent that the risks of a PET/CT scan.

The results presented in this thesis indicate that including PET into the radiation therapy treatment planning process does not increase the risks of the treatment related side effects studied. Provided that the tumor control is unchanged, the quality of the plans is maintained when PET-data is available to the target volume delineators. The plans appear to be of comparable quality (provided that the therapeutic efficacy is maintained) and the risk of long-term complications is not changed.

Published results from more than a decade of clinical experience, emphasizes the usefulness of PET/CT in the care of cancer patients and for now there is no reason to assume that this would be different for children (4, 12, 17, 23-28, 32-35). Adding this knowledge to the results presented in this work, there seem to be no apparent reason to avoid PET/CT scanning of pediatric cancer patients to help define the target volume. In fact, the only possible conclusion is that PET should be used as a complementary tool in target volume delineation for radiation therapy planning of pediatric patients.

# 7. Future prospects

Despite the low effective doses from a PET/CT scan of a pediatric patient, it is always mandatory to justify the medical use of ionizing radiation – especially when exposing pediatric patients.

The improvements in diagnostic accuracy and a target delineation more coherent with biopsy results achieved with PET/CT has been shown in many studies (15, 24, 121). Without a doubt, the PET scan can be of great importance for the treatment of the individual patient, but in the present study it does not appear to impact the estimated risks of NTC or SC.

Is there any general impact of including PET in radiation therapy planning for pediatric cancer?
Assuming the target volumes delineated with PET can be regarded as true, what happens if the no-PET plans are applied onto the PET-based volumes?

The resulting target coverage and dose-distribution is evaluated, mainly from the DVH:s (Appendix E):
For some patients, where PTV(+PET) is smaller than PTV(-PET), the dose-coverage is better for the smaller PTV (e.g. patient nr 1 (PETped01)).
As could be expected, the equivalence is also seen: a poorer dose-coverage for PTV(+PET) when this volume is larger than PTV(-PET) (e.g. patient nr 2 (PETped09), patient nr 4 (PETped10), patient nr 11 (PETped12) and the PTV in the neck of patient nr 5 (PETped04)). In two of the four patients where this could be seen, the decreased dose-coverage is evident in all modalities, while for the other two patients it is most distinct in the IMRT-, IMPT- and IMAT-plans.
There are patients with more or less identical dose-coverage of the PTV:s, regardless of the PET-based PTV being smaller (e.g. patient nr 3 (PETped03) and patient nr 6 (PETped20)) or larger than PTV(-PET) (e.g. patient nr 10 (PETped11)).

The most interesting observation is found in the DVH:s of patient number 7 (PETped06). The target coverage of PTV(+PET) is deteriorated for all modalities but 3DCRT, even though this PET-based PTV is smaller than PTV(-PET). This indicates that the change of the shape of the PTV, caused by including the PET-information, is enough to have an impact of the target coverage. In other words, the PET-based PTV may be smaller than the PTV(-PET), but the PET-information results in a PTV(+PET) with a different shape. This shape discrepancy can be large enough to compromise the dose-coverage of the PTV(+PET) in a plan optimized for the PTV(-PET).
The same tendency is visible for the target volume in the lower back of patient nr 5 (PETped04), where the dose-distribution to the PTV(+PET) is inferior in two of the modalities (IMAT and IMPT). However, since this is one of the PET-negative patients, the effect cannot entirely be explained by whether or not information from a PET scan is included into the delineation process.

Whether proton therapy would benefit from different margins cannot be determined from these eleven patients. A vague tendency towards an increased importance of PET in the most conformal treatment modalities can be seen, but this study is too small to make any definitive statements. Further studies are required to provide generally applicable results regarding the impact of PET on the most conform treatment modalities.

# Abbreviations and terminology

| | |
|---|---|
| CBCT | Cone-Beam CT |
| CCSS | Childhood Cancer Survivor Study<br>The CCSS is a retrospective cohort study investigating health outcomes of cancer survivor diagnosed and treated between 1970 and 1986, compared to a sibling cohort. It is an American multi-institutional collaborative study of individuals who survived at least five years after being diagnosed with cancer during childhood or adolescence. |
| CI | Confidence Interval (statistical) |
| CI | Conformity Index |
| (3D)CRT | (Three-dimensional) Conformal Radiation Therapy |
| CTV | Clinical Target Volume<br>The CTV is a tissue volume that contains the GTV and any subclinical microscopic malignant disease (as defined by ICRU and ICRU 62). Thus, the CTV is an anatomical concept. |
| EAR | Exess Absolute Risk<br>The rate of disease in an exposed population minus the rate of disease in an unexposed population |
| EHR | Excess Hazard Ratio |
| EPID | Electronic Portal Imaging Device |
| ERR | The rate of disease in an exposed population divided by the rate of disease in an unexposed population, minus 1.0. |
| GTV | Gross Tumor Volume.<br>The GTV is the gross palpable or visible/demonstrable extent and location of the malignant growth (as defined by ICRU and ICRU 62). In this work, the notations GTV(-PET) and GTV(+PET) means GTV delineated with and without PET information. |
| HR | Hazard Ratio |
| IMAT | Intensity-Modulated Arc Therapy |
| IMPT | Intensity-Modulated Proton Therapy |
| IMRT | Intensity-Modulated Radiation Therapy |
| MRI | Magnetic Resonance Imaging |
| NAL | No Action Limit |
| NTCP | Normal Tissue Complication Probability |
| OAR (OR) | Organs At Risk<br>Normal tissues whose radiation sensitivity may significantly influence the treatment planning and/or the prescribed dose. |
| PET | Positron Emission Tomography |
| PRV | Planning Risk Volume |
| PTV | Planning Target Volume.<br>The PTV is a geometrical concept encompassing the CTV. The PTV must be large enough to ensure that the prescribed dose is delivered to the CTV, taking into consideration the net effect of all possible geometrical variations and inaccuracies (as defined by ICRU and ICRU 62). |
| QUANTEC | Quantitative Analyses of Normal Tissue Effects in the Clinic |

| | |
|---|---|
| RR | Relative Risk |
| RTOG | Radiation Therapy Oncology Group.<br>A scoring criteria commonly used to report toxicities induced by radiation therapy. |
| SC | Secondary Cancer/s |
| SD | Standard Deviation |
| US | Ultrasound |

# Appendix A

## **Patient 1** (PETped01)

| | Heart Failure HR (95% CI) | Myoc. Infarction HR (95% CI) | Peric. Disease HR (95% CI) | Valvular Abnorm. HR (95% CI) | Radiation nephropathy bilateral P (95% CI) | Liver disease P | GI toxicity P | Late rectal toxicity P |
|---|---|---|---|---|---|---|---|---|
| **CRT noPET** | 1.09 (1.02-1.19) | 1.07 (1.00-1.23) | 1.09 (1.00-1.27) | 1.11 (1.00-1.37) | 91.40% (79.69-100) | 0.00% | 100% | 0.00% |
| **CRT wPET** | 1.09 (1.02-1.17) | 1.06 (1.00-1.22) | 1.09 (1.00-1.25) | 1.11 (1.00-1.35) | 89.75% (76.36-100) | 0.00% | 100% | 0.00% |
| **IMRT noPET** | 1.08 (1.02-1.15) | 1.05 (1.00-1.18) | 1.07 (1.00-1.21) | 1.09 (1.00-1.30) | 90.79% (78.45-100) | 0.00% | 100% | 0.00% |
| **IMRT wPET** | 1.07 (1.02-1.15) | 1.05 (1.00-1.18) | 1.07 (1.00-1.21) | 1.09 (1.00-1.30) | 90.51% (77.89-100) | 0.00% | 100% | 0.00% |
| **IMPT noPET** | 1.00 (1.00-1.00) | 1.00 (1.00-1.00) | 1.00 (1.00-1.00) | 1.00 (1.00-1.00) | 73.10% (54.89-100) | 0.00% | 100% | 0.00% |
| **IMPT wPET** | 1.00 (1.00-1.00) | 1.00 (1.00-1.00) | 1.00 (1.00-1.00) | 1.00 (1.00-1.00) | 73.63% (48.91-98.36) | 0.00% | 99.99% | 0.00% |
| **IMAT noPET** | 1.08 (1.02-1.15) | 1.06 (1.00-1.19) | 1.07 (1.00-1.22) | 1.09 (1.00-1.31) | 80.90% (60.22-100) | 0.00% | 100% | 0.00% |
| **IMAT wPET** | 1.08 (1.02-1.15) | 1.06 (1.00-1.19) | 1.07 (1.00-1.22) | 1.10 (1.00-1.31) | 81.00% (60.38-100) | 0.00% | 100% | 0.00% |

Table 26: NTCP, Patient 1.

| | V95 PTV | V107 PTV | CI PTV | CI Volume for symmetric bone irradiation |
|---|---|---|---|---|
| **CRT noPET** | 0.89 | 0.01 | 0.89 | 0.99 |
| **CRT wPET** | 0.91 | 0.00 | 0.91 | 0.99 |
| **IMRT noPET** | 0.91 | 0.01 | 0.91 | 1.00 |
| **IMRT wPET** | 0.92 | 0.00 | 0.92 | 1.00 |
| **Proton noPET** | 0.96 | 0.00 | 0.96 | 1.00 |
| **Proton wPET** | 0.96 | 0.00 | 0.96 | 1.00 |
| **RA noPET** | 0.84 | 0.01 | 0.84 | 0.99 |
| **RA wPET** | 0.88 | 0.00 | 0.88 | 1.00 |

Table 27: Target coverage, Patient 1.

| | Breast cancer | Lung cancer | Thyroid cancer | Ventricle cancer |
|---|---|---|---|---|
| CRT noPET | -- | -- | -- | 52.67% |
| CRT wPET | -- | -- | -- | 51.45% |
| IMRT noPET | -- | -- | -- | 44.77% |
| IMRT wPET | -- | -- | -- | 49.99% |
| IMPT noPET | -- | -- | -- | 22.43% |
| IMPT wPET | -- | -- | -- | 22.61% |
| IMAT noPET | -- | -- | -- | 40.41% |
| IMAT wPET | -- | -- | -- | 42.09% |

Table 28: Cumulative lifetime risk of secondary cancer, Patient 1.

| | NTCP | Conformity Index, PTV | Secondary Cancer |
|---|---|---|---|
| 3DCRT | 0.180 | 0.109 | 0.273 |
| IMRT | 0.180 | | |
| IMPT | 0.655 | | |
| IMAT | 0.180 | | |

Table 29: Significance, p-values (related samples Wilcoxon signed rank test), Patient 1.

For Patient 1, including PET did not significantly change the NTCP, the conformity indexes or the risk of developing secondary cancer.

## **Patient 2** (PETped09)

| | Heart Failure HR (95% CI) | Myoc. Infarction HR (95% CI) | Peric. Disease HR (95% CI) | Valvular Abnorm. HR (95% CI) | Pneum. P (95% CI) | Radiation nephropathy bilateral P (95% CI) | Liver disease P | GI toxicity P | Late rectal toxicity P |
|---|---|---|---|---|---|---|---|---|---|
| **CRT noPET** | 1.00 (1.00-1.00) | 1.00 (1.00-1.00) | 1.00 (1.00-1.00) | 1.00 (1.00-1.00) | 2.03% (0.85-3.20) | 0.05% (0.00-0.10) | 0.00% | 63.05% | 0.26% |
| **CRT wPET** | 1.00 (1.00-1.00) | 1.00 (1.00-1.00) | 1.00 (1.00-1.00) | 1.00 (1.00-1.00) | 2.03% (0.85-3.20) | 0.05% (0.00-0.10) | 0.00% | 66.19% | 0.26% |
| **IMRT noPET** | 1.00 (1.00-1.00) | 1.00 (1.00-1.00) | 1.00 (1.00-1.00) | 1.00 (1.00-1.00) | 2.03% (0.85-3.20) | 0.05% (0.00-0.10) | 0.00% | 56.55% | 0.20% |
| **IMRT wPET** | 1.00 (1.00-1.00) | 1.00 (1.00-1.00) | 1.00 (1.00-1.00) | 1.00 (1.00-1.00) | 2.03% (0.85-3.20) | 0.05% (0.00-0.10) | 0.00% | 54.75% | 0.22% |
| **IMPT noPET** | 1.00 (1.00-1.00) | 1.00 (1.00-1.00) | 1.00 (1.00-1.00) | 1.00 (1.00-1.00) | 2.03% (0.85-3.20) | 0.05% (0.00-0.10) | 0.00% | 46.34% | 0.15% |
| **IMPT wPET** | 1.00 (1.00-1.00) | 1.00 (1.00-1.00) | 1.00 (1.00-1.00) | 1.00 (1.00-1.00) | 2.03% (0.85-3.20) | 0.05% (0.00-0.10) | 0.00% | 46.96% | 0.14% |
| **IMAT noPET** | 1.00 (1.00-1.00) | 1.00 (1.00-1.00) | 1.00 (1.00-1.00) | 1.00 (1.00-1.00) | 2.03% (0.85-3.20) | 0.05% (0.00-0.10) | 0.00% | 46.35% | 0.09% |
| **IMAT wPET** | 1.00 (1.00-1.00) | 1.00 (1.00-1.00) | 1.00 (1.00-1.00) | 1.00 (1.00-1.00) | 2.03% (0.85-3.20) | 0.05% (0.00-0.10) | 0.00% | 46.54% | 0.10% |

Table 30: NTCP, Patient 2.

| | V95 PTV | V107 PTV | CI PTV | CI Volume for symmetric bone irradiation |
|---|---|---|---|---|
| **CRT noPET** | 0.97 | 0.00 | 0.96 | 1.00 |
| **CRT wPET** | 0.97 | 0.00 | 0.97 | 1.00 |
| **IMRT noPET** | 0.99 | 0.00 | 0.99 | 0.99 |
| **IMRT wPET** | 1.00 | 0.00 | 1.00 | 0.99 |
| **Proton noPET** | 0.96 | 0.00 | 0.96 | 1.00 |
| **Proton wPET** | 0.99 | 0.00 | 0.99 | 1.00 |
| **RA noPET** | 1.00 | 0.00 | 1.00 | 1.00 |
| **RA wPET** | 1.00 | 0.00 | 1.00 | 1.00 |

Table 31: Target coverage, Patient 2.

| | Breast cancer | Lung cancer | Thyroid cancer | Ventricle cancer |
|---|---|---|---|---|
| CRT noPET | 0.04% | 0.03% | -- | 0.03% |
| CRT wPET | 0.04% | 0.03% | -- | 0.03% |
| IMRT noPET | 0.04% | 0.03% | -- | 0.00% |
| IMRT wPET | 0.04% | 0.03% | -- | 0.03% |
| IMPT noPET | 0.04% | 0.03% | -- | 0.03% |
| IMPT wPET | 0.04% | 0.03% | -- | 0.03% |
| IMAT noPET | 0.04% | 0.03% | -- | 0.03% |
| IMAT wPET | 0.04% | 0.03% | -- | 0.03% |

Table 32: Cumulative lifetime risk of secondary cancer, Patient 2.

| | NTCP | Conformity Index, PTV | Secondary Cancer |
|---|---|---|---|
| 3DCRT | 0.317 | 0.102 | 0.317 |
| IMRT | 0.655 | | |
| IMPT | 0.655 | | |
| IMAT | 0.180 | | |

Table 33: Significance, p-values (related samples Wilcoxon signed rank test), Patient 2.

For Patient 2, including PET did not significantly change the NTCP, the risk of developing secondary cancer or the conformity index.

## **Patient 3** (PETped03)

| | Heart Failure HR (95% CI) | Myoc. Infarction HR (95% CI) | Peric. Disease HR (95% CI) | Valvular Abnorm. HR (95% CI) | Pneum. P (95% CI) | Esophag. complic. P | Xero. Bilateral P | Hypothyr. P (95% CI) | Blindness P (95% CI) | Ototox. P (95% CI) |
|---|---|---|---|---|---|---|---|---|---|---|
| **CRT noPET** | 1.06 (1.02-1.12) | 1.05 (1.00-1.15) | 1.06 (1.00-1.18) | 1.08 (1.00-1.25) | 3.06% (1.48-4.64) | 20.00% | 4.42% | 92.99% (83.54-100) | 0.70% (0.63-1.30) | 0.12% (0.00-0.75) |
| **CRT wPET** | 1.04 (1.01-1.09) | 1.03 (1.00-1.10) | 1.04 (1.00-1.12) | 1.05 (1.00-1.17) | 2.89% (1.38-4.41) | 18.22% | 4.20% | 92.90% (83.37-100) | 0.69% (0.62-1.28) | 0.12% (0.00-0.75) |
| **IMRT noPET** | 1.04 (1.01-1.08) | 1.03 (1.00-1.10) | 1.04 (1.00-1.11) | 1.05 (1.00-1.16) | 4.00% (2.10-5.90) | 14.22% | 2.98% | 91.86% (81.49-100) | 0.67% (0.61-1.16) | 0.10% (0.00-0.63) |
| **IMRT wPET** | 1.04 (1.01-1.08) | 1.03 (1.00-1.10) | 1.04 (1.00-1.12) | 1.05 (1.00-1.16) | 4.12% (2.18-6.06) | 13.62% | 3.10% | 91.21% (80.34-100) | 0.68% (0.62-1.24) | 0.10% (0.00-0.64) |
| **IMPT noPET** | 1.00 (1.00-1.00) | 1.00 (1.00-1.00) | 1.00 (1.00-1.00) | 1.00 (1.00-1.00) | 2.71% (1.26-4.15) | 14.14% | 1.80% | 91.07% (80.10-100) | 0.53% (0.53-0.55) | 0.09% (0.00-0.60) |
| **IMPT wPET** | 1.00 (1.00-1.00) | 1.00 (1.00-1.00) | 1.00 (1.00-1.00) | 1.00 (1.00-1.00) | 2.66% (1.23-4.09) | 13.67% | 1.80% | 90.72% (79.49-100) | 0.53% (0.53-0.55) | 0.09% (0.00-0.60) |
| **IMAT noPET** | 1.12 (1.03-1.24) | 1.09 (1.00-1.29) | 1.12 (1.00-1.34) | 1.15 (1.00-1.48) | 5.11% (2.88-7.35) | 14.51% | 1.68% | 91.38% (80.63-100) | 0.88% (0.73-2.12) | 0.11% (0.00-0.70) |
| **IMAT wPET** | 1.09 (1.00-1.17) | 1.06 (1.00-1.21) | 1.08 (1.00-1.24) | 1.10 (1.00-1.34) | 4.67% (2.57-6.78) | 14.43% | 1.89% | 91.32% (80.53-100) | 0.89% (0.74-2.18) | 0.13% (0.00-0.77) |

**Table 34: NTCP, Patient 3.**

| | V95 PTV | V107 PTV | CI PTV |
|---|---|---|---|
| **CRT noPET** | 0.87 | 0.00 | 0.87 |
| **CRT wPET** | 0.86 | 0.00 | 0.86 |
| **IMRT noPET** | 0.94 | 0.00 | 0.94 |
| **IMRT wPET** | 0.98 | 0.00 | 0.97 |
| **Proton noPET** | 0.95 | 0.00 | 0.95 |
| **Proton wPET** | 0.94 | 0.00 | 0.94 |
| **RA noPET** | 0.95 | 0.00 | 0.95 |
| **RA wPET** | 0.91 | 0.00 | 0.91 |

**Table 35: Target coverage, Patient 3.**

| | Breast cancer | Lung cancer | Thyroid cancer | Ventricle cancer |
|---|---|---|---|---|
| CRT noPET | 1.99% | 7.01% | 0.15% | -- |
| CRT wPET | 1.85% | 6.08% | 0.16% | -- |
| IMRT noPET | 0.62% | 11.61% | 0.26% | -- |
| IMRT wPET | 0.66% | 12.12 % | 0.31% | -- |
| IMPT noPET | 0.04% | 4.92 % | 0.36 | -- |
| IMPT wPET | 0.04% | 4.65% | 0.48% | -- |
| IMAT noPET | 1.44% | 15.86% | 0.30% | -- |
| IMAT wPET | 1.21% | 14.31% | 0.32% | -- |

Table 36: Cumulative lifetime risk of secondary cancer, Patient 3.

| | NTCP | Conformity Index, PTV | Secondary Cancer |
|---|---|---|---|
| 3DCRT | 0.007 | 0.461 | 0.424 |
| IMRT | 0.684 | | |
| IMPT | 0.109 | | |
| IMAT | 0.114 | | |

Table 37: Significance, p-values (related samples Wilcoxon signed rank test), Patient 3.

For Patient 3, including PET did not significantly change the NTCP, except for the 3DCRT plans (significance level is 0.05): the estimated risks of normal tissue complications are significantly lower with PET.
PET did not significantly change the risk of developing secondary cancer or the conformity index.

## **Patient 4** (PETped10)

| | Heart Failure HR (95% CI) | Myoc. Infarction HR (95% CI) | Peric. Disease HR (95% CI) | Valvular Abnorm. HR (95% CI) | Pneum. P (95% CI) | Radiation nephropathy bilateral P (95% CI) | Liver disease P | GI toxicity P | Late rectal toxicity P |
|---|---|---|---|---|---|---|---|---|---|
| **CRT noPET** | 1.00 (1.00-1.00) | 1.00 (1.00-1.00) | 1.00 (1.00-1.00) | 1.00 (1.00-1.00) | 2.03% (0.85-3.20) | 0.05% (0.00-0.10) | 0.00% | 0.84% | 0.00% |
| **CRT wPET** | 1.00 (1.00-1.00) | 1.00 (1.00-1.00) | 1.00 (1.00-1.00) | 1.00 (1.00-1.00) | 2.03% (0.85-3.20) | 0.05% (0.00-0.10) | 0.00% | 0.90% | 0.00% |
| **IMRT noPET** | 1.00 (1.00-1.00) | 1.00 (1.00-1.00) | 1.00 (1.00-1.00) | 1.00 (1.00-1.00) | 2.03% (0.85-3.20) | 0.05% (0.00-0.10) | 0.00% | 0.72% | 0.00% |
| **IMRT wPET** | 1.00 (1.00-1.00) | 1.00 (1.00-1.00) | 1.00 (1.00-1.00) | 1.00 (1.00-1.00) | 2.03% (0.85-3.20) | 0.05% (0.00-0.10) | 0.00% | 0.59% | 0.00% |
| **IMPT noPET** | 1.00 (1.00-1.00) | 1.00 (1.00-1.00) | 1.00 (1.00-1.00) | 1.00 (1.00-1.00) | 2.03% (0.85-3.20) | 0.05% (0.00-0.10) | 0.00% | 0.46% | 0.00% |
| **IMPT wPET** | 1.00 (1.00-1.00) | 1.00 (1.00-1.00) | 1.00 (1.00-1.00) | 1.00 (1.00-1.00) | 2.03% (0.85-3.20) | 0.05% (0.00-0.10) | 0.00% | 0.44% | 0.00% |
| **IMAT noPET** | 1.00 (1.00-1.00) | 1.00 (1.00-1.00) | 1.00 (1.00-1.00) | 1.00 (1.00-1.00) | 2.03% (0.85-3.20) | 0.05% (0.00-0.10) | 0.00% | 0.45% | 0.00% |
| **IMAT wPET** | 1.00 (1.00-1.00) | 1.00 (1.00-1.00) | 1.00 (1.00-1.00) | 1.00 (1.00-1.00) | 2.03% (0.85-3.20) | 0.05% (0.00-0.10) | 0.00% | 0.46% | 0.00% |

Table 38: NTCP, Patient 4.

| | V95 PTV | V107 PTV | CI PTV |
|---|---|---|---|
| **CRT noPET** | 0.96 | 0.00 | 0.95 |
| **CRT wPET** | 0.94 | 0.00 | 0.93 |
| **IMRT noPET** | 0.97 | 0.00 | 0.97 |
| **IMRT wPET** | 0.98 | 0.00 | 0.98 |
| **Proton noPET** | 1.00 | 0.00 | 1.00 |
| **Proton wPET** | 1.00 | 0.00 | 1.00 |
| **RA noPET** | 0.98 | 0.00 | 0.98 |
| **RA wPET** | 0.99 | 0.00 | 0.99 |

Table 39: Target coverage, Patient 4.

| | Breast cancer | Lung cancer | Thyroid cancer | Ventricle cancer |
|---|---|---|---|---|
| CRT noPET | -- | 0.03% | -- | 0.04% |
| CRT wPET | -- | 0.03% | -- | 0.04% |
| IMRT noPET | -- | 0.03% | -- | 0.01% |
| IMRT wPET | -- | 0.03% | -- | 0.01% |
| IMPT noPET | -- | 0.03% | -- | 0.02% |
| IMPT wPET | -- | 0.03% | -- | 0.02% |
| IMAT noPET | -- | 0.03% | -- | 0.02% |
| IMAT wPET | -- | 0.03% | -- | 0.03% |

Table 40: Cumulative lifetime risk of secondary cancer, Patient 4.

| | NTCP | Conformity Index, PTV | Secondary Cancer |
|---|---|---|---|
| 3DCRT | 0.317 | 1.000 | 0.317 |
| IMRT | 0.317 | | |
| IMPT | 0.317 | | |
| IMAT | 0.317 | | |

Table 41: Significance, p-values (related samples Wilcoxon signed rank test), Patient 4.

For Patient 4, including PET did not significantly change the NTCP, the risk of developing secondary cancer or the conformity index.

## Patient 5 (PETped04)

| | Heart Failure HR (95% CI) | Myoc. Infarction HR (95% CI) | Peric. Disease HR (95% CI) | Valvular Abnorm. HR (95% CI) | Pneum. P (95% CI) | GI toxicity P | Xero. Bilateral P | Hypothyr. P (95% CI) | Blindness P (95% CI) | Ototox. P (95% CI) |
|---|---|---|---|---|---|---|---|---|---|---|
| **CRT noPET** | 1.00 (1.00-1.01) | 1.00 (1.00-1.01) | 1.00 (1.00-1.01) | 1.00 (1.00-1.01) | 2.06% (0.87-3.26) | 0.10% | 4.20% | 29.22% (21.12-37.31) | 0.99% (0.80-2.64) | 0.85% (0.00-4.23) |
| **CRT wPET** | 1.00 (1.00-1.01) | 1.00 (1.00-1.01) | 1.00 (1.00-1.01) | 1.00 (1.00-1.01) | 2.07% (0.88-3.27) | 0.10% | 4.34% | 29.50% (21.34-37.65) | 0.99% (0.80-2.64) | 0.87% (0.00-4.29) |
| **IMRT noPET** | 1.00 (1.00-1.01) | 1.00 (1.00-1.01) | 1.00 (1.00-1.01) | 1.00 (1.00-1.01) | 2.05% (0.87-3.24) | 0.07% | 1.94% | 19.37% (12.68-26.05) | 1.55% (1.13-5.16) | 0.40% (0.00-2.13) |
| **IMRT wPET** | 1.00 (1.00-1.01) | 1.00 (1.00-1.01) | 1.00 (1.00-1.01) | 1.00 (1.00-1.01) | 2.06% (0.87-3.25) | 0.05% | 1.91% | 21.71% (14.77-28.64) | 1.52% (1.11-5.02) | 0.33% (0.00-1.80) |
| **IMPT noPET** | 1.00 (1.00-1.00) | 1.00 (1.00-1.00) | 1.00 (1.00-1.00) | 1.00 (1.00-1.00) | 2.02% (0.85-3.20) | 0.05% | 1.21% | 18.07% (11.51-24.63) | 0.53% (0.53-0.55) | 0.23% (0.00-1.28) |
| **IMPT wPET** | 1.00 (1.00-1.00) | 1.00 (1.00-1.00) | 1.00 (1.00-1.00) | 1.00 (1.00-1.00) | 2.03% (0.85-3.20) | 0.04% | 1.31% | 17.54% (11.03-24.05) | 0.53% (0.53-0.55) | 0.24% (0.00-1.35) |
| **IMAT noPET** | 1.00 (1.00-1.01) | 1.00 (1.00-1.01) | 1.00 (1.00-1.01) | 1.00 (1.00-1.01) | 2.05% (0.86-3.24) | 0.03% | 1.45% | 17.99% (11.43-24.54) | 0.76% (0.66-1.60) | 0.62% (0.00-3.17) |
| **IMAT wPET** | 1.00 (1.00-1.01) | 1.00 (1.00-1.01) | 1.00 (1.00-1.01) | 1.00 (1.00-1.01) | 2.06% (0.87-3.25) | 0.03% | 1.50% | 18.09% (11.53-24.65) | 0.72% (0.64-1.40) | 0.60% (0.00-3.04) |

Table 42: NTCP, Patient 5.

| | V95 PTV | V107 PTV | CI PTV neck | CI PTV Lower back | CI PTV Mean |
|---|---|---|---|---|---|
| **CRT noPET** | 0.99 | 0.00 | 0.99 | 0.98 | 0.99 |
| **CRT wPET** | 0.99 | 0.00 | 0.99 | 0.98 | 0.98 |
| **IMRT noPET** | 0.95 | 0.00 | 0.94 | 0.94 | 0.94 |
| **IMRT wPET** | 0.96 | 0.00 | 0.98 | 0.94 | 0.96 |
| **Proton noPET** | 0.97 | 0.00 | 0.94 | 0.99 | 0.97 |
| **Proton wPET** | 0.97 | 0.00 | 0.93 | 0.99 | 0.96 |
| **RA noPET** | 0.96 | 0.00 | 0.93 | 0.97 | 0.95 |
| **RA wPET** | 0.96 | 0.00 | 0.97 | 0.97 | 0.97 |

Table 43: Target coverage, Patient 5.

| | Breast cancer | Lung cancer | Thyroid cancer | Ventricle cancer |
|---|---|---|---|---|
| CRT noPET | 0.20% | 0.33% | 30.78% | 0.16% |
| CRT wPET | 0.21% | 0.40% | 30.89% | 0.72% |
| IMRT noPET | 0.16% | 0.25% | 19.90% | 0.01% |
| IMRT wPET | 0.17% | 0.29% | 23.48% | 0.21% |
| IMPT noPET | 0.04% | 0.01% | 16.35% | 0.03 % |
| IMPT wPET | 0.04% | 0.02% | 15.38% | 0.03 % |
| IMAT noPET | 0.08% | 0.22% | 17.29% | 0.06% |
| IMAT wPET | 0.14% | 0.28% | 17.31% | 0.17% |

Table 44: Cumulative lifetime risk of secondary cancer, Patient 5.

| | NTCP | Conformity Index, PTV | Secondary Cancer |
|---|---|---|---|
| 3DCRT | 0.068 | 0.458 | 0.013 |
| IMRT | 0.462 | | |
| IMPT | 0.891 | | |
| IMAT | 0.500 | | |

Table 45: Significance, p-values, Patient 5.

For Patient 5, including PET did not significantly change the NTCP or the conformity index. However, the risk of developing secondary cancer was significantly increased for the PET-based plans. The numbers for secondary stomach cancer are the main contributors to this result, and it should be noticed that for no modality – without or with PET – is the lifetime cumulative risk above 1%.

## **Patient 6** (PETped20)

| | Heart Failure HR (95% CI) | Myoc. Infarction HR (95% CI) | Peric. Disease HR (95% CI) | Valvular Abnorm. HR (95% CI) | Pneum. P (95% CI) | Xero. Bilateral P | Hypothyr. P (95% CI) | Blindness P (95% CI) | Ototox. P (95% CI) |
|---|---|---|---|---|---|---|---|---|---|
| **CRT noPET** | 1.01 (1.00-1.02) | 1.01 (1.00-1.02) | 1.01 (1.00-1.02) | 1.01 (1.00-1.03) | 2.09% (0.89-3.29) | 77.78% | 26.46% (18.86-34.05) | 0.76% (0.60-1.60) | 0.95% (0.00-4.66) |
| **CRT wPET** | 1.01 (1.00-1.01) | 1.01 (1.00-1.02) | 1.01 (1.00-1.02) | 1.01 (1.00-1.03) | 2.08% (0.88-3.28) | 75.63% | 26.00% (18.47-33.52) | 0.70% (0.58-1.34) | 0.43% (0.00-2.25) |
| **IMRT noPET** | 1.01 (1.00-1.02) | 1.01 (1.00-1.02) | 1.01 (1.00-1.03) | 1.01 (1.00-1.04) | 2.12% (0.90-3.33) | 62.75% | 27.86% (20.02-35.69) | 0.96% (0.66-2.53) | 3.06% (0.00-14.14) |
| **IMRT wPET** | 1.01 (1.00-1.02) | 1.01 (1.00-1.02) | 1.01 (1.00-1.02) | 1.01 (1.00-1.03) | 2.11% (0.90-3.32) | 59.60% | 27.27% (19.53-35.00) | 0.83% (0.62-1.95) | 1.08% (0.00-5.23) |
| **IMPT noPET** | 1.00 (1.00-1.00) | 1.00 (1.00-1.00) | 1.00 (1.00-1.00) | 1.00 (1.00-1.00) | 2.02% (0.85-3.20) | 53.54% | 30.20% (21.90-38.50) | 2.75% (1.24-10.81) | 0.87% (0.00-4.29) |
| **IMPT wPET** | 1.00 (1.00-1.00) | 1.00 (1.00-1.00) | 1.00 (1.00-1.00) | 1.00 (1.00-1.00) | 2.02% (0.85-3.20) | 52.38% | 34.76% (25.40-44.12) | 2.26% (1.08-8.57) | 0.97% (0.00-4.77) |
| **IMAT noPET** | 1.01 (1.00-1.02) | 1.01 (1.00-1.03) | 1.01 (1.00-1.03) | 1.01 (1.00-1.04) | 2.38% (1.06-3.71) | 47.57% | 23.56% (16.39-30.72) | 2.73% (1.23-10.71) | 0.78% (0.00-3.90) |
| **IMAT wPET** | 1.01 (1.00-1.02) | 1.01 (1.00-1.02) | 1.01 (1.00-1.03) | 1.01 (1.00-1.04) | 2.30% (1.01-3.58) | 45.13% | 20.86% (14.02-27.70) | 2.51% (1.16-9.72) | 0.69% (0.00-3.47) |

Table 46: NTCP, Patient 6.

| | V95 PTV | V107 PTV | CI PTV | CI PTV-E |
|---|---|---|---|---|
| **CRT noPET** | 0.94 | 0.00 | 0.93 | 0.93 |
| **CRT wPET** | 0.93 | 0.00 | 0.92 | 0.94 |
| **IMRT noPET** | 1.00 | 0.00 | 0.99 | 0.93 |
| **IMRT wPET** | 1.00 | 0.00 | 0.99 | 0.97 |
| **Proton noPET** | 1.00 | 0.00 | 1.00 | 0.96 |
| **Proton wPET** | 0.99 | 0.00 | 0.99 | 0.96 |
| **RA noPET** | 0.96 | 0.00 | 0.95 | 0.93 |
| **RA wPET** | 0.94 | 0.00 | 0.93 | 0.83 |

Table 47: Target coverage, Patient 6.

| | Breast cancer | Lung cancer | Thyroid cancer | Ventricle cancer |
|---|---|---|---|---|
| CRT noPET | 0.04% | 0.54% | 17.04% | 0.01% |
| CRT wPET | 0.03% | 0.49% | 16.73% | 0.01% |
| IMRT noPET | 0.63% | 0.76% | 27.37% | 0.06% |
| IMRT wPET | 0.61% | 0.70% | 25.18% | 0.05% |
| IMPT noPET | 0.04% | 0.00% | 22.82% | 0.03% |
| IMPT wPET | 0.04% | 0.00% | 31.41% | 0.03% |
| IMAT noPET | 0.68% | 2.77% | 27.14% | 0.06% |
| IMAT wPET | 0.58% | 2.14% | 25.55% | 0.05% |

Table 48: Cumulative lifetime risk of secondary cancer, Patient 6.

| | NTCP | Conformity Index, PTV | Secondary Cancer |
|---|---|---|---|
| 3DCRT | 0.043 | 0.092 | 0.034 |
| IMRT | 0.043 | | |
| IMPT | 1.000 | | |
| IMAT | 0.043 | | |

Table 49: Significance, p-values, Patient 6.

For Patient 6, including PET did significantly change the NTCP, except for the IMPT plans (significance level is 0.05). For the other three modalities, the estimated risks of normal tissue complications are significantly lower with PET. The conformity indexes were not significantly changed. The risk of developing secondary cancer was significantly changed: the risk was lower for the PET-based plans.

## **Patient 7** (PETped06)

| | Heart Failure HR (95% CI) | Myoc. Infarction HR (95% CI) | Peric. Disease HR (95% CI) | Valvular Abnorm. HR (95% CI) | Pneum. P (95% CI) | Esophag. complic. P | Xero. Bilateral P | Hypothyr. P (95% CI) | Blindness P (95% CI) | Ototox. P |
|---|---|---|---|---|---|---|---|---|---|---|
| **CRT noPET** | 1.08 (1.02-1.17) | 1.06 (1.00-1.20) | 1.08 (1.00-1.24) | 1.10 (1.00-1.33) | 3.12% (1.52-4.73) | 1.24% | 5.47% | 37.43% (27.37-47.50) | 0.85% (0.71-1.98) | 0.75% (0.00-3.76) |
| **CRT wPET** | 1.08 (1.02-1.16) | 1.06 (1.00-1.20) | 1.08 (1.00-1.23) | 1.10 (1.00-1.32) | 3.16% (1.54-4.77) | 1.25% | 5.50% | 37.40% (27.34-47.45) | 0.85% (0.71-1.98) | 0.76% (0.00-3.79) |
| **IMRT noPET** | 1.01 (1.00-1.02) | 1.01 (1.00-1.03) | 1.01 (1.00-1.03) | 1.01 (1.00-1.05) | 2.44% (1.09-3.78) | 1.06% | 5.62% | 29.11% (21.03-37.18) | 0.80% (0.69-1.76) | 0.12% (0.00-0.76) |
| **IMRT wPET** | 1.01 (1.00-1.03) | 1.01 (1.00-1.03) | 1.01 (1.00-1.04) | 1.02 (1.00-1.05) | 2.47% (1.11-3.83) | 0.99% | 5.62% | 29.05% (20.99-37.12) | 0.88% (0.73-2.12) | 0.13% (0.00-0.81) |
| **IMPT noPET** | 1.00 (1.00-1.00) | 1.00 (1.00-1.00) | 1.00 (1.00-1.01) | 1.00 (1.00-1.01) | 2.22% (0.96-3.47) | 0.97% | 5.63% | 27.96% (20.10-35.81) | 0.53% (0.53-0.55) | 0.14% (0.00-0.84) |
| **IMPT wPET** | 1.00 (1.00-1.00) | 1.00 (1.00-1.00) | 1.00 (1.00-1.00) | 1.00 (1.00-1.01) | 2.23% (0.97-3.49) | 0.95% | 5.56% | 26.93% (19.25-34.60) | 0.55% (0.54-0.64) | 0.23% (0.00-1.31) |
| **IMAT noPET** | 1.04 (1.01-1.08) | 1.03 (1.00-1.09) | 1.04 (1.00-1.11) | 1.05 (1.00-1.16) | 2.88% (1.37-4.40) | 0.95% | 5.48% | 26.82% (19.17-34.48) | 1.10% (0.86-3.12) | 0.17% (0.00-0.98) |
| **IMAT wPET** | 1.04 (1.01-1.08) | 1.03 (1.00-1.09) | 1.03 (1.00-1.10) | 1.04 (1.00-1.14) | 2.82% (1.33-4.31) | 0.97% | 5.59% | 27.04% (19.30-34.68) | 1.20% (0.93-3.58) | 0.21% (0.00-1.22) |

**Table 50: NTCP, Patient 7.**

| | V95 PTV | V107 PTV | CI PTV |
|---|---|---|---|
| **CRT noPET** | 0.88 | 0.02 | 0.87 |
| **CRT wPET** | 0.88 | 0.02 | 0.87 |
| **IMRT noPET** | 0.94 | 0.00 | 0.94 |
| **IMRT wPET** | 0.96 | 0.00 | 0.95 |
| **Proton noPET** | 0.98 | 0.00 | 0.98 |
| **Proton wPET** | 0.99 | 0.00 | 0.98 |
| **RA noPET** | 0.87 | 0.00 | 0.86 |
| **RA wPET** | 0.89 | 0.00 | 0.89 |

**Table 51: Target coverage, Patient 7.**

| | Breast cancer | Lung cancer | Thyroid cancer | Ventricle cancer |
|---|---|---|---|---|
| CRT noPET | -- | 7.56% | 27.01% | 0.09% |
| CRT wPET | -- | 7.75 % | 27.02% | 0.09% |
| IMRT noPET | -- | 3.21% | 26.24% | 0.01% |
| IMRT wPET | -- | 3.47% | 26.40% | 0.01% |
| IMPT noPET | -- | 1.58% | 25.77% | 0.02% |
| IMPT wPET | -- | 1.69% | 25.42% | 0.02% |
| IMAT noPET | -- | 6.16% | 25.06% | 0.04% |
| IMAT wPET | -- | 5.78% | 26.04% | 0.04% |

Table 52: Cumulative lifetime risk of secondary cancer, Patient 7.

| | NTCP | Conformity Index, PTV | Secondary Cancer |
|---|---|---|---|
| 3DCRT | 0.276 | 0.180 | 0.484 |
| IMRT | 0.752 | | |
| IMPT | 0.674 | | |
| IMAT | 0.161 | | |

Table 53: Significance, p-values, Patient 7.

For Patient 7, including PET did not significantly change the NTCP, the risk of developing secondary cancer or the conformity index.

## **Patient 8** (PETped07)

| | Heart Failure HR (95% CI) | Myoc. Infarction HR (95% CI) | Peric. Disease HR (95% CI) | Valvular Abnorm. HR (95% CI) | Pneum. P (95% CI) | Esophag. complic. P | Radiation nephropathy bilateral P (95% CI) | Liver disease P | GI toxicity P | Late rectal toxicity P | Hypothyr. P (95% CI) |
|---|---|---|---|---|---|---|---|---|---|---|---|
| **CRT noPET** | 2.74 (1.42-4.41) | 2.25 (0.00-5.20) | 2.66 (0.00-5.89) | 3.10 (0.00-7.89) | 47.61% (39.06-56.16) | 21.53% | 0.05% (0.00-0.10) | 0.00% | 0.00% | 0.00% | 13.15% (7.11-19.20) |
| **CRT wPET** | 2.71 (1.41-4.36) | 2.23 (0.00-5.13) | 2.63 (0.00-5.81) | 3.07 (0.00-7.78) | 44.08% (53.86-52.29) | 20.46% | 0.05% (0.00-0.10) | 0.00% | 0.00% | 0.00% | 13.05% (7.02-19.09) |
| **IMRT noPET** | 1.89 (1.21-2.74) | 1.64 (0.13-3.14) | 1.85 (0.20-3.50) | 2.08 (0.00-4.52) | 37.09% (29.65-44.52) | 17.22% | 0.05% (0.00-0.10) | 0.00% | 0.00% | 0.00% | 13.22% (7.17-19.28) |
| **IMRT wPET** | 2.04 (1.25-3.04) | 1.75 (0.00-3.51) | 1.99 (0.06-3.92) | 2.26 (0.00-5.12) | 35.46% (28.22-42.69) | 14.94% | 0.05% (0.00-0.10) | 0.00% | 0.00% | 0.00% | 13.13% (7.09-19.17) |
| **IMPT noPET** | 1.62 (1.15-2.23) | 1.45 (0.39-2.51) | 1.60 (0.44-2.76) | 1.76 (0.03-3.48) | 21.02% (15.75-26.30) | 13.21% | 0.05% (0.00-0.10) | 0.00% | 0.00% | 0.00% | 12.36% (6.42-18.30) |
| **IMPT wPET** | 1.57 (1.14-2.12) | 1.41 (0.44-2.37) | 1.54 (0.49-2.60) | 1.69 (0.12-3.26) | 20.87% (15.62-26.12) | 12.78% | 0.05% (0.00-0.10) | 0.00% | 0.00% | 0.00% | 12.36% (6.42-18.30) |
| **IMAT noPET** | 1.59 (1.14-2.17) | 1.43 (0.41-2.44) | 1.57 (0.46-2.67) | 1.72 (0.08-3.36) | 39.39% (31.68-47.09) | 13.94% | 0.05% (0.00-0.10) | 0.00% | 0.00% | 0.00% | 13.25% (7.19-19.31) |
| **IMAT wPET** | 1.69 (1.17-2.35) | 1.49 (0.32-2.66) | 1.66 (0.38-2.93) | 1.83 (0.00-3.73) | 32.97% (26.05-39.90) | 12.92% | 0.05% (0.00-0.10) | 0.00% | 0.00% | 0.00% | 13.26% (7.19-19.31) |

**Table 54: NTCP, Patient 8.**

| | V95 PTV | V107 PTV | CI PTV |
|---|---|---|---|
| **CRT noPET** | 0.95 | 0.00 | 0.95 |
| **CRT wPET** | 0.95 | 0.00 | 0.95 |
| **IMRT noPET** | 0.91 | 0.04 | 0.91 |
| **IMRT wPET** | 0.91 | 0.03 | 0.90 |
| **Proton noPET** | 0.98 | 0.00 | 0.98 |
| **Proton wPET** | 0.99 | 0.00 | 0.99 |
| **RA noPET** | 0.93 | 0.00 | 0.93 |
| **RA wPET** | 0.96 | 0.00 | 0.96 |

**Table 55: Target coverage, Patient 8.**

| | Breast cancer | Lung cancer | Thyroid cancer | Ventricle cancer |
|---|---|---|---|---|
| CRT noPET | -- | 64.17% | 2.78% | 2.38% |
| CRT wPET | -- | 61.76% | 2.45% | 2.06% |
| IMRT noPET | -- | 56.83% | 3.01% | 0.87% |
| IMRT wPET | -- | 55.64% | 2.69% | 0.97% |
| IMPTnoPET | -- | 43.35% | 0.03% | 0.02% |
| IMPT wPET | -- | 43.19% | 0.03% | 0.02% |
| IMAT noPET | -- | 58.48% | 3.11% | 1.08% |
| IMAT wPET | -- | 53.76% | 3.12% | 1.04% |

Table 56: Cumulative lifetime risk of secondary cancer, Patient 8.

| | NTCP | Conformity Index, PTV | Secondary Cancer |
|---|---|---|---|
| 3DCRT | 0.026 | 0.414 | 0.017 |
| IMRT | 0.917 | | |
| IMPT | 0.028 | | |
| IMAT | 0.917 | | |

Table 57: Significance, p-values, Patient 8.

For Patient 8, including PET did not significantly change the NTCP, except for 3DCRT and IMPT where the estimated risks were significantly lower for the PET-based plans. Including PET significantly reduce the risk of developing secondary cancer but had no impact on the conformity index.

## **Patient 9** (PETped08)

| | Esophag. complic. P | Xero. Bilateral P | Hypothyr. P (95% CI) | Blindness P (95% CI) | Ototox. P |
|---|---|---|---|---|---|
| **CRT noPET** | 0.38% | 13.46% | 16.90% (10.46-23.35) | 0.66% (0.60-1.14) | 0.62% (0.00-3.14) |
| **CRT wPET** | 0.38% | 12.70% | 16.88% (10.44-23.33) | 0.65% (0.60-1.10) | 0.61% (0.00-3.09) |
| **IMRT noPET** | 0.30% | 7.29% | 13.34% (7.27-19.41) | 0.67% (0.61-1.16) | 0.12% (0.00-0.75) |
| **IMRT wPET** | 0.30% | 4.56% | 13.43% (7.35-19.51) | 0.64% (0.59-1.06) | 0.12% (0.00-0.71) |
| **IMPT noPET** | 0.27% | 7.31% | 12.43% (6.48-18.38) | 0.53% (0.53-0.55) | 0.10% (0.00-0.60) |
| **IMPT wPET** | 0.27% | 6.14% | 12.48% (6.53-18.44) | 0.53% (0.53-0.55) | 0.09% (0.00-0.60) |
| **IMAT noPET** | 0.30% | 4.56% | 13.31% (7.25-19.38) | 0.66% (0.60-1.12) | 0.13% (0.00-0.80) |
| **IMAT wPET** | 0.30% | 4.68% | 13.37% (7.30-19.44) | 0.64% (0.59-1.04) | 0.12% (0.00-0.75) |

Table 58: NTCP, Patient 9.

| | V95 PTV | V107 PTV | CI PTV | CI Volume for symmetric bone irradiation |
|---|---|---|---|---|
| **CRT noPET** | 0.93 | 0.00 | 0.93 | 0.95 |
| **CRT wPET** | 0.94 | 0.00 | 0.94 | 0.95 |
| **IMRT noPET** | 1.00 | 0.00 | 1.00 | 1.00 |
| **IMRT wPET** | 1.00 | 0.00 | 1.00 | 1.00 |
| **Proton noPET** | 1.00 | 0.00 | 0.99 | 1.00 |
| **Proton wPET** | 0.99 | 0.00 | 0.99 | 1.00 |
| **RA noPET** | 0.96 | 0.00 | 0.96 | 1.00 |
| **RA wPET** | 0.94 | 0.00 | 0.94 | 1.00 |

Table 59: Target coverage, Patient 9.

| | Breast cancer | Lung cancer | Thyroid cancer | Ventricle cancer |
|---|---|---|---|---|
| CRT noPET | -- | -- | 13.26% | -- |
| CRT wPET | -- | -- | 13.23% | -- |
| IMRT noPET | -- | -- | 3.36% | -- |
| IMRT wPET | -- | -- | 3.64% | -- |
| IMPT noPET | -- | -- | 0.28% | -- |
| IMPT wPET | -- | -- | 0.48% | -- |
| IMAT noPET | -- | -- | 3.30% | -- |
| IMAT wPET | -- | -- | 3.48% | -- |

Table 60: Cumulative lifetime risk of secondary cancer, Patient 9.

| | NTCP | Conformity Index, PTV | Secondary Cancer |
|---|---|---|---|
| 3DCRT | 0.042 | 0.655 | 0.144 |
| IMRT | 0.273 | | |
| IMPT | 0.273 | | |
| IMAT | 0.225 | | |

Table 61: Significance, p-values, Patient 9.

For Patient 9, including PET did not significantly change the NTCP, except for 3DCRT where the estimated risks were significantly lower for the PET-based plan. The risk of developing secondary cancer and the conformity indexes were not significantly changed.

## Patient 10(PETped11)

| | Heart Failure HR (95% CI) | Myoc. Infarction HR (95% CI) | Peric. Disease HR (95% CI) | Valvular Abnorm. HR (95% CI) | Pneum. P (95% CI) | Esophag. complic. P | Xero. Bilateral P | Hypothyr. P (95% CI) | Blindness P (95% CI) | Ototox. P (95% CI) |
|---|---|---|---|---|---|---|---|---|---|---|
| **CRT noPET** | 1.01 (1.00-1.01) | 1.00 (1.00-1.01) | 1.01 (1.00-1.01) | 1.01 (1.00-1.02) | 2.24% (0.97-3.50) | 1.49% | 96.77% | 49.85% (36.24-63.45) | 6.22% (3.89-26.15) | 85.47% (1.57-100) |
| **CRT wPET** | 1.00 (1.00-1.01) | 1.00 (1.00-1.01) | 1.00 (1.00-1.01) | 1.01 (1.00-1.02) | 2.19% (0.95-3.44) | 1.21% | 97.15% | 37.67% (47.80-27.54) | 6.24% (3.91-26.25) | 88.81% (19.00-100) |
| **IMRT noPET** | 1.01 (1.00-1.02) | 1.01 (1.00-1.02) | 1.01 (1.00-1.03) | 1.01 (1.00-1.04) | 2.27% (0.99-3.54) | 1.91% | 68.19% | 87.66% (74.52-100) | 9.65% (5.92-41.57) | 80.00% (0.00-100) |
| **IMRT wPET** | 1.01 (1.00-1.01) | 1.01 (1.00-1.02) | 1.01 (1.00-1.02) | 1.01 (1.00-1.03) | 2.20% (0.95-3.45) | 1.29% | 73.93% | 82.85% (67.61-98.09) | 10.11% (6.19-43.63) | 86.46% (0.00-100) |
| **IMPT noPET** | 1.00 (1.00-1.00) | 1.00 (1.00-1.00) | 1.00 (1.00-1.00) | 1.00 (1.00-1.00) | 2.04% (0.86-3.23) | 1.58% | 62.38% | 85.33% (71.05-99.61) | 5.43% (3.42-22.59) | 61.67% (0.00-100) |
| **IMPT wPET** | 1.00 (1.00-1.00) | 1.00 (1.00-1.00) | 1.00 (1.00-1.00) | 1.00 (1.00-1.00) | 2.04% (0.86-3.23) | 1.07% | 61.18% | 83.61% (68.64-98.58) | 5.96% (3.74-24.97) | 67.31% (0.00-100) |
| **IMAT noPET** | 1.01 (1.00-1.01) | 1.01 (1.00-1.02) | 1.01 (1.00-1.02) | 1.01 (1.00-1.03) | 2.33% (1.03-3.63) | 1.39% | 66.83% | 83.80% (67.92-98.24) | 8.80% (5.42-37.75) | 58.06% (0.00-100) |
| **IMAT wPET** | 1.01 (1.00-1.01) | 1.00 (1.00-1.01) | 1.01 (1.00-1.02) | 1.01 (1.00-1.02) | 2.22% (0.96-3.48) | 0.94% | 62.82% | 72.54% (55.48-89.60) | 9.10% (5.60-39.11) | 65.62% (0.00-100) |

Table 62: NTCP, Patient 10.

| | V95 PTV | V107 PTV | CI PTV | CI PTV-EI |
|---|---|---|---|---|
| **CRT noPET** | 0.81 | 0.32 | 0.81 | 0.91 |
| **CRT wPET** | 0.80 | 0.33 | 0.80 | 0.92 |
| **IMRT noPET** | 0.93 | 0.02 | 0.93 | 1.00 |
| **IMRT wPET** | 0.96 | 0.00 | 0.96 | 0.98 |
| **Proton noPET** | 0.93 | 0.01 | 0.93 | 0.99 |
| **Proton wPET** | 0.96 | 0.00 | 0.96 | 0.98 |
| **RA noPET** | 0.86 | 0.10 | 0.86 | 0.99 |
| **RA wPET** | 0.82 | 0.17 | 0.81 | 0.97 |

Table 63: Target coverage, Patient 10.

| | Breast cancer | Lung cancer | Thyroid cancer | Ventricle cancer |
|---|---|---|---|---|
| CRT noPET | -- | 1.73% | 15.19% | -- |
| CRT wPET | -- | 1.38% | 12.66% | -- |
| IMRT noPET | -- | 1.97% | 1.41% | -- |
| IMRT wPET | -- | 1.44% | 3.50% | -- |
| IMPT noPET | -- | 0.18% | 3.02% | -- |
| IMPT wPET | -- | 0.16% | 3.57% | -- |
| IMAT noPET | -- | 2.45% | 5.77% | -- |
| IMAT wPET | -- | 1.60% | 10.44% | -- |

Table 64: Cumulative lifetime risk of secondary cancer, Patient 10.

| | NTCP | Conformity Index, PTV | Secondary Cancer |
|---|---|---|---|
| 3DCRT | 0.779 | 1.000 | 1.000 |
| IMRT | 0.600 | | |
| IMPT | 0.893 | | |
| IMAT | 0.463 | | |

Table 65: Significance, p-values, Patient 10.

For Patient 10, including PET did not significantly change the NTCP, the conformity indexes or the risk of developing secondary cancer.

## **Patient 11**(PETped12)

| | Heart Failure HR (95% CI) | Myoc. Infarction HR (95% CI) | Peric. Disease HR (95% CI) | Valvular Abnorm. HR (95% CI) | Pneum. P (95% CI) | Esophag. complic. P | Xero. Bilateral P | Hypothyr. P (95% CI) | Blindness P (95% CI) | Ototox. P |
|---|---|---|---|---|---|---|---|---|---|---|
| **CRT noPET** | 1.02 (1.00-1.04) | 1.01 (1.00-1.05) | 1.02 (1.00-1.06) | 1.02 (1.00-1.08) | 3.36% (1.68-5.05) | 2.31% | 96.27% | 89.18% (76.92-100) | 5.80% (3.65-24.27) | 89.41% (22.37-100) |
| **CRT wPET** | 1.02 (1.01-1.04) | 1.02 (1.00-1.06) | 1.02 (1.00-1.06) | 1.03 (1.00-1.09) | 3.41% (1.71-5.11) | 2.07% | 96.35% | 88.62% (76.03-100) | 6.51% (4.06-27.45) | 90.36% (27.87-100) |
| **IMRT noPET** | 1.02 (1.00-1.03) | 1.01 (1.00-1.04) | 1.02 (1.00-1.05) | 1.02 (1.00-1.07) | 2.61% (1.20-4.02) | 1.62% | 92.15% | 92.26% (82.21-100) | 6.90% (4.29-29.19) | 43.33% (0.00-100) |
| **IMRT wPET** | 1.02 (1.01-1.04) | 1.02 (1.00-1.05) | 1.02 (1.00-1.06) | 1.03 (1.00-1.09) | 2.84% (1.34-4.33) | 1.59% | 90.84% | 92.27% (82.22-100) | 7.40% (4.59-31.47) | 51.87% (0.00-100) |
| **IMPT noPET** | 1.00 (1.00-1.00) | 1.00 (1.00-1.00) | 1.00 (1.00-1.00) | 1.00 (1.00-1.00) | 2.22% (0.96-3.47) | 1.46% | 77.96% | 90.49% (79.10-100) | 4.11% (2.64-16.66) | 25.12% (0.00-100) |
| **IMPT wPET** | 1.00 (1.00-1.00) | 1.00 (1.00-1.00) | 1.00 (1.00-1.00) | 1.00 (1.00-1.00) | 2.21% (0.96-3.47) | 1.25% | 73.59% | 90.26% (78.71-100) | 4.11% (2.65-16.68) | 30.63% (0.00-100) |
| **IMAT noPET** | 1.02 (1.01-1.04) | 1.01 (1.00-1.05) | 1.02 (1.00-1.06) | 1.03 (1.00-1.08) | 2.70% (1.26-4.15) | 1.14% | 74.24% | 91.71% (81.21-100) | 7.05% (4.38-29.89) | 58.10% (0.00-100) |
| **IMAT wPET** | 1.02 (1.01-1.05) | 1.02 (1.00-1.06) | 1.02 (1.00-1.06) | 1.03 (1.00-1.09) | 2.77% (1.30-4.24) | 1.28% | 75.84% | 92.68% (82.97-100) | 7.41% (4.59-31.49) | 61.86% (0.00-100) |

**Table 66: NTCP, Patient 11.**

| | V95 PTV | V107 PTV | CI PTV | CI PTV-EI |
|---|---|---|---|---|
| **CRT noPET** | 0.93 | 0.00 | 0.93 | 0.98 |
| **CRT wPET** | 0.91 | 0.00 | 0.91 | 0.99 |
| **IMRT noPET** | 0.97 | 0.00 | 0.97 | 0.99 |
| **IMRT wPET** | 0.97 | 0.00 | 0.97 | 0.99 |
| **Proton noPET** | 0.97 | 0.00 | 0.97 | 0.98 |
| **Proton wPET** | 0.96 | 0.00 | 0.96 | 0.98 |
| **RA noPET** | 0.92 | 0.00 | 0.91 | 0.99 |
| **RA wPET** | 0.88 | 0.00 | 0.88 | 0.99 |

**Table 67: Target coverage, Patient 11.**

| | Breast cancer | Lung cancer | Thyroid cancer | Ventricle cancer |
|---|---|---|---|---|
| CRT noPET | -- | 8.85% | 0.65% | -- |
| CRT wPET | -- | 9.10% | 0.69% | -- |
| IMRT noPET | -- | 4.41% | 0.21% | -- |
| IMRT wPET | -- | 5.87% | 0.19% | -- |
| IMPT noPET | -- | 1.57% | 0.37% | -- |
| IMPT wPET | -- | 1.56% | 0.39% | -- |
| IMAT noPET | -- | 5.04% | 0.27% | -- |
| IMAT wPET | -- | 5.46% | 0.17% | -- |

Table 68: Cumulative lifetime risk of secondary cancer, Patient 11.

| | NTCP | Conformity Index, PTV | Secondary Cancer |
|---|---|---|---|
| 3DCRT | 0.326 | 0.109 | 0.183 |
| IMRT | 0.325 | | |
| IMPT | 0.500 | | |
| IMAT | 0.018 | | |

Table 69: Significance, p-values, Patient 11.

For Patient 11, including PET did not significantly change the NTCP, except for the IMAT where the PET-based plans resulted in a significantly higher risk of NTC. The risk of developing secondary cancer and the conformity indexes were not significantly changed.

# Appendix B

## DVHs of the treatment plans

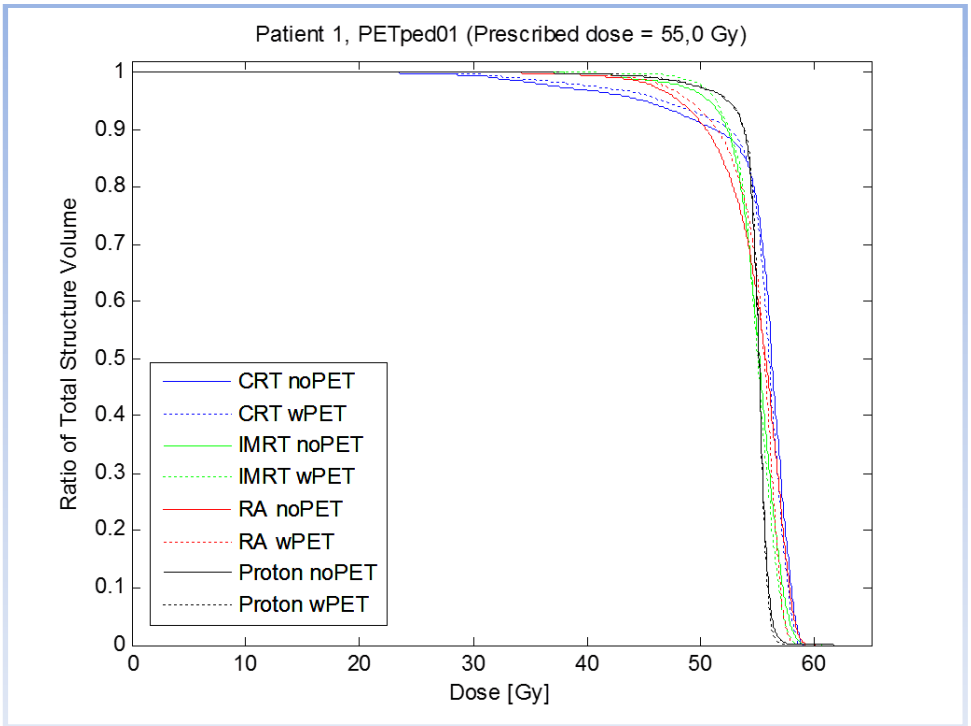


Figure 36: DVH:s, Patient 1.

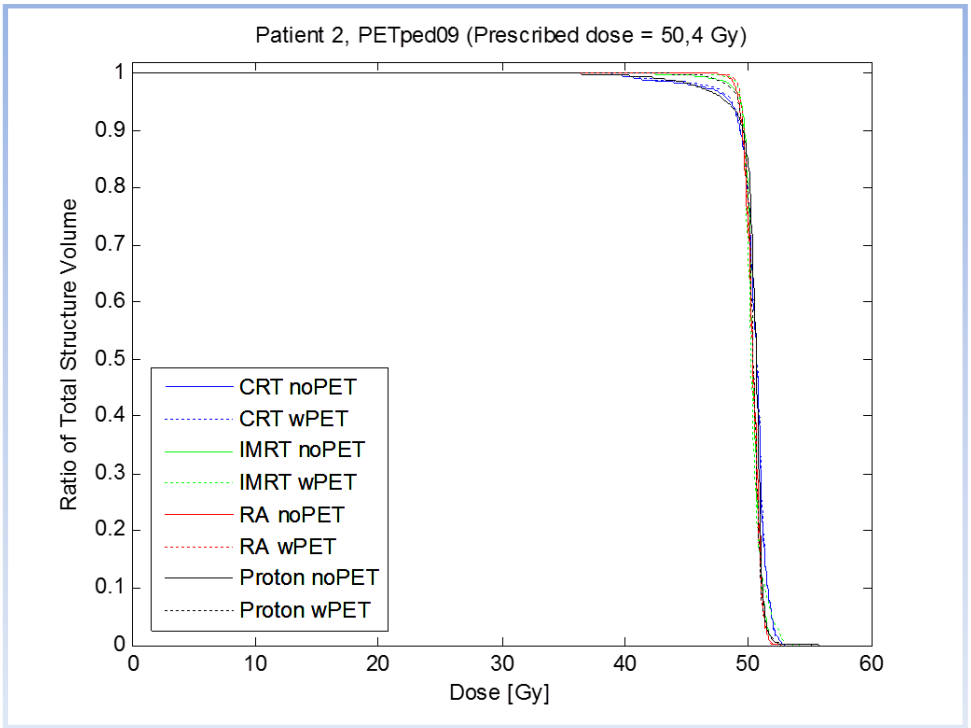


Figure 37: DVH:s, Patient 2.

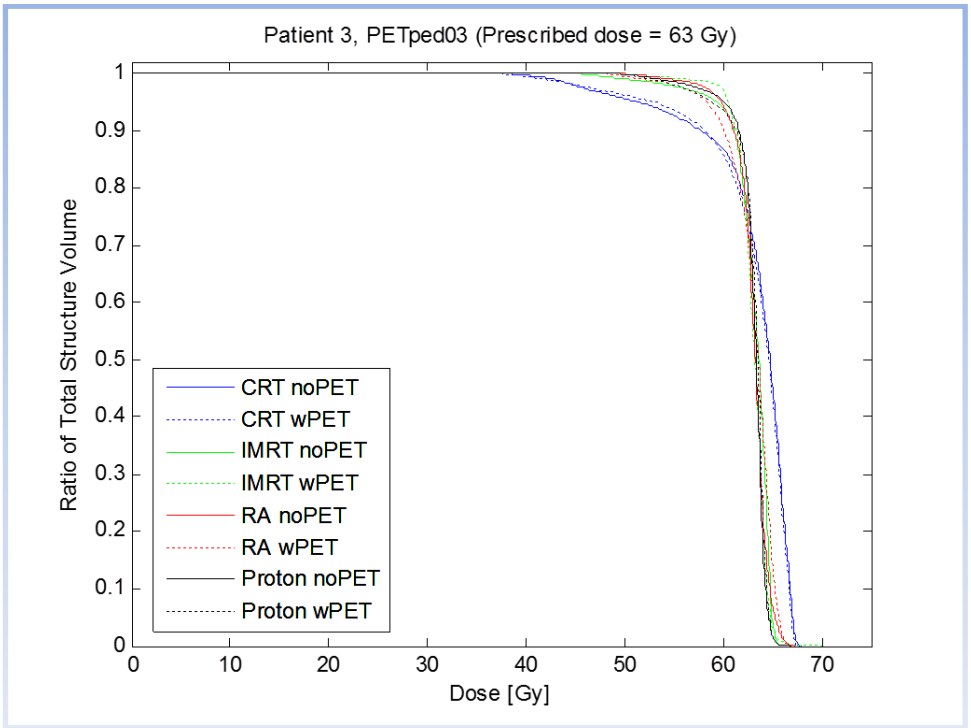


Figure 38: DVH:s, Patient 3.

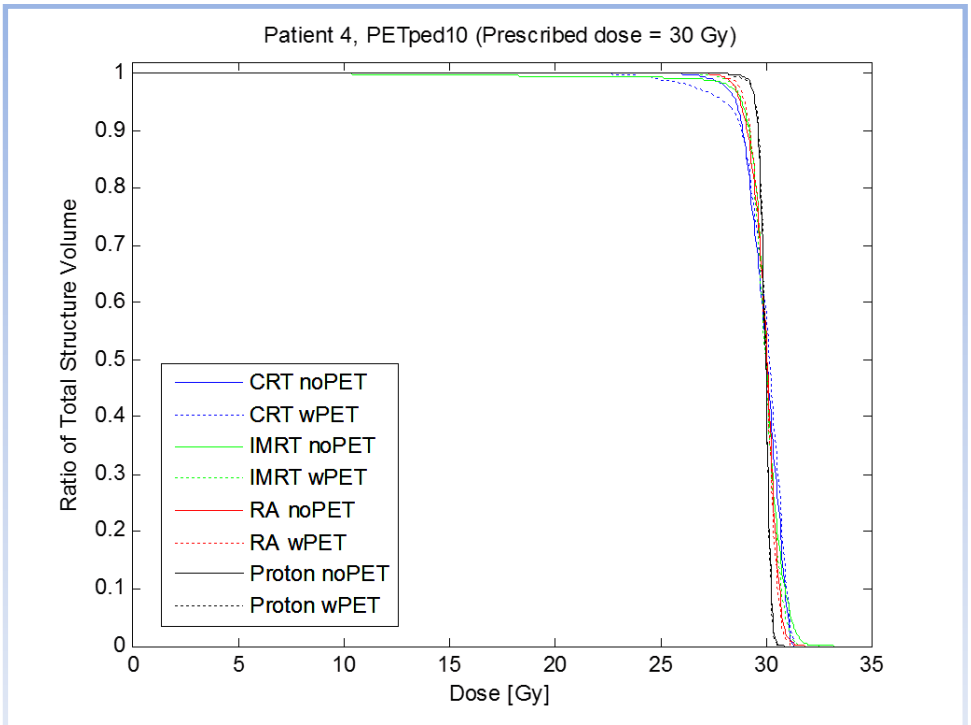


Figure 39: DVH:s, Patient 4.

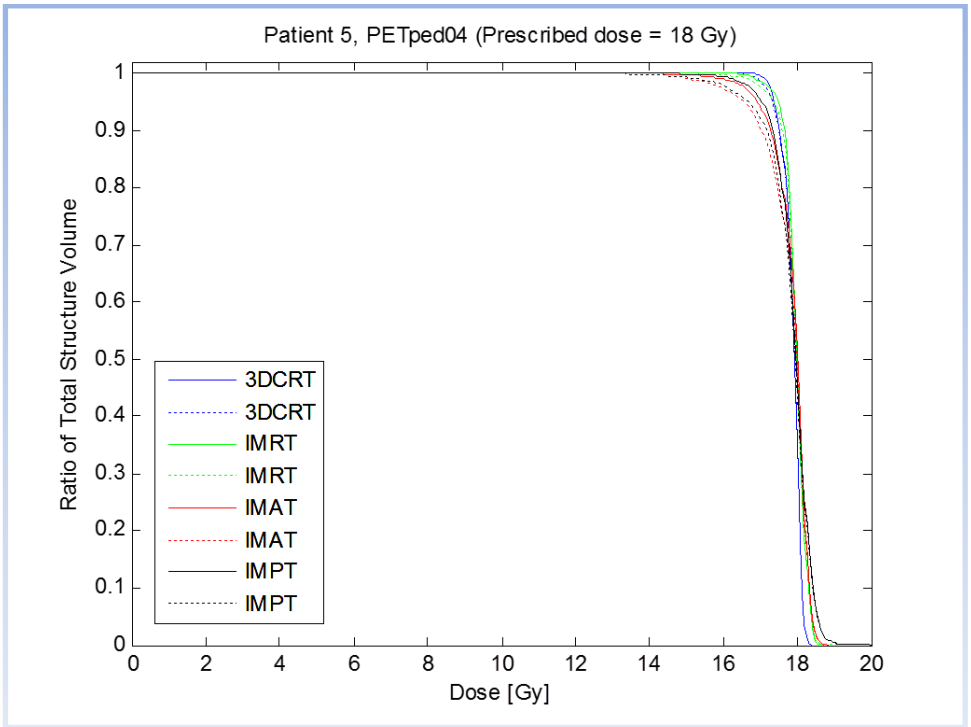


Figure 40: DVH:s, Patient 5 (PTV neck).

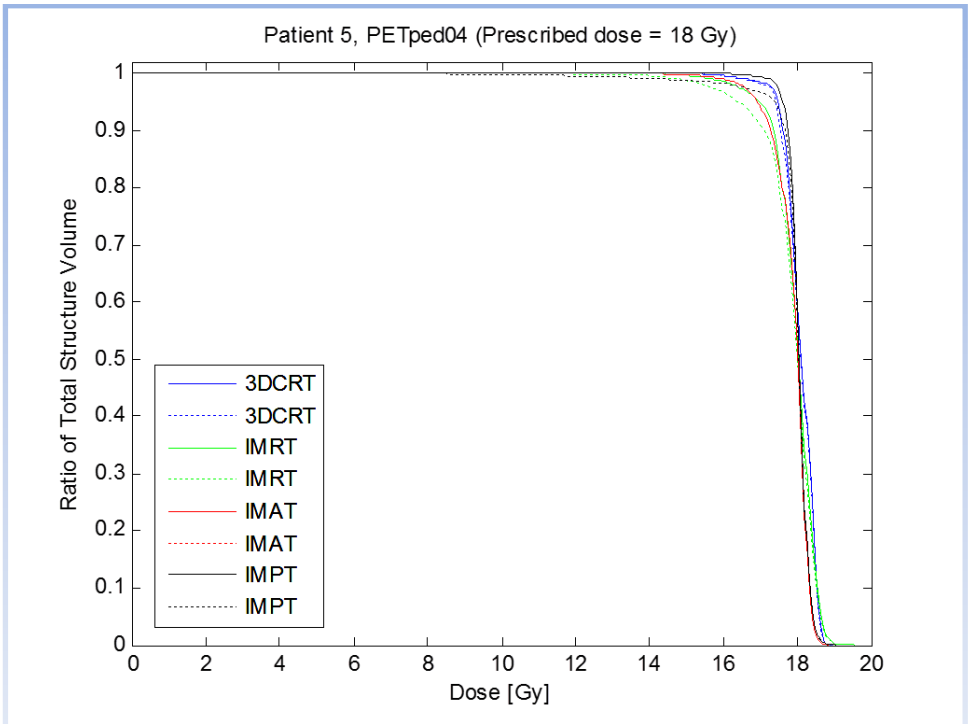


Figure 41: DVH:s, Patient 5 (PTV lower back).

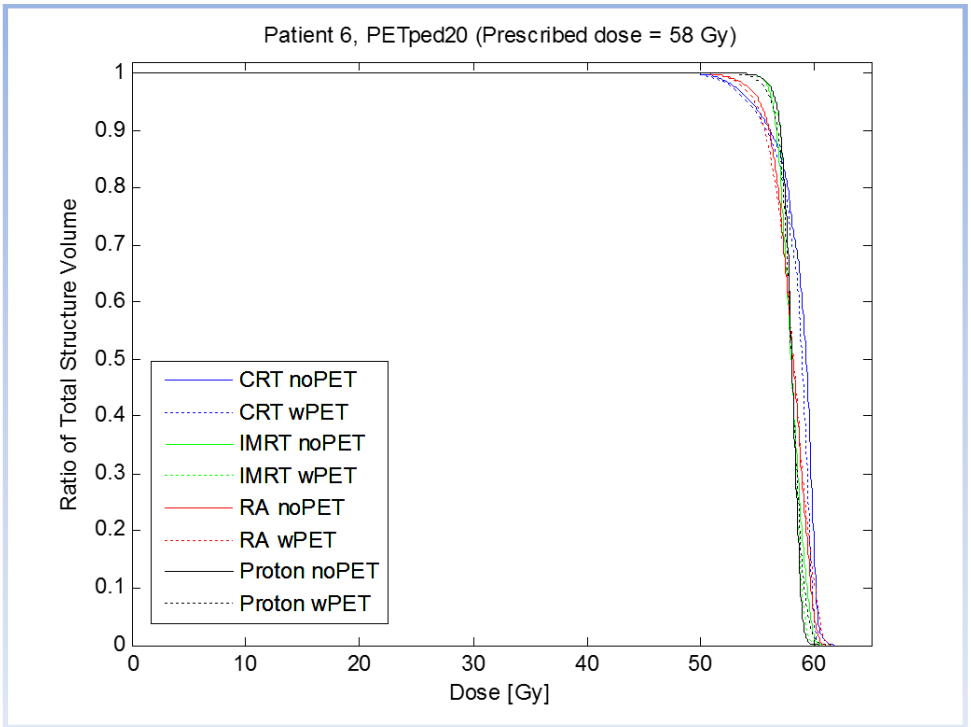


Figure 42: DVH:s, Patient 6.

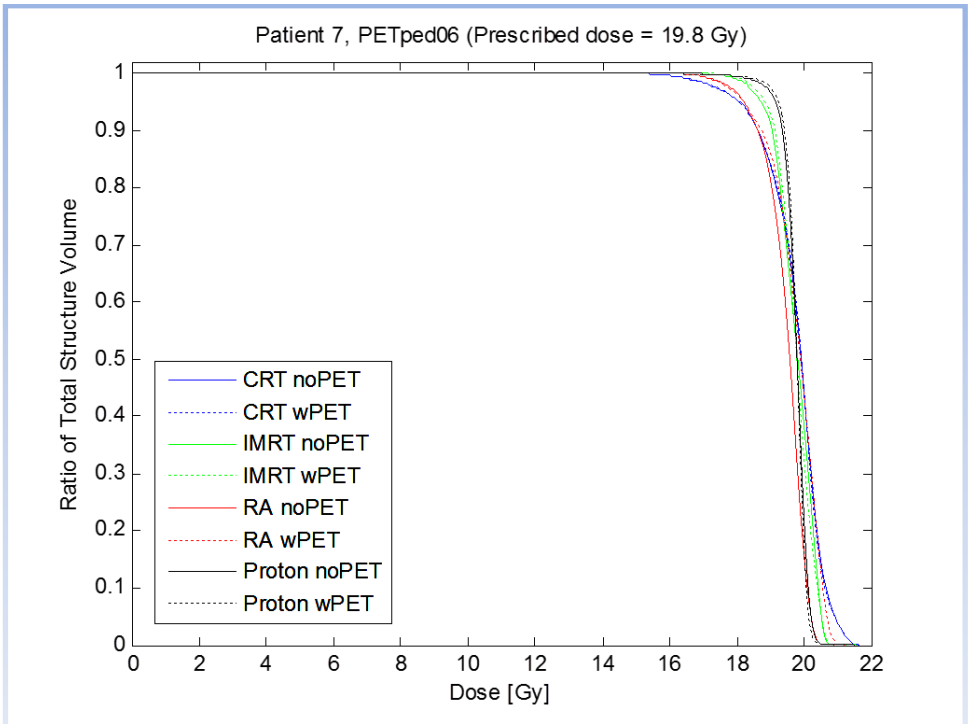


Figure 43: DVH:s, Patient 7.

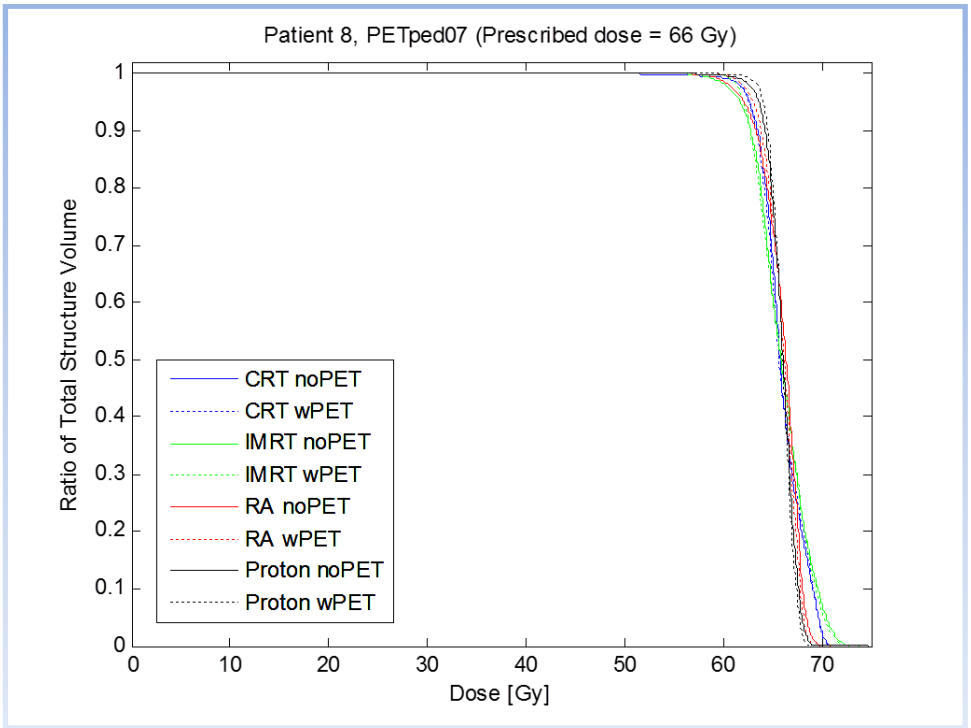


Figure 44: DVH:s, Patient 8.

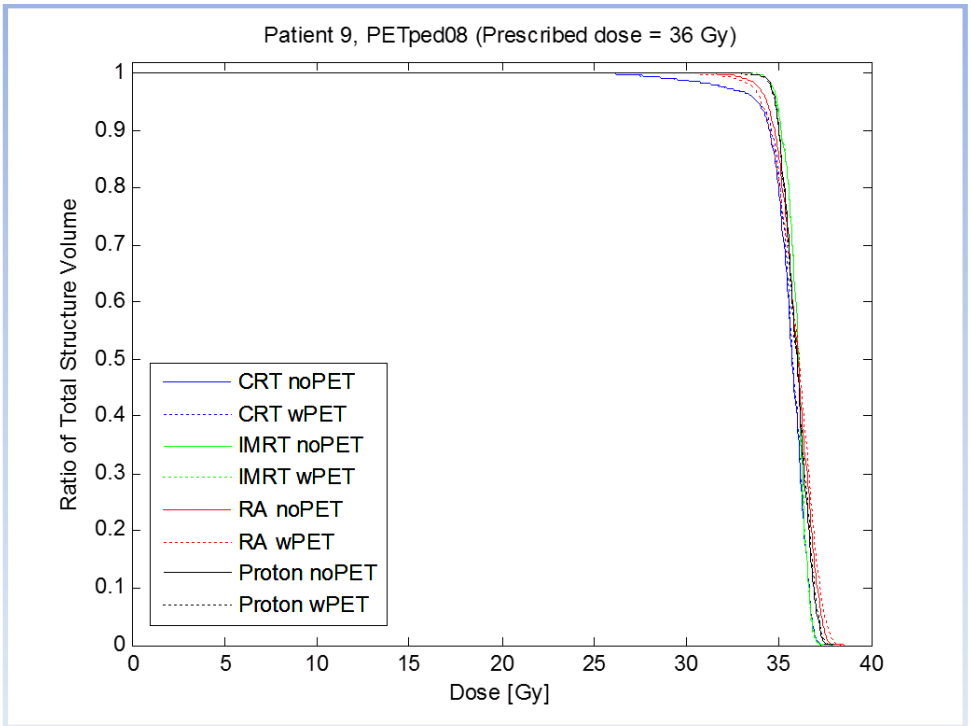


Figure 45: DVH:s, Patient 9.

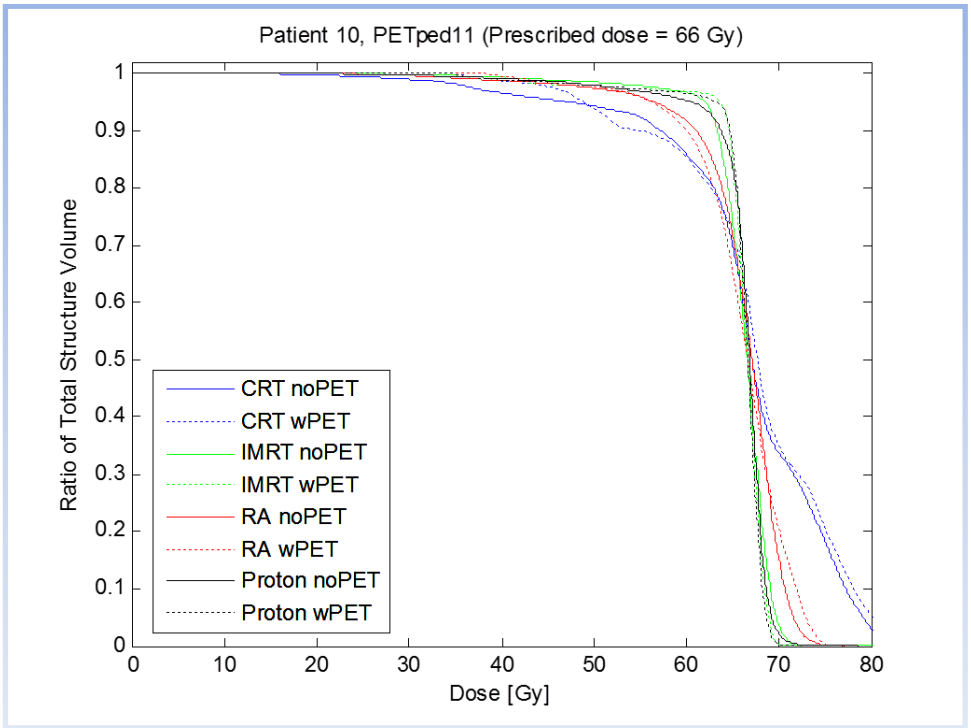


Figure 46: DVH:s, Patient 10.

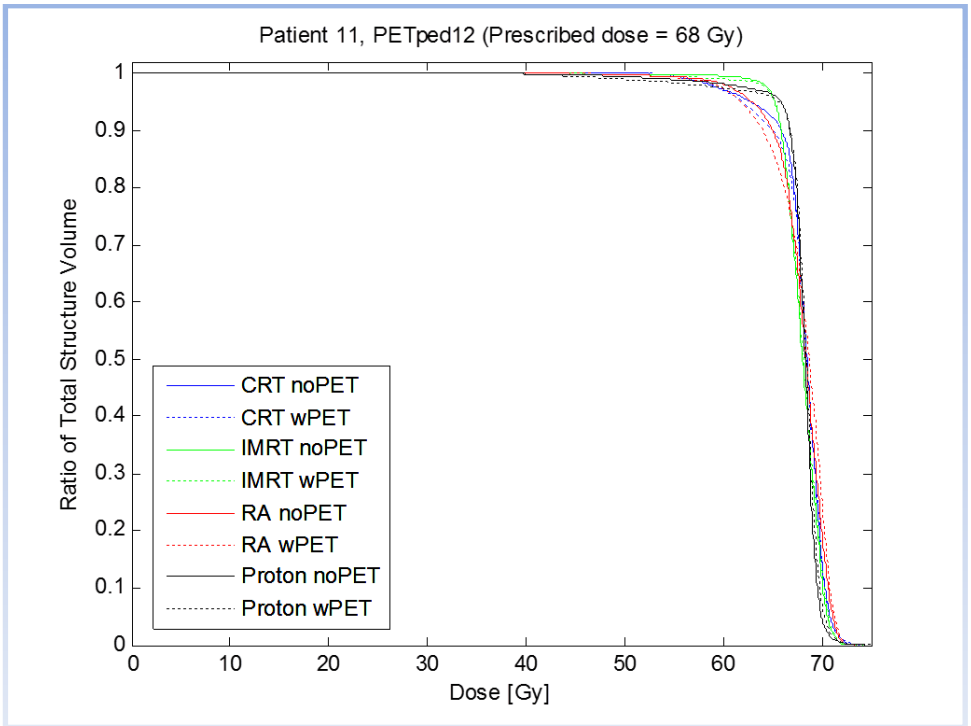


Figure 47: DVH:s, Patient 11.

# Appendix C

## Estimations of the statistical uncertainties in the linear dose-response models

To estimate the confidence interval (CI) of the linear functions describing the risks of cardiac complications, the curve-fitting tool in MATLAB was used. This tool estimates symmetric confidence intervals from the variance of the data.

The confidence interval for the linear NTCP-function of the eye was generated from a line fitted through the endpoints of the confidence intervals of each data point. The confidence interval from the curve fitting tool in MATLAB was too small to be reliable.

## Estimations of the statistical uncertainties in the logistic dose-response models

For some of the logistic models the 95% confidence interval for the parameters was available, or could be derived. However, inserting them directly into the models did not render useful confidence intervals. For example, combining the extreme-values of the parameters in a logistic function in an attempt to render the most sensitive and the least sensitive models, resulted in crossing curves. This would imply that there are no uncertainties in the estimated NTCP for certain doses.

Instead, a propagation of uncertainty formula was used to give some idea about the magnitude of the statistical uncertainties. Any uncertainties in the model itself are not accounted for.

In a logistic dose-response model, the risk of developing a complication is described by the formula below:

$$P(\gamma_{50}, TD_{50}, D) = \frac{1}{1 + e^{4\gamma_{50}\left(1-\frac{D}{TD_{50}}\right)}}$$

The statistical uncertainty of the probability can be estimated:

$$\sigma_P{}^2 = \left(\frac{\partial P}{\partial \gamma_{50}}\right)^2 \cdot \left(\sigma_{\gamma_{50}}\right)^2 + \left(\frac{\partial P}{\partial TD_{50}}\right)^2 \cdot \left(\sigma_{TD_{50}}\right)^2 + \left(\frac{\partial P}{\partial D}\right)^2 \cdot (\sigma_D)^2$$

where the partial derivatives are:

$$\frac{\partial P}{\partial \gamma_{50}} = \frac{-4 \cdot \left(1 - \frac{D}{TD_{50}}\right) \cdot e^{4\gamma_{50}\left(1-\frac{D}{TD_{50}}\right)}}{\left(e^{4\gamma_{50}\left(1-\frac{D}{TD_{50}}\right)} + 1\right)^2}$$

$$\frac{\partial P}{\partial TD_{50}} = \frac{-4D \cdot \gamma_{50} \cdot e^{4\gamma_{50}\left(1-\frac{D}{TD_{50}}\right)}}{(TD_{50})^2 \cdot \left(e^{4\gamma_{50}\left(1-\frac{D}{TD_{50}}\right)} + 1\right)^2}$$

$$\frac{\partial P}{\partial D} = \frac{-4\gamma_{50} \cdot e^{4\gamma_{50}\left(1-\frac{D}{TD_{50}}\right)}}{TD_{50} \cdot \left(e^{4\gamma_{50}\left(1-\frac{D}{TD_{50}}\right)} + 1\right)^2}$$

The standard deviations, σ, of $\gamma_{50}$ and $TD_{50}$ were calculated from the variance v of each parameter ($\sigma^2 = v$). The standard deviation of D was approximated to 0.5 Gy.

# Appendix D

## The incidence of blindness in the sibling cohort

The incidence of blindness among the cancer survivors can be estimated from the data in CCSS (70).

First, the ratio of the number of patients developing blindness (383 during the first five years after diagnosis and 107 developing blindness more than five years after diagnosis) and the number of patients never developing blindness is calculated. The quotient is then divided by the relative risk (12.4 during the first 5 years and 2.6 five years or more after diagnosis.

$$\frac{383/13782}{12{,}4} = 0{,}00224$$

$$\frac{107/13782}{2{,}6} = 0{,}00299$$

The sum of these quotients equals the incidence of legal blindness in the sibling cohort and is approximately 0.5%:

$$0{,}00224 + 0{,}00299 = 0{,}00523$$

# Appendix E

## NoPET-plans applied onto PTV(+PET)

Conformity index for PTV delineated without PET (PTV(-PET)) and with PET (PTV(+PET)), in the plan optimized for the PTV(-PET).Solid lines are PTV(-PET) and dashed curves are PTV(+PET).

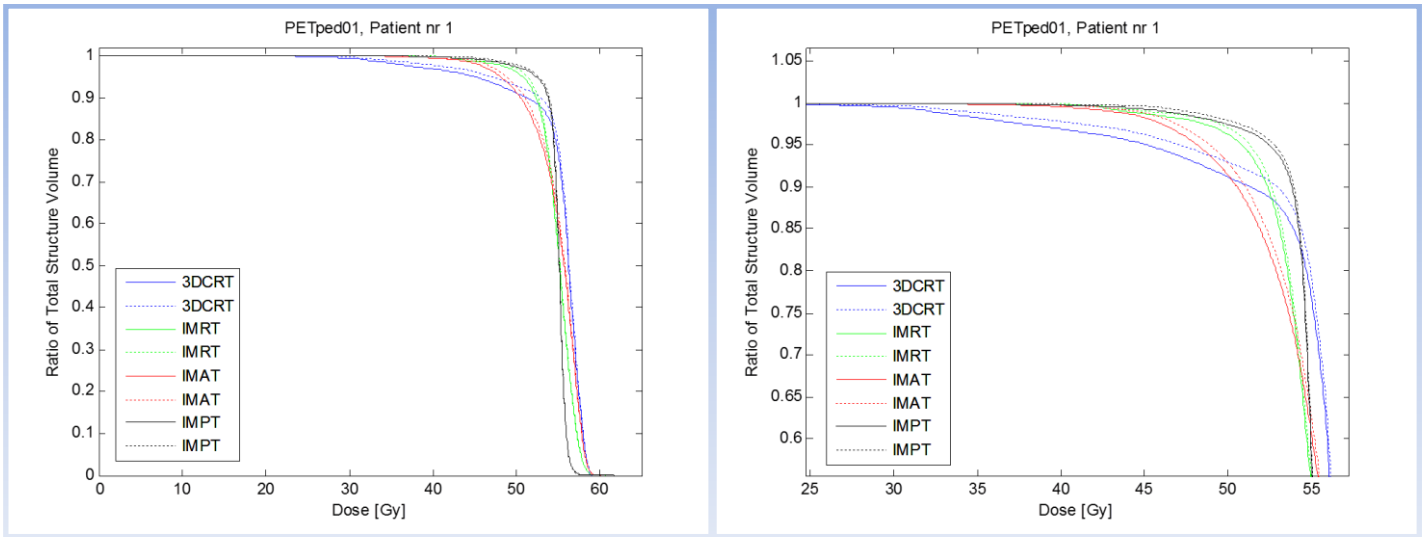


Figure 48: Patient 1 (PETped01).

For patient number 1: slightly better target coverage of the PTV(+PET) than the PTV(-PET) in the noPET-plans. PTV(+PET) is smaller than PTV(-PET).

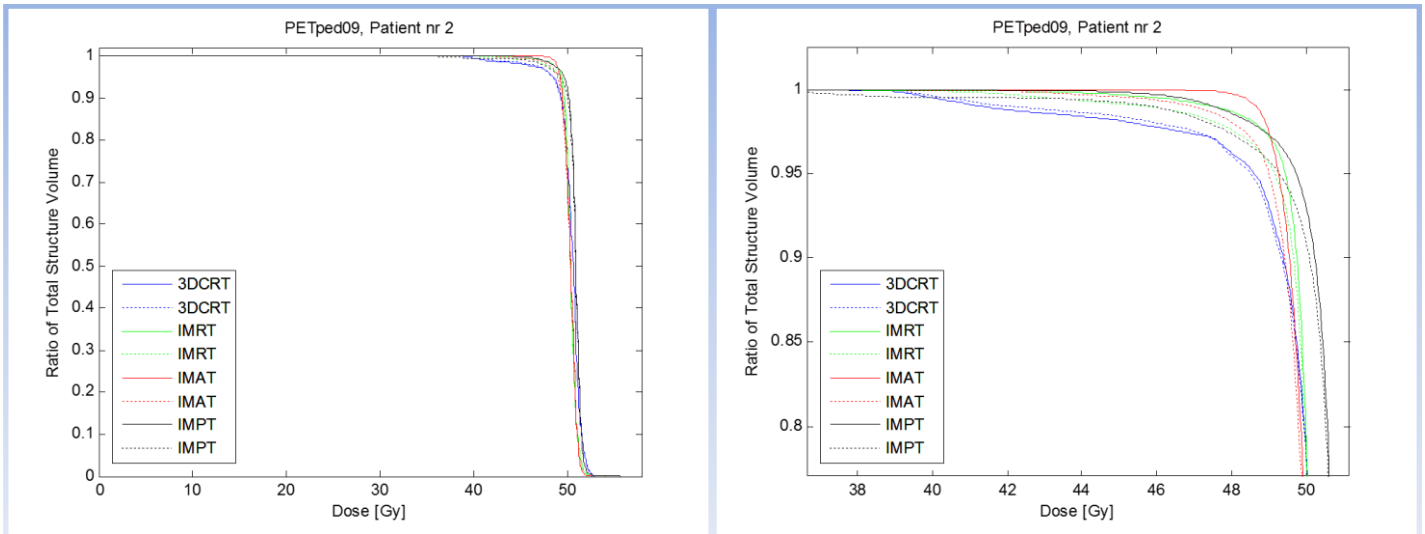


Figure 49: Patient 2 (PETped09).

For patient number 2, the dose coverage of PTV(+PET) is poorer than that of the PTV(-PET) in the IMRT-, IMAT- and IMPT plans. PTV(+PET) is slightly larger than PTV(-PET).

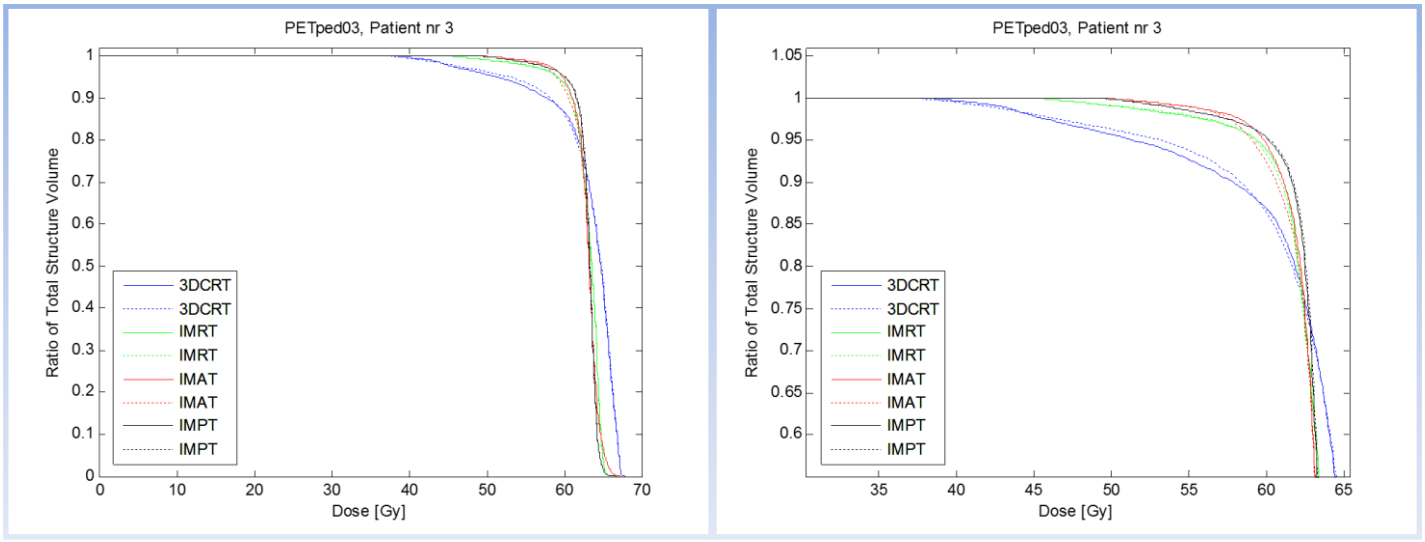


Figure 50: Patient 3 (PETped03).

For patient number 3, the dose coverage of PTV(+PET) was not considerably different than that of the PTV(-PET) for any of the treatment modalities.
PTV(+PET) is smaller than PTV(-PET).

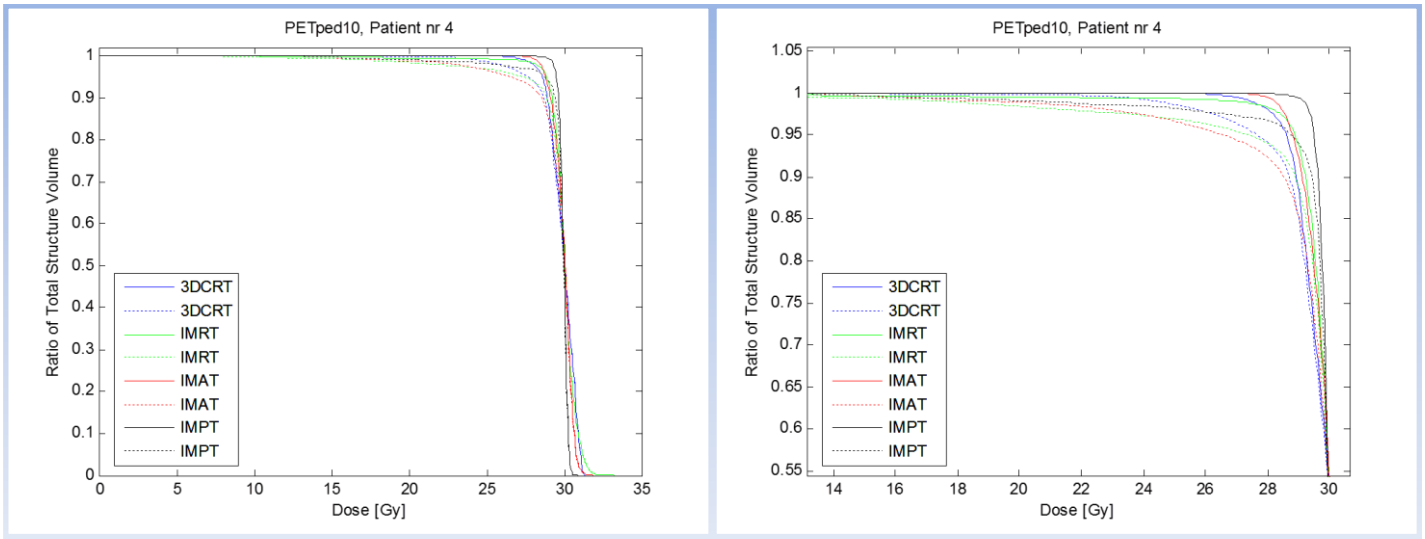


Figure 51: Patient 4 (PETped10).

For patient number 4 the DVH of the PTV(+PET) revealed a unsatisfactory target coverage for all treatment modalities compared to the DVH:s of PTV(-PET).
PTV(+PET) is larger than PTV(-PET).

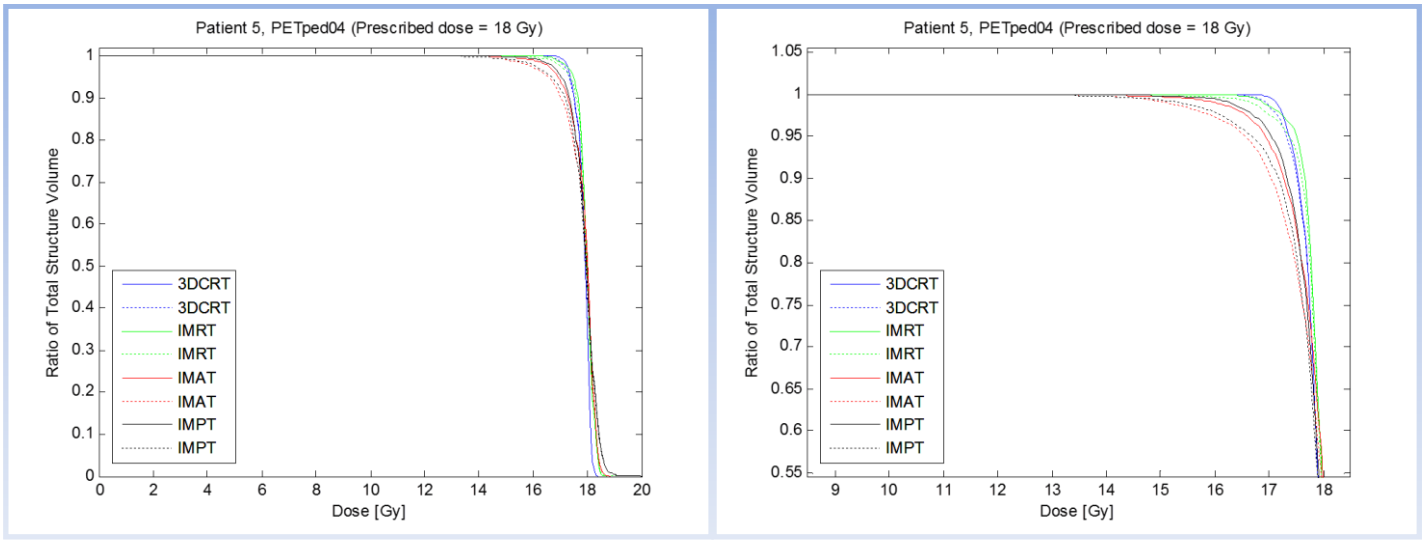


Figure 52: Patient 5 (PETped04) (PTV neck).

For patient number 5 the dose-coverage of the PTV(+PET) in the neck was mostly deteriorated for the IMAT- and IMPT-plans, while the PTV(+PET) in the lower back suffered mostly in the IMRT- and IMPT-noPET-plans.
PTV(+PET) in the neck is larger than PTV(-PET) whereas PTV(+PET) in the lower back is smaller than PTV(-PET).

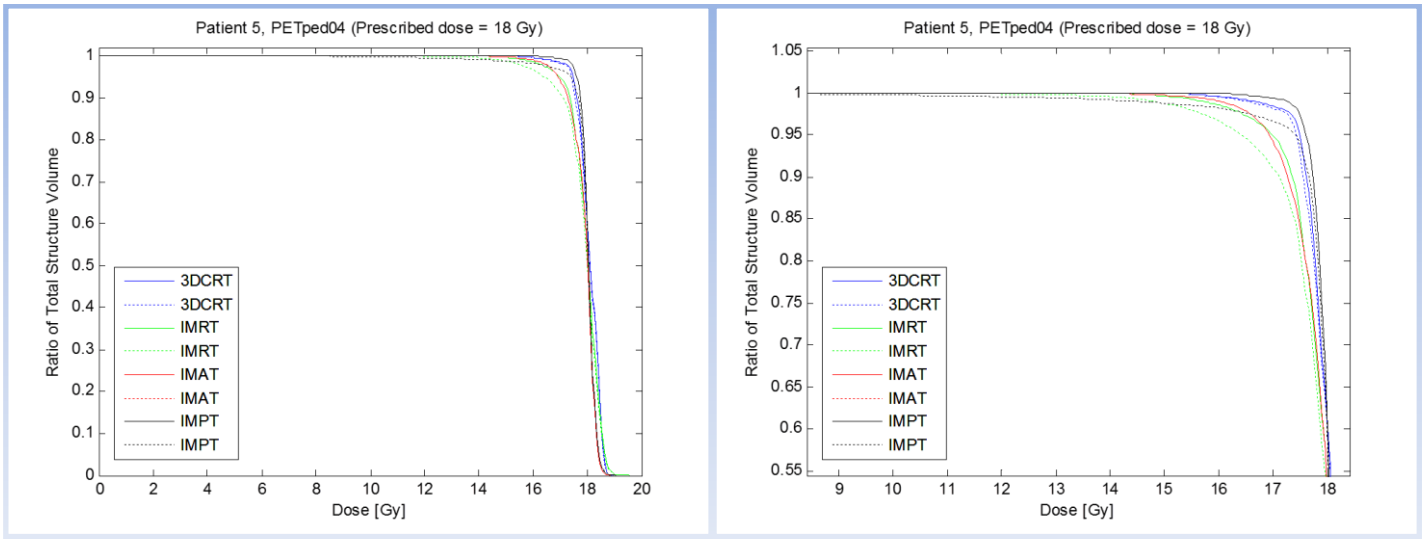


Figure 53: Patient 5 (PETped04) (PTV lower back).

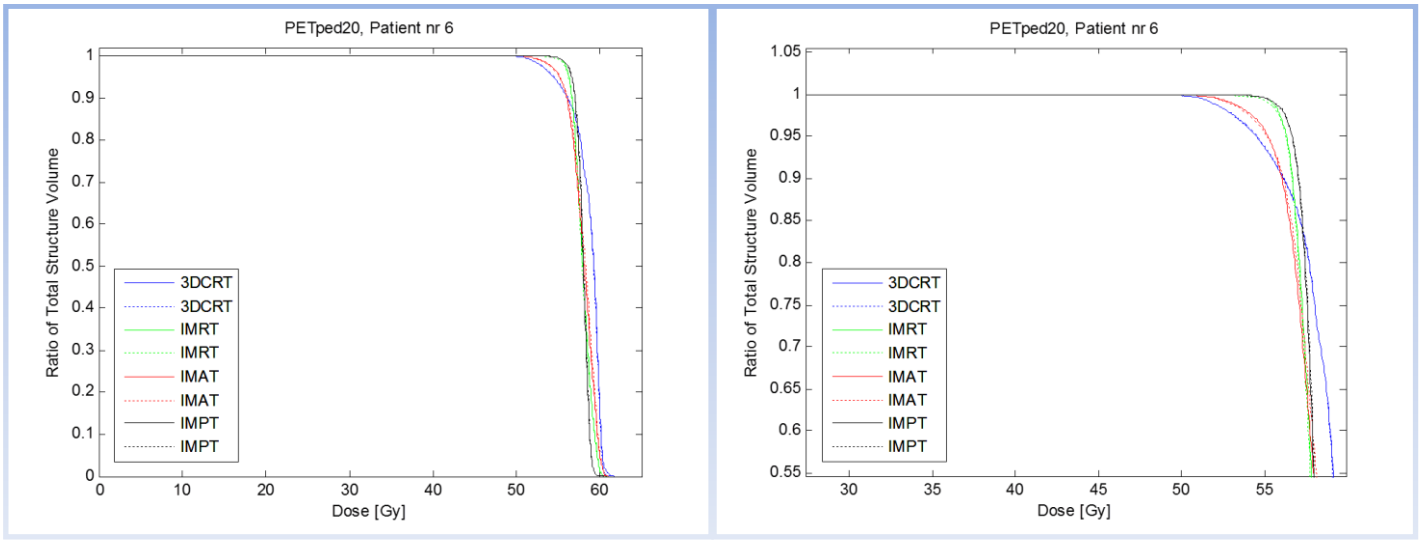


**Figure 54: Patient 6 (PETped20).**

For patient number 6, there are no visible differences between the target coverage of PTV(+PET) and PTV(-PET) in the plans made for the target volumes without PET.
PTV(+PET) is smaller than PTV(-PET).

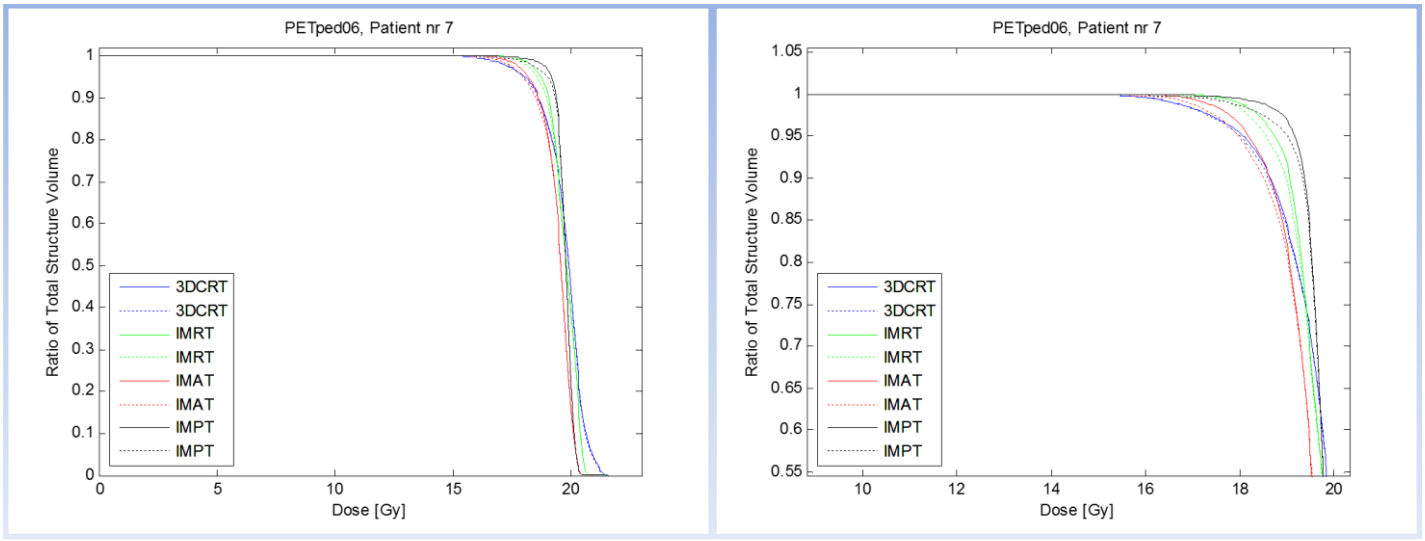


**Figure 55: Patient 7 (PETped06).**

For patient number 7, the target coverage of PTV(+PET) is slightly worse for all modalities but 3DCRT.
PTV(+PET) is smaller than PTV(-PET).

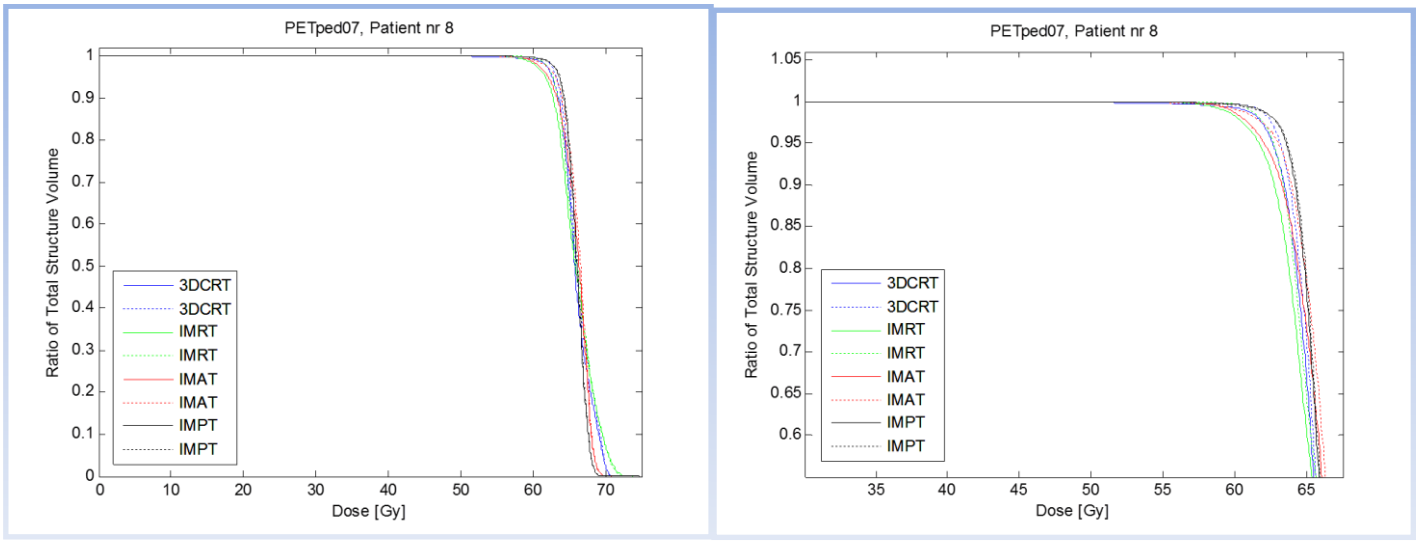


Figure 56: Patient 8 (PETped07).

For patient number 8, the differences in target coverage are very small. For all modalities but IMPT, where there is no visible difference, the dose-coverage is slightly better for the PTV(+PET).
PTV(+PET) is quite a lot smaller than PTV(-PET).

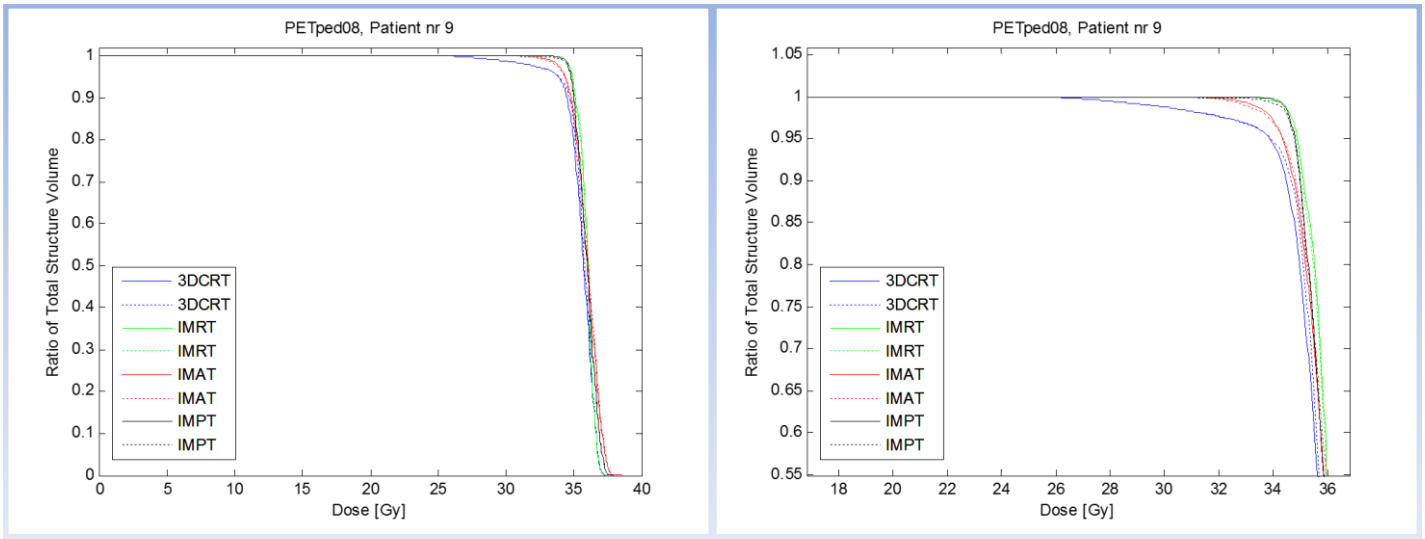


Figure 57: Patient 9 (PETped08).

For patient number 9, there are no noteworthy differences in target coverage.
PTV(+PET) is smaller than PTV(-PET).

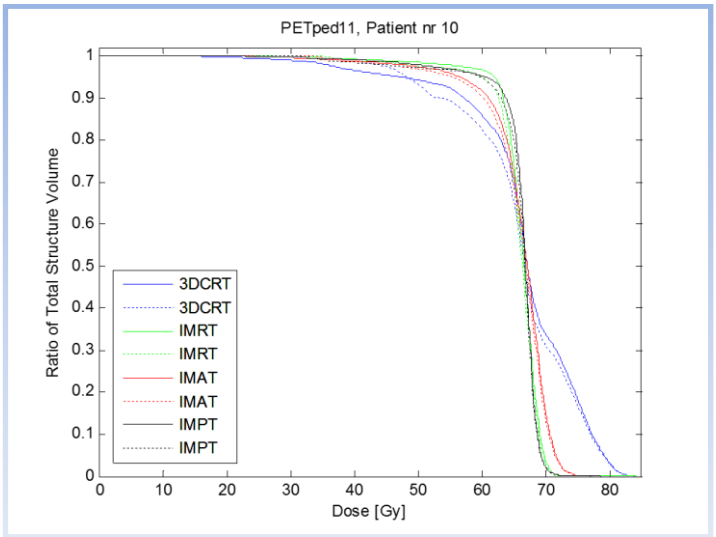


Figure 58: Patient 10 (PETped11).

For patient number 10, there are no noteworthy differences in target coverage.
PTV(+PET) is larger than PTV(-PET).

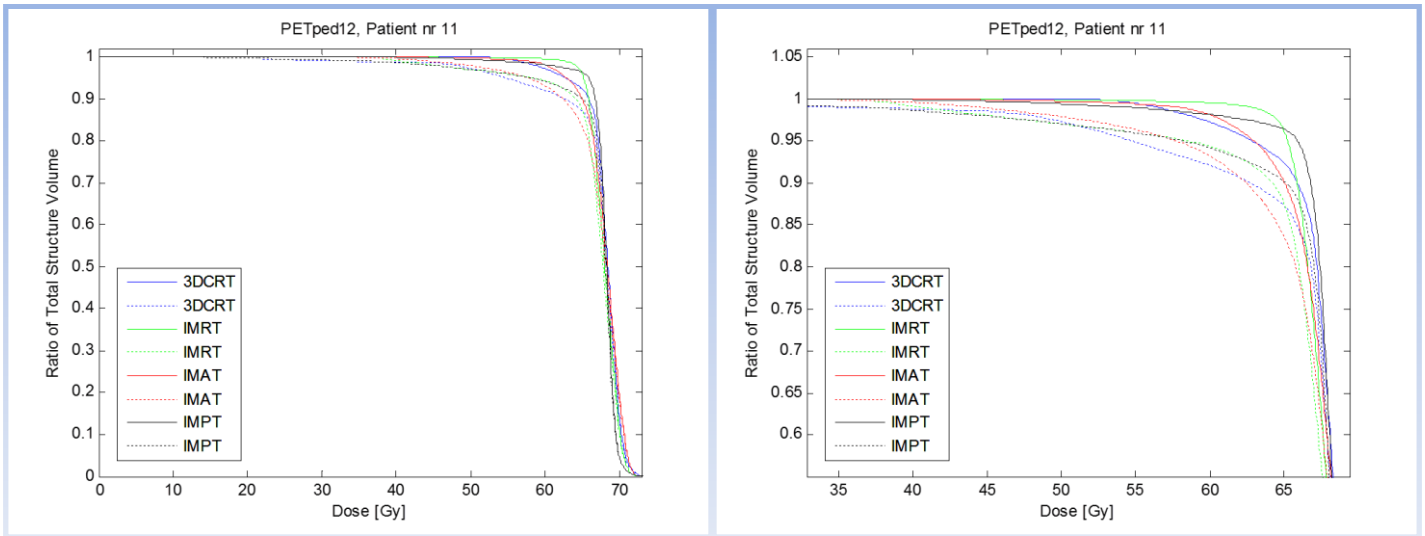


Figure 59: Patient 11 (PETped12).

For patient number 11, there dose-coverage is clearly poorer for the PTV(+PET) than the PTV(-PET).
PTV(+PET) is a lot larger than PTV(-PET).

# References

1. **DA Mulrooney, MW Yeazel, T Kawashima, AC Mertens, P Mitby, M Stovall, SS Donaldson, DM Green, CA Sklar, LL Robison and WM Leisenring.** Cardiac outcomes in a cohort of adult survivors of childhood and adolescent cancer: Retrospective analysis of the Childhood Cancer Survivor Study cohort. *British Medical Journal.* 2009, 339.

2. **SC Chawla, N Federman, D Zhang, K Nagata, S Nuthakki, M McNitt-Gray and MI Boechat.** Estimated cumulative radiation dose from PET/CT in children with malignancies: a 5-year retrospective review. *Pediatric Radiology.* 2010, 40, pp. 681-686.

3. **Cancerfonden.** http://www.cancerfonden.se/sv/cancer/Undersokningar-och-behandlingar/Behandlingar/Stralbehandling/?gclid=CO-I1siB07ACFecumAodbEU01A. *www.cancerfonden.se.* 2009.

4. **EGC Troost, DAX Schinagl, J Bussink, WJG Oyen and JHAM Kaanders.** Clinical evidence on PET-CT for radiation therapy planning in head and neck tumors. *Radiotherapy and Oncology.* 2010, 96, pp. 324-334.

5. **SB Jensen, AML Pedersen, A Vissink, E Andersen, CG Brown, AN Davies, J Dutilh, JS Fulton, L Jankovic, NNF Lopes, ALS Mello, LV Muniz, CA Murdoch-Kinch, RG Nair, JJ Napeñas, A Nogueira-Rodrigues, D Saunders, B Stirling, I von Bültzingslöwen et al.** A systematic review of salivary gland hypofunction and xerostomia induced by cancer therapies: Prevalence, severity and impact on quality of life. *Support Cancer Care.* 2010, 18, pp. 1039-1060.

6. **L Cozzi, A Fogliata, A Lomax and A Bolsi.** A treatment planning comparision of 3D Conformal Therapy, Intensity Modulated Photon Therapy and Proton Therapy for treatment of advanced head and neck tumors. *Radiotherapy and Oncology.* 2001, 61, pp. 287-297.

7. **F Sterzing, EM Stoiber, S Nill, H Bauer, P Huber, J Debus and MW Münter.** Intensity Modulated Radiotherapy (IMRT) in the treatment of children and adoloscents - A single institution's experience and a review of the literature. *Radiation Oncology.* 2009, 4.

8. **W Dörr, S Köst, K Keinert, F-H Glaser, G ENdert and T Herrmann.** Early intenstinal changes following abdominal radiotherapy. *Strahlentherapie und Onkologie.* 2006, 1.

9. **P Munck af Rosenschöld, S Engelholm, L Ohlhues, I Law, I Vogelius and SA Engelholm.** Photon and proton therapy planning comparison for malignant glioma based on CT, FDG-PET, DTI-MRI and fiber tracking. *Acta Oncologica.* 2011, 50, pp. 777-783.

10. **R Miralbell, A Lomax, L Cella and U Schneider.** Potential reduction of the incidence of radiation-induced second cancers by using proton beams in the treatment of pediatric tumors. *International Journal of Radiation Oncology, Biology and Physics.* 2002, Vol. 54, 3, pp. 824-829.

11. **X Mu, T Björk-Eriksson, S Nill, U Oelfke, KA Johansson, G Gagliardi, L Johansson, M Karlsson and B Zackrisson.** Does electron and proton therapy reduce the risk of radiation induced cancer after spinal irradiation for childhood medulloblastoma? A comparative treatment planning study. *Acta Oncologica.* 2005, 44, pp. 554-562.

12. **A van Baardwijk, BG Baumert, G Bosmans, M van Kroonenburgh, S Stroobants, V Gregoire, P Lambin and D de Ruysscher.** The current status of FDG-PET in tumour volume definition in radiotherapy treatment planning. *Cancer Treatment Reviews.* 2006, 32, pp. 245-260.

13. **International Atomic Energy Agency, IAEA officers N Watanabe and B Jeremic.** IAEA-TECDOC-1603: The role of PET/CT in radiation treatment planning of cancer patient treatment. 2008.

14. **Phelps, ME.** Positron emission tomography provides molecular imaging of biological processes. *Proceedings of the National Academy of Sciences.* 2000, Vol. 97, 16, pp. 9226-9233.

15. **Z Bar-Zever, Z Keidar, A Ben-Barak, R bar-Shalom, S Postovsky, L Guralnik, MW Ben Arush and O Israel.** The incremental value of 18F-FDG PET/CT in paediatric malignancies. *European Journal of Nuclear Medicine and Molecular Imaging.* 2007, 34, pp. 630-637.

16. **L Xing, B Wessels and WR Hendee.** The value of PET/CT is being over-sold as a clinical tool in radiation oncology (Point/Counterpoint). *Medical Physics.* 2005, Vol. 6, 32, pp. 1457-1459.

17. **Erdi, YE.** The use of PET for radiotherapy. *Current Medical Imaging Reviews.* 2007, 3, pp. 3-16.

18. **G Antoch, N Saoudi, H Kuehl, G Dahmen, SP Mueller, T Beyer, A Bockisch, JF Debatin and LS Freudenberg.** Accuracy of whole-body dual-modality Fluorine-18-2-Fluoro-2-Deoxy-D-Glucose Positron Emission Tomography and Computed Tomography (FDG-PET/CT) for tumor staging in solid tumors: Comparison with CT and PET. *Journal of Clinical Oncology.* 2004, Vol. 22, 21, pp. 4357-4368.

19. **M MacManus, T Leong.** Incorporating PET information in radiation therapy planning. *Biomedical Imaging and Intervention Journal.* 2007, 3.

20. **EA Wegner, SF Barrington, JE Kingston, RO Robinson, RE Ferner, M Taj, MA Smith and MJ O'Doherty.** The impact of PET scanning on management of paediatric oncology patients. *European Journal of Nuclear Medicine and Molecular Imaging.* 2005, Vol. 32, 1, pp. 23-30.

21. **RR Boktor, WS Omar, E Mousa, I Attia, A Refaat, MH ElTawdy, AG Pitman and HM Abdel-Dayem.** A preliminary report on the impact of 18F-FDG PET/CT in the management of paediatric head and neck cancer. *Nuclear Medicine Communications.* 2012, 33, pp. 21-28.

22. **MM Hudson, MJ Krasin and SC Kaste.** PET imaging in pediatric Hodgkin's lymphoma. *Pediatric Radiology.* 2004, 34, pp. 190-198.

23. **G Delouya, L Igidbashian, A Houle, M Bélair, L Boucher, C Cohade, S Beaulieu, ÉJ Filion, G Coulombe, M Hinse, C Martel, P Després and PF Nguyen-Than.** 18F-FDG-PET imaging in radiotherapy tumor volume delineation in treatment of head and neck cancer. *Radiotherapy and Oncology.* 2011, Vol. 101, 3, pp. 362-368.

24. **MWB Arush, O Israel, S Postovsky, D Militianau, I Meller, I Zaidman, A E Sapir and R Bar-Shalom.** Positron Emission Tomography/ Computed Tomography with 18Fluoro-Deoxyglucose in the detection of local recurrence and distant metastases of pediatric sarcoma. *Pediatric Blood Cancer.* 2007, 49, pp. 901-905.

25. **T Völker, T Denecke, I Steffen, D Misch, S Schönberger, m Plotkin, J Ruf, C Furth, B Stöver, H Hautzel, G Henze and H Amthauer.** Positron Emission Tomography for staging of pediatric sarcoma patients: Results of a prospective multicenter trial. *Journal of Clinical Oncology.* 2007, Vol. 25, 34, pp. 5435-5441.

26. **D de Ruysscher, U Nestle, R Jeraj and M MacManus.** PET Scans in radiotherapy planning of lung cancer. *Lung Cancer.* 2012, Vol. 75, 2, pp. 141-145.

27. **DAX Schinagl, JHAM Kaanders and WJG Oyen.** From anatomical to biological target volumes: the role of PET in radiation treatment planning. *Cancer Imaging.* 2006, 6, pp. 107-116.

28. **PH Jarrit, KJ Carson, AR Hounsell and D Visvikis.** The role of PET/CT scanning in radiotherapy planning. *The British Journal of Radiology.* 2006, 79, pp. 27-35.

29. **CC Ling, J Humm, S Larson, H Amols, Z Fuks, S Leibel and JA Koutcher.** Towards multidimensional radiotherapy (MD-CRT): Biological imaging and biological conformality. *International Journal of Radiation Oncology, Biology and Physics.* 2000, Vol. 47, 3, pp. 551-560.

30. **DAX Schinagl, WV Vogel, AL Hoffmann, JA van Dalen, WJ Oyen and JHAM Kaanders.** Comparison of five segmentation tools for 18F-Fluoro- Deoxy- Glucose- Positron Emission Tomography- based target volume definition in head and neck cancer. *International Journal of Radiation Oncology, Biology & Physics.* 2007, Vol. 69, 4, pp. 1282-1289.

31. **I ElNaqa, H Zaidi.** PET-guided delineation of radiation therapy treatment volumes: A survey of image segmentation techniques. *European Journal of Nuclear Medicine Molecular Imaging.* 2010, 37, pp. 2165-2187.

32. **R Eakin, J Foster, G Hanna, A Hounsell, T Lynch, J McAleese, O McNally, W Page, D Stewart and Y Summers.** The role of PET/CT in radiotherapy planning. *Oncology News.* 2007, Vol. 1, 6, pp. 13-15.

33. **V Grégoire, K Haustermans, X Geets, S Roels and M Lonneux.** PET-based treatment planning in radiotherapy: A new standard? *The Journal of Nuclear Medicine.* 2007, Vol. 48, 1, pp. 68-76.

34. **M Lambrecht, K Haustermans.** Clinical evidence on PET-CT for radiation therapy planning in gastro-intestinal tumors. *Radiotherapy and Oncology.* 2010, 96, pp. 339-346.

35. **C Franzius, KU Juergens.** PET/CT in paediatric oncology: Indications and pitfalls. *Pediatric Radiology.* 2009, 39, pp. 446-449.

36. **JC Mitchell, F Grant, AR Evenson, JA Parker, P-O Hasselgren and S Parangi.** Preoperative evaluation of thyroid nodules with 18FDG-PET/CT. *Surgery.* 2005, 6, pp. 1166-1174.

37. **KC Oeffinger, AC Mertens, MM Hudson, JG Gurney, J Casillas, H Chen, J Whitton, M Yeazel, Y Yasui, and LL Robison.** Health care of young adult survivors of childhood cancer: A report from the Childhood Cancer Survivor Study. *The Annals of Family Medicine.* 2004, 2, pp. 61-70.

38. **IR Vogelius, SM Bentzen, MV Maraldo, PM Petersen and L Specht.** Risk factors for radiation- induced hypothyroidism. *Cancer.* 2011, Vol. 117, 23, pp. 5250-5260.

39. **G Gagliardi, LS Constine, V Moiseenko, C Correa, LJ Pierce, AM Allen and LB Marks.** QUANTEC Organ-specific paper: radiation dose-volume effects in the heart. *International Journal of Radiation Oncology, Biology and Physics.* 2010, Vol. 76, 3, pp. 77-85.

40. **Lee, Y-H.** Late physical effects of childhood cancer survivors. *Korean Journal of Pediatrics.* 2010, Vol. 53, 4.

41. **VA Semenenko, XA Li.** Lyman-Kutcher-Burman NTCP model parameters for radiation pneumonitis and xerostomia based on combined analysis of published data. *Physics in Medicine and Biology.* 2008, 53, pp. 737-755.

42. **LB Marks, SM Bentzen, JO Deasy, F-M Kong, JD Bradley, IS Vogelius, I ElNaqa, JL Hubbs, JV Lebesque, RD Timmerman, MK Martel and A Jackson.** QUANTEC Organ-Specific Paper: Radiation dose- volume effects in the lung. *International Journal of Radiation Oncology, Biology & Physics.* 2010, Vol. 76, 3, pp. 70-76.

43. **M Werner-Wasik, E Yorke, J Deasy, J Nam and LB Marks.** QUANTEC Organ-Specific Paper: Radiation dose-volume effects in the esophagus. *International Journal of Radiation Oncology, Biology & Physics.* 2010, Vol. 76, 3, pp. 86-93.

44. **T Bölling, N Willich and I Ernst.** Late effects of abdominal irradiation in children: A review of the literature. *Anticancer Research.* 2010, 30, pp. 227-232.

45. **LR Meacham, CA Sklar, S Li, Q Liu, N Gimpel, Y Yasui, JA Whitton, M Stovall, LL Robison and KC Oeffinger.** Diabetes mellitus in long-term survuvors of childhood cancer. Increased risk associated with radiation therapy: A report for the Childhood Cancer Survivor Study. *Archives of Internal Medicine.* Vol. 169, 15, pp. 1381-1387.

46. **AN Viswanathan, ED Yorke, LB Marks, PJ Eifel and WU Shipley.** QUANTEC Organ-Specific Paper: Radiation dose-volume effects of the urinary bladder. *International Journal of Radiation Oncology, Biology & Physics.* 2010, Vol. 76, 3, pp. 116-122.

47. **LB Marks, PR Carroll, TC Dugan and MS Anscher.** The response of the urinary bladder, urethra and ureter to radiation and chemotherapy. *International Journal of Radiation Oncology, Biology & Physics.* 1995, Vol. 31, 5, pp. 1257-1280.

48. **LA Dawson, BD Kavanagh, AC Paulino, SK Das, M Miften, XA Li, C Pan, RKT Haken and TE Schulteiss.** QUANTEC Organ-Specific Paper: Radiation-associated kidney injury. *International Journal of Radiation Oncology, Biology & Physics.* 2010, Vol. 76, 3, pp. 108-115.

49. **HB Kal, M Loes van Kempen-Harteveld.** Induction of severe cataract and late renal dysfunction following total body irradiation: Dose-effect relationships. *Anticancer Research.* 2009, 29, pp. 3305-3310.

50. **JC Cheng, TE Schultheiss and JYC Wong.** Impact of drug therapy, radiation dose and dose rate on renal toxicity following bone marrow transplantation. *International Journal of Radiation Oncology, Biology and Physics.* 2008, Vol. 71, 5, pp. 1436-1443.

51. **LA Dawson, RKT Haken.** Partial volume tolerance of the liver to radiation. *Seminars in Radiation Oncology.* 2005.

52. **CC Pan, BD Kavanagh, LA Dawson, XA Li, SK Das, M Miften and RKT Haken.** QUANTEC Organ-Specific Paper: Radiation-associated liver injury. *International Journal of Radiation Oncology, Biology & Physics.* 2010, Vol. 76, 3, pp. 94-100.

53. **LA Dawson, D Normolle, JM Balter, CJ McGinn, TS Lawrence and RKT Haken.** Analysis of radiation-induced liver disease using the Lyman NTCP model. *International Journal of Radiation Oncology, Biology and Physics.* 2002, Vol. 53, 4, pp. 810-821.

54. **BD Kavanagh, CC Pan, LA Dawason, SK Das, XA Li, RKT Haken and M Miften.** QUANTEC Organ Specific Paper: Radiation dose-volume effects in the stomach and small bowel. *International Journal of Radiation Oncology, Biology and Physics.* 2010, Vol. 76, 3, pp. 101-107.

55. **A Gunnlaugsson, E Kjellén, P Nilsson, P-O Bendahl, J Willner and A Johnsson.** Dose-volume relationships between enteritis and irradiated bowel volumes during 5-Fluoracil and Oxaliplatin based chemoradiotherapy in locally advanced rectal cancer. *Acta Oncologica.* 2007, 46, pp. 937-944.

56. **E-Y Huang, C-C Sung, S-F Ko, C-J Wang and KD Yang.** The different volume effects of small-bowel toxicity during pelvic irradiation between gynecological patients with and without abdominal surgery: A prospective study with Computed Tomography-based dosimetry. *International Journal of Radiation Oncology, Biology and Physics.* 2007, Vol. 69, 3, pp. 732-739.

57. **LM Tho, M Glegg, J Paterson, C Yap, A MacLeod, M McCabe and AC McDonald.** Acute small bowel toxicity and preoperative chemoradiotherapy for rectal cancer: Investigating dose-volume relationships and role for inverse planning. *International Journal of Radiation Oncology Biology and Physics.* 2006, Vol. 66, 2, pp. 505-513.

58. **HT Eich, U Haverkamp, A Engert, M Kocher, R Skripnitchenko, C Brilliant, S Sehlen, E Dühmke, V Diehl and R-P Müller.** Biophysical analysis of the acute toxicity of radiotherapy in Hodgkin's Lymphoma - A comparison between extended field and involved field radiotherapy based on the data of the german Hodgkin study group. *International Journal of Radiation Oncology, Biology & Physics.* 2005, Vol. 63, 3, pp. 860-865.

59. **Brenner, DJ.** Fractionation and late rectal toxicity. *International Journal of Radiation Oncology, Biology and Physics.* 2004, Vol. 60, 4, pp. 1013-1015.

60. **JC Roeske, AJ Mundt, H Halpern, P Sweeney, H Sutton, C Powers, J Rotmensch, S Waggoner and RR Weichselbaum.** Late rectal sequelae following definitive raditaion therapy for carcinoma of the uterine cervix: A dosimetric analysis. *International Journal of Radiation Oncology, Biology and Physics.* 1997, Vol. 37, 2, pp. 351-358.

61. **JM Michalski, H Gay, A Jackson, SL Tucker and JO Deasy.** QUANTEC Organ-Specific Paper: Radiation dose-volume effects in radiation-induced rectal injury. *International Journal of Radiation Oncology, Biology & Physics.* 2010, Vol. 76, 3, pp. 123-129.

62. **EH Huang, A Pollack, L Levy, G Starkschall, L Dong, I Rosen and DA Kuban.** Late rectal toxicity: Dose-volume effects of conformal radiotherapy for prostate cancer. *International Journal of Radiation Oncology, Biology and Physics.* 2002, Vol. 54, 5, pp. 1314-1321.

63. **T Rancati, M Schwarz, AM Allen, F Feng, A Popovtzer, B Mittal and A Eisbruch.** Radiation dose volume effects in the larynx and pharynx. *International Journal of Radiation Oncology, Biology and Physics.* 2010, 76, pp. 64-69.

64. **S Beier-Jensen, AM Pedersen, J Reibel and B Nauntofte.** Xerostomia and hypofunction of the salivary glands in cancer therapy. *Support Cancer Care.* 2003, 11, pp. 207-225.

65. **AC Houweling, MEP Philippens, T Dijkema, JM Roesink, CHJ Terhaard, C Schilstra, RKT Haken, A Eisbruch and CPJ Raaijmakers.** A comparison of dose-response models for the parotid gland in a large group of head- and- neck cancer patients. *International Journal of Radiation Oncology, Biology & Physics.* 2010, Vol. 76, 4, pp. 1259-1265.

66. **T Dijkema, CPJ Raaijmakers, RKT Haken, JM Joesink, PM Braam, AC Houweling, MA Moerland, A Eisbruch and CHJ Terhaard.** Parotid gland function after radiotherapy: The combined Michigan and Utrecht experience. *International Journal of Radiation Oncology, Biology and Physics.* 2010, Vol. 78, 2, pp. 449-453.

67. **JO Deasy, V Moiseenko, L Marks, KSC Chao, J Nam and A Eisbruch.** QUANTEC Organ-Specific Paper: Radiotherapy dose-volume effects on salivary gland function. *International Journal of Radiation Oncology, Biology and Physics.* 2010, Vol. 76, 3, pp. 58-63.

68. **S Bhatia, NK Ramsay, JP Bantle, A Mertens and LL Robison.** Thyroid abnormalities after therapy for Hodgkin's Disease in childhood. *Oncologist.* 1996, 1, pp. 62-67.

69. **U Ricardi, A Corrias, A Einaudi, L Genitori, A Sandri, LC Di Montezemolo, L Besenzon, E Madon and A Urgesi.** Thyroid dysfunction as a late effect in childhood medulloblastoma: A comparison of hyperfractionated versus conventionally fractionated craniospinal radiotherapy. *International Journal of Radiation Oncology, Biology & Physics.* 2001, Vol. 50, 5, pp. 1287-1294.

70. **KF Whelan, K Stratton, T Kawashima, JW Waterbor, RP Castleberry, M Stovall, CA Sklar, RJ Packer, P Mitby, CL Aitken, J Blatt, LL Robison and AC Mertens.** Ocular late effects in childhood and adolescent cancer survivors: A report from the Childhood Cancer Survivor Study. *Pediatric Blood Cancer.* 2010, Vol. 54, 1, pp. 103-109.

71. **Kempen-Harteveld, HB Kal and M Loes van.** Induction of severe cataract and late renal dysfunction following total body irradiation: Dose-effect relationships. *Anticancer Research.* 2009, 29, pp. 3305-3310.

72. **K Muller, PJCM Nowak, N Naus, C de Pan, CA van Santen, P Levendag and GPM Luyten.** Lacrimal gland radiosensitivity in uveal melanoma patients. *International Journal of Radiation Oncocolgy, Biology and Physics.* 2009, Vol. 74, 2, pp. 497-502.

73. **Finger, P T.** Radiation therapy for orbital tumors: Concepts, current use and ophthalmic radiation side effects. *Survey of Ophtalmology.* 2009, Vol. 54, 5, pp. 545-568.

74. **N Bhandare, A Jackson, A Eisbruch, CC Pan, JC Flickinger, P Antonelli and WM Mendenhall.** QUANTEC Organ-Specific Paper: Radiation therapy and hearing loss. *International Journal of Radiation Oncology, Biology and Physics.* 2010, Vol. 76, 3, pp. 50-57.

75. **C Hua, JK Bass, R Khan, LE Kun and TE Merchant.** Hearing loss after radiotherapy for pediatric brain tumors: Effect of cochlear dose. *International Journal of Radiation Oncology, Biology and Physics.* 2008, Vol. 72, 3, pp. 892-899.

76. **E Huang, BS Teh, DR Strother, QG Davis, JK Chiu, HH Lu, LS Carpenter, W-Y Mai, MM Chintagumpala, M South, WH Grant, EB Butler and SY Woo.** Intensity-Modulated Radiation Therapy for pediatric medulloblastoma: Early report on the reduction of ototoxicity. *International Journal of Radiation Oncology, Biology & Physics.* 2002, Vol. 52, 3, pp. 599-605.

77. **A Ottolenghi, V Smyth and KR Trott.** The risks to healthy tissues from the use of existing and emerging techniques for radiation therapy. *Radiation Protection Dosimetry.* 2011, Vol. 143, 2, pp. 533-535.

78. **Lyman, JT.** Complication probability as assessed from dose-volume histograms. *Radiation Research Supplement.* 1985, 8, pp. 13-19.

79. **C Burman, GJ Kutcher.** Calculation of complication probability factors for non-uniform normal tissue irradiation: The effective volume method. *International Journal of Radiation Oncology, Biology & Physics.* 1989, Vol. 6, 16, pp. 1623-1630.

80. **Niemierko, A.** Reporting and analyzing dose distributions: A concept of equivalent uniform dose. *Medical Physics.* 1997, Vol. 24, 1, pp. 103-110.

81. **A Tai, B Erickson and XA Li.** Extrapolation of Normal Tissue Complication Probability for different fractionations in liver irradiation. *International Journal of Radiation Oncology, Biology and Physics.* 2009, Vol. 74, 1, pp. 283-289.

82. **J Tward, M Glenn, M Pulsipher, P Barnette and D Gaffney.** Incidence, risk factors and pathogenesis of second malignancies in patients with non-Hodgkin lymfoma. *Leukemia & Lymphoma.* 2007, 48, pp. 1482-1495.

83. **W Dörr, T Herrmann.** Cancer induction by radiotherapy: Dose dependence and spatial relationship to irradiated volume. *Journal of Radiological Protection.* 2002, 22, pp. 117-121.

84. **G Svahn-Tapper, S Garwicz, H Anderson, A Shamsaldin, F DeVathaire, JH Olsen, H Doellner, H Hertz, G Jonmundsson, F Langmark, M Lanning, R Sankila, H Tulinius and T Möller.** Radiation Dose and Relapse are Predictors for Development of Second Malignant Solid Tumors After Cancer in Childhood and Adolescence: A Population-Based Case-Control Study in the Five Nordic Countries. *Acta Oncologica.* 2006, 45, pp. 438-448.

85. **Kleinerman, RA.** Cancer risks following diagnostic and therapeutic radiation exposure in children. *Pediatric Radiology.* 2006, 36, pp. 121-125.

86. **LE Kun, C Beltran.** Radiation therapy for children: Evolving technologies in the era of ALARA. *Pediatric Radiology.* 2009, 39, pp. 65-70.

87. **Schneider, U.** Modeling the risk of secondary malignancies after radiotherapy. *Genes.* 2011, 2, pp. 1033-1049.

88. **NP Brodin, IR Vogelius, MV Maraldo, P Munck af Rosenschöld, MC Aznar, A Kiil-Berthelsen, P Nilsson, T Björk-Eriksson, L Specht and SM Bentzen.** Life Years Lost - Comparing potentially fatal late complications after radiotherapy for pediatric medulloblastoma on a common scale. *Cancer.* 2012.

89. **U Schneider, M Sumila and J Robotka.** Site-Specific Dose-Response Relationships For Cancer Induction From The Combined Japanese A-bomb and Hodgkin Cohorts For Doses Relevant To Radiotherapy. *Theoretical Biology And Medical Modelling.* 2011, Vol. 8, 27.

90. **M van Herk, P Remeijer, C Rasch and JV Lebesque.** The probability of correct target dosage: Dose-population histograms for deriving treatment margins in radiotherapy. *International Journal of Radiation Oncology, Biology & Physics.* 2000, Vol. 47, 4, pp. 1121-1135.

91. **Herk, Marcel van.** Errors and margins in radiotherapy. *Seminars in Radiation Oncology.* 2004, Vol. 14, 1, pp. 52-64.

92. **E Eldebawy, E Attalla, I Eldesoky and MS Zaghloul.** Geometrical uncertainty margins in 3D conformal radiotherapy in the pediatric age group. *Journal of the Egyptian National Cancer Institute.* 2011, 23, pp. 55-60.

93. **MS Zaghloul, AG Mousa, E Eldebawy, E Attalla, H Shafik and S Ezzat.** Comparison of electronic portal imaging and Cone Beam Computed Tomography for position verification in children. *Clinical Oncology.* 2010, 22, pp. 850-861.

94. **XA Li, XS Qi, M Pitterle, K Kalakota, K Mueller, BA Erickson, D Wang, CJ Schultz, SY Firat and JF Wilson.** Interfractional variations in patient setup and anatomic change assessed by daily Computed Tomography. *International Journal of Radiation Oncology, Biology & Physics.* 2007, Vol. 68, 2, pp. 581-591.

95. **T Gupta, S Chopra, A Kadam, JP Agarwal, PR Devi, S Ghosh-Laskar and KA Dinshaw.** Assessment of three-dimensional set-up-errors in conventional head and neck radiotherapy using electronic portal imaging device. *Radiation Oncology.* 2007, Vol. 2, 44.

96. **C Beltran, MJ Krasin and TE Merchant.** Inter- and intrafractional positional uncertainties in pediatric radiotherapy patients with brain and head and neck tumors. *International Journal of Radiation Oncology, Biology & Physics.* 2011, Vol. 79, 4, pp. 1266-1274.

97. **Thomas, SJ.** Margins for treatment planning of proton therapy. *Physics in Medicine and Biology.* 2006, 51, pp. 1491-1501.

98. **F Albertini, EB Hug and AJ Lomax.** Is it necessary to plan with safety margins for actively scanned proton therapy? *Physics in Medicine and Biology.* 2011, 56, pp. 4399-4413.

99. **Lomax, AJ.** Intensity Modulated Proton Therapy and its sensitivity to treatment uncertainties 2: The potential effects of inter-fraction and inter-field motions. *Physics in Medicine and Biology.* 2008, 53, pp. 1043-1056.

100. **J Lambert, N Suchowerska, DR McKenzie and M Jackson.** Intrafractional motion during proton beam scanning. *Physics in Medicine and Biology.* 2005, 50, pp. 4853-4862.

101. **AL McKenzie, M van Herk and B Mijnheer.** The width of margins in radiotherapy treatment plans. *Physics in Medicine & Biology.* 2000, 45, pp. 3331-3342.

102. **PJ Eifel, SS Donaldson and PRM Thomas.** Response of growing bone to irradiation: A proposed late effects scoring system. *International Journal of Radiation Oncology, Biology & Physics.* 1995, Vol. 31, 5, pp. 1301-1307.

103. **SALUB, Svenska arbetsgruppen för långtidsuppföljning efter barncancer.** Uppföljning efter barncancer. 2010, Vol. Version: 5.0.

104. **SE Combs, W Behnisch, AE Kulozik, PE Huber, J Debus and D Schulz-Ertner.** Intensity-Modulated Radiotherapy (IMRT) and Fractionated Stereotactic Radiotherapy (FSRT) for children with head- and- neck rhabdomyosarcoma. *BMC Cancer.* 2007, Vol. 7, 1.

105. **JF Daisne, T Duprez, B Weynand, M Lonneux, M Hamoir, H Reychler and V Grégoire.** Tumor volume in pharyngolaryngeal squamous cell carcinoma: Comparison at CT, MR imaging and FDG PET and validation with surgical specimen. *Radiology.* 2004, 233, pp. 93-100.

106. **NP Brodin, P Munck af Rosenschöld, MC Aznar, A Kiil- Berthelsen, IR Vogelius, P Nilsson, B Lannering and T Björk-Eriksson.** Radiobiological risk estimates of adverse events and secondary cancer for proton and photon radiation therapy of pediatric medulloblastoma patients. *Acta Oncologica.* 2011, 50, pp. 806-816.

107. **MT Milano, LS Constine and P Okunieff.** Normal tissue tolerance dose metrics for radiation therapy of major organs. *Radiation Oncology.* 2006, 11, pp. 131-140.

108. **JN Healy, MF Borg.** Paediatric nasopharyngeal rhabdomyosarcoma: A case series and literature review. *Journal of Medical Imaging and Radiation Oncology.* 2010, 54, pp. 388-394.

109. **T Knöös, I Kristensen and P Nilsson.** Volumetric and dosimetric evaluation of radiation treatment plans: Radiation conformity index. *International Journal of Radiation Oncology, Biology & Physics.* 1998, Vol. 42, 5, pp. 1169-1176.

110. **J Deng, T Pawlicki, Y Chen, J Li, SB Jiang and CM Ma.** The MLC tongue-and-groove effect on IMRT dose distributions. *Physics in Medicine and Biology.* 2001, Vol. 46, pp. 1039-1060.

111. **Cassady, JR.** Clinical radiation nephropathy. *International Journal of Radiation Oncology, Biology & Physics.* 1995, Vol. 31, 5, pp. 1249-1256.

112. **M Liu, V Moiseenko, A Agranovich, A Karvat, W Kwan, ZH Saleh, AA Apte and JO Deasy.** Normal Tissue Complication Probability (NTCP) modeling of late rectal bleeding following external beam radiotherapy for prostate cancer: A test of the QUANTEC-recommended NTCP model. *Acta Oncologica.* 2010, 49, pp. 1040-1044.

113. **A Kursheed, HC Hillier, PC Shrimpton and BF Wall.** Influence of patient age on normalized effective doses calculated for CT examinations. *British Journal of Radiology.* 2002, 75, pp. 819-830.

114. **Committee to Assess Health Risks from Exposure of Low Levels of Ionizing Radiation, Nuclear and Studies Board, Division on Earth and Life Studies, National Research Council of the National Academies.** Health risks from exposure to low levels of ionizing radiation: BEIR VII, Phase 2. *Washington DC, National Academy Press.* 2006.

115. **KN Prasad, WC Cole and GM Hasse.** Health risks of low dose ionizing radiation in humans: A review. *Experimental Biology and Meidcine.* 2004, Vol. 229, 5, pp. 378-382.

116. **DJ Brenner, R Doll, DT Goodhead, EJ Hall, CE Land, JB Little, JH Lubin, DL Preston, RJ Preston, JS Puskin, E Ron, RK Sachs, JM Samet, RB Setlow and M Zaider.** Cancer risks attributable to low doses of ionizing radiation: Assessing what we really know. *Proceedings of the National Academy of Sciences (PNAS).* 2003, Vol. 100, 24.

117. **MP Little, R Wakeford, WJ Tawn, SD Bouffler and AB de Gonzales.** Risks associated with low doses and low dose rates of ionizing radiation: Why linearity may be (almost) the best we can do. *Radiology.* 2009, Vol. 251, 1, pp. 6-12.

118. **JM Yeh, L Nekhlyudov, SJ Goldie, AC Mertens and L Diller.** A model-based estimate of cumulative excess mortality in survivors of childhood cancer. *Annals of Internal Medicine.* 2010, Vol. 152, pp. 409-417.

119. **T Murano, U Tateishi, T Iinuma, N Shimada, H Daisaki, T Terauchi, N Moriyama and T Inoue.** Evaluation of the risk of radiation exposure from new 18FDG PET/CT plans versus conventional X-ray plans in patients with pediatric cancers. *Annals of Nuclear Medicine.* 2010, 24, pp. 261-267.

120. **J Staaf, H Jacobsson and A Sanchez-Crespo.** A revision of the organ radiation doses from 2-Fluoro-2-Deoxy-D-Glucose with reference to tumor presence. *Radiation Protection Dosimetry.* 2012.

121. **M Tatsumi, JH Miller and RL Wahl.** 18F-FDG PET/CT in evaluating non-CNS pediatric malignancies. *Journal of Nuclear Medicine.* 2007, 48, pp. 1923-1931.

122. **J Stauss, C Franzius, T Pfluger, KU Juergens, L Biassoni, J Begent, R Kluge, H Amthauer, T Voelker, L Hojgaard, S Barrington, S Hain, T Lynch and K Hahn.** Guidelines for 18F-FDG PET and PET-CT imaing in paediatric oncology. *European Journal of Nuclear Medicine and Molecular Imaging.* 2007.

123. **GJ Kutcher, C Burman.** Calculation of Complication Probability Factors for Non-Uniform Normal Tissue Irradiation: the Effective Volume Method. *International Journal of Radiation Oncology, Biology & Physics.* 1989, 6, pp. 1623-1630.

124. **Lyman, JT.** Complication probability as assessed from dose-volume-histograms. *Radiation Research Supplement.* 1985, 8, pp. 13-19.

125. **Z-Y Xu, S-X Liang, J Zhu, X-D Zhu, J-D Zhao, H-J Lu, Y-L Yang, L Chen, A-Y Wang, X-L Fu and G-L Jiang.** Prediction of radiation-induced liver disease by Lyman Normal-Tissue Complication Probability model in three-dimensional conformal radiation therapy for primary liver carcinoma. *International Journal of Radiation Oncology, Biology and Physics.* 2006, Vol. 65, 1, pp. 189-195.

LUND UNIVERSITY
Faculty of Science

Rigshospitalet